Universidade de Aveiro Departamento de Química
2010

Ana Rita Ribeiro Teles

Electrospinning de Celulose a Partir de Soluções de Líquido Iónicos

Electrospinning of Cellulose From Ionic Liquids Solutions

Universidade de Aveiro Departamento de Química
2010

Ana Rita Ribeiro Teles

Electrospinning de Celulose a Partir de Soluções de Líquido Iónicos

Electrospinning of Cellulose From Ionic Liquids Solutions

Dissertação apresentada à Universidade de Aveiro para cumprimento dos requisitos necessários à obtenção do grau de Mestre em Materiais Derivados de Recursos Renováveis, realizada sob a orientação científica do Doutor João Manuel da Costa e Araújo Pereira Coutinho, Professor Associado com Agregação do Departamento de Química da Universidade de Aveiro e Doutor José António Teixeira Lopes da Silva, Professor Auxiliar do Departamento de Química da Universidade de Aveiro

Obrigado por estares sempre ao meu lado…

o júri

presidente

Prof. Doutor Armando Jorge Domingues Silvestre

Professor Associado com Agregação do Departamento de Química da Universidade de Aveiro

Prof. Doutor João Manuel da Costa e Araújo Pereira Coutinho
Professor Associado com Agregação do Departamento de Química da Universidade de Aveiro

Prof. Doutor José António Teixeira Lopes da Silva
Professor Auxiliar do Departamento de Química da Universidade de Aveiro

Doutora Carmen Sofia da Rocha Freire Barros
Investigadora do CICECO da Universidade de Aveiro

Doutora Mara Guadalupe Freire Martins
Estagiária de Pós-Doutoramento do Instituto de Tecnologia Química e Biológica - ITQB2 da Universidade Nova de Lisboa

Agradecimentos

Em primeiro lugar quero agradecer aos meus orientadores, Professor João Coutinho e Professor José António, a oportunidade de conhecer o mundo da investigação e a orientação ao longo deste trabalho.

Uma palavra muito especial ao Professor João Coutinho, pois para além desta tese proporcionou-me todo o conhecimento que tenho sobre líquidos iónicos e a entrada num grupo de investigação fantástico que me ajudou a crescer não só profissionalmente mas também como pessoa.

A todos os Path's, o meu muito obrigado. Acho que nesta tese há um bocadinho de todos vós, sem a vossa ajuda não teria conseguido chegar até aqui. Acho que os piores e os melhores momentos da minha vida até agora foram partilhados convosco e jamais o esquecerei.

Não posso deixar de agradecer aquelas pessoas que fizeram parte do meu percurso e que considero amigos para a vida.

Agradeço também à minha família que sempre me apoiou e acreditou em mim. Pai, Mãe…não há palavras para vos agradecer.

Carlos, cada dia é passado a pensar em ti. És sem duvida o meu porto de abrigo, o meu suporte…vou agradecer-te o resto da vida.

palavras-chave Líquidos iónicos, celulose, electrofiação, monossacarídeos, solubilidade.

resumo

Os líquidos iónicos (LIs) têm sido alvo de um vasto estudo numa tentativa de substituir os solventes orgânicos voláteis comummente utilizados na indústria. Os LIs possuem uma grande capacidade de solvatação e pressões de vapor desprezáveis, tornando-os assim uma mais valia na solubilização das mais diversas biomoléculas (desde a própria madeira que é um biocompósito, até aos hidratos de carbono mais simples – monossacarídeos). A presente dissertação centra-se na solubilização de biomassa em LIs (celulose e monossacarídeos). A primeira secção desta tese teve como objectivo a dissolução de celulose em LIs para processamento por electrofiação de forma a conseguir micro e nanofibras de celulose. Para optimizar o tamanho e morfologia das fibras obtidas foram estudados vários parâmetros: tipo de celulose, tempo de dissolução, concentração de celulose e tensão superficial do solvente (LI). Observou-se que após 72 h e à temperatura ambiente era possível obter uma solução de 8 % (m/m) de celulose em líquido iónico na qual já não se observavam cristais de celulose em microscopia óptica de luz polarizada. Esta solução permitiu fazer electrofiação que resultou numa diminuição do tamanho das fibras de celulose original de 10 μm para 500 nm. De modo a diminuir a tensão superficial do solvente e obter fibras de ainda menor diâmetro, foi utilizado um segundo LI como tensioactivo. As fibras obtidas apresentaram um diâmetro próximo de 300 nm após a electrofiação. Os resultados obtidos demonstraram que é possível obter fibras nanométricas por electrofiação utilizando um solvente não volátil.

Não obstante o seu baixo custo e elevada importância dos hidratos de carbono para áreas como a dos biocombustíveis, a indústria alimentar e farmacêutica, estes compostos são ainda pouco explorados no que respeita à sua solubilidade em líquidos iónicos. Neste domínio foram determinadas solubilidades de 6 monossacarídeos em LIs hidrofóbicos e hidrofílicos numa gama de temperaturas de (288.15 a 348.15) K. Os LIs hidrofílicos mostraram possuir uma elevada capacidade de solvatação dos monossacarídeos que é da mesma ordem de grandeza daquela observada em solventes moleculares comuns – água. Da dependência das solubilidades dos açúcares com a temperatura demonstrou-se que o anião do LI apresenta um papel primordial na solvatação de açúcares. A variação da solubilidade em função da temperatura indica que a entalpia de solução dos monossacarídeos depende essencialmente da natureza do LI e não do açúcar.

keywords Ionic liquids, cellulose, electrospinning, monosaccharides, solubility.

abstract

Ionic liquids (ILs) have been largely explored attempting the substitution of the hazardous volatile organic solvents usually employed in industry. ILs possess high solvent capacity and negligible vapour pressures, which makes them enhanced solvents for the most diverse biomolecules (from wood, that is a biocomposite to its infamous isolated compound – monosaccharides). The present dissertation focuses in the solubility of biomass in ILs (cellulose and monosaccharides). The first section of this thesis aims the cellulose dissolution in ILs for the subsequent processing by electrospinning seeking the obtention of cellulose micro- and nanofibers for industrial applications. In order to optimize the size and morphology of the electrospun fibers several operational parameters were evaluated: nature of cellulose, time of dissolution, concentration of cellulose, and the surface tension of the solvent. Optimized results indicated that after 72 h at room temperature it was possible to obtain a solution of 8 wt % of cellulose in IL, in which no cellulose crystals were observed by optical polarized light microscopy. This solution allow the performance of electrospinning, which resulted in the downsize of the fibers, from 10 μm to 500nm μm. In order to diminish the surface tension of the solvent and lead towards even smaller fibers, a second IL was used as a tensioactive. The electrospun fibers obtained had a diameter near 300 nm. The obtained results showed that it is possible to obtain nanosized cellulose fibers through electrospinning by using a non-volatile solvent.

Despite the carbohydrates low cost and upmost importance to industries, such as fuel manufacturing, food industries and pharmaceuticals, these compounds are lagged behind regarding their phase equilibria in novel solvents, such as ILs. In this thesis a systematic study of 6 monosaccharides in both hydrophobic and hydrophilic ILs was conducted in a large temperature range from (288.15 to 348.15) K. Hydrophilic ILs presented enhanced solvation capacity for carbohydrates and of the same order of magnitude as that observed in a common molecular solvent – water. From the solubilities temperature dependence it was demonstrated that the IL anion plays a major role in defining the carbohydrates saturation limits. Critical temperature turnovers in solubility values were observed indicating that the enthalpy of solution of carbohydrates in ILs is largely dependent on the ILs nature, and not that of the sugar.

Contents

List of Tables

List of Figures

Notation

List of symbols

T	Temperature
T_m	Melting Temperature
n	Number of Carbon Atoms
X	Halogens
wt %	Weight Percentage
x	Mole Fraction
R^2	Correlation Coefficient
$\Delta_f H$	Enthalpy of Fusion
R	Universal Gas Constant

Greek Symbols

β	Hydrogen Bond Basicity Parameter
γ	Activity Coefficient
λ	Wave Length
ρ	Density
σ	Surface Tension
$\Delta\sigma$ %	Surface Tension Relative Deviation

List of Abbreviations

Abs	Absorvance
AGU	Anhydrous Glucose Unit
DMSO	Dimethylsulfoxide
DNS	3,5-Dinitrosalicylic Acid
DP	Degree of Polymerization
ILs	Ionic Liquids
NMR	Nuclear Magnetic Resonance
POM	Polarized Optical Microscopy
rpm	Rotations *per* Minute
RTILs	Room Temperature Ionic Liquids
SEM	Scan Electron Microscopy
UV-VIS	Ultraviolet-Visible
VOC's	Volatile Organic Compounds
XRD	X-ray Diffraction
$[CF_3SO_3]^-$	Triflate anion
$[CF_3CO_2]^-$	Trifluoroacetate anion
$[C_4mim][N(CN)_2]$	1-butyl-3-methylimidazolium Dicyanamide
[C4mim][DMP]	1-butyl-3-methylimidazolium Dimethylphosphate
$[C_4mim][BF_4]$	1-butyl-3-methylimidazolium Tetrafluoroborate
$[C_4mim][NTf_2]$	1-butyl-3-methylimidazolium Bis(trifluoromethylsulfonyl)imide
$[C_8mim][BF_4]$	1-methyl-3-octylimidazolium Tetrafluoroborate

$[C_8mim][PF_6]$	1-methyl-3-octylimidazolium Hexafluorophosphate
$[C_8mim][NTf_2]$	1-methyl-3-octylimidazolium Bis(trifluoromethylsulfonyl)imide
$[C_{10}mim][Cl]$	1-methyl-3-decylimidazolium Chloride
$[P_{66614}][Cl]$	Trihexyltetradecylphosphonium Chloride
$[P_{66614}][N(CN)_2]$	Trihexyltetradecylphosphonium Dicyanamide

1. General Introduction

1.1 Objectives and Scopes

The declining resources of fossil fuels, as well as the global heating caused by greenhouse gas emissions, have become unquestionable threats. It is, therefore, crucial to find new resources of raw materials and energy in order to produce day-to-day products aiming at allowing us to keep our living standards [1]. In the last century this subject did not received a great deal of attention until the conception that the fossil resources scarcity is a real case in point [2]. Nowadays, trying to overcome that problem, the scientific community is making large efforts to find renewable sources of chemicals, materials and energy [3]. Their production from biomass is the aim of the biorefinery concept development [4]. Vegetable biomass is essentially made up of carbohydrates, lignin, proteins, and fats. The biorefinery major goal is to transform such biological materials into useful products using an adequate combination of technologies and processes. Figure 1 shows the principal elements making part of the biorefinery process where biomass is converted into the most diverse products, such as fuels, power and chemicals using biological and chemical conversion processes [4].

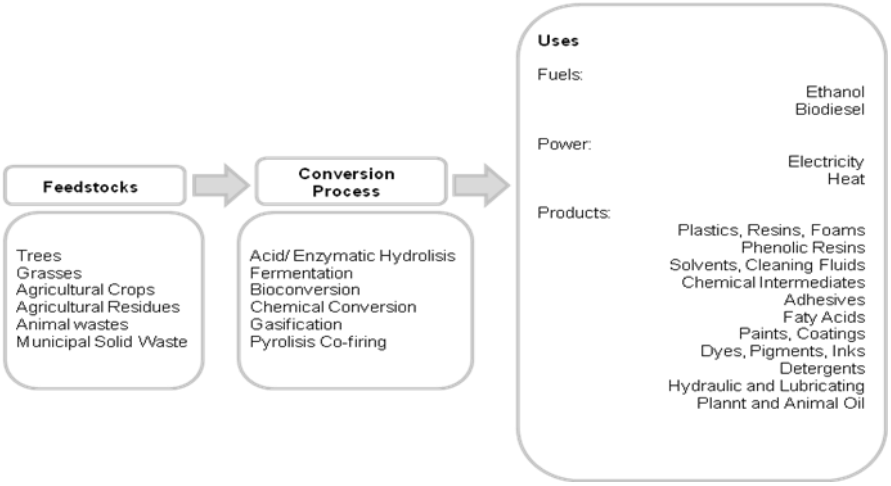

Figure 1 Simple three-step biomass-to-products process [4]

One of the major constituents of biomass is cellulose: a renewable, biodegradable and biocompatible polysaccharide. Cellulose-based products have significant applications in the pulp and paper, textile, polymer, membrane and paint industries. Nevertheless, its crystalline structure makes impossible the dissolution in water and common organic solvents. Solvents capable of cellulose dissolution are usually volatile, toxic and noxious to the environment, namely e.g. dimethylacetamide/LiCl or cupri-ethylenediamine [5]. This is thus the example of a process where a sustainable and environmentally friendly resource is actually processed by non-sustainable and environmentally damaging processes. Environmentally friendly processes making use of biomass

must address the actual critical concerns related to the declining resources of fossil fuels and global heating. This has been pushing research towards the discovery of valuable "green" solvents to be used in the biorefinery field. In this context, ionic liquids (ILs) appear as greener solvents than typical volatile organic solvents used in industry. ILs appealing characteristics, such as their low melting points, negligible vapor pressures, general nonflammability, large solvation capability and recycling simplicity, among others, largely contributed for such a classification.

The main objective of this work is the production of micro- and nanofibers of cellulose by electrospinning using ILs (non-volatile compounds) as alternative solvents to the typical nonoxious organic solvents largely employed. Co-Solvents such as dimethylsulfoxide (DMSO) [6], and solvents like lithium chloride (LiCl)/N,N-dimethyl acetamide (DMAc) and N-methylmorpholine oxide (NMMO)/water [7] are commonly used aiming cellulose electrospinning purposes. During this process the release of high levels and harmful volatile solvents to the atmosphere, and the impossibility of an effective recovery and recycling step, are the major drawbacks associated to the electrospinning process.

Electrospinning is a very versatile method for obtaining cellulose fibers with dimensions in the order of micro and nanometers. Electrospun fibers have great potential in several applications, such as in membranes, biosensors, electronic and optical devices, as well as in catalytic and enzymatic supports [8]. At the industrial level, the supreme areas regarding the application of electrospun fibers are in the textile, pharmaceutical and packaging areas. There are already few studies concerning the electrospinning of cellulose fibers using ILs [6, 9-10]. Nevertheless, those studies used an extremely viscous IL (requiring high temperatures and thus an high energy consumption) or a mixture between an IL and DMSO (still not a complete benign process) [6, 9]. Attempts to use pure ILs, with low melting temperatures, as main solvents of cellulose for electrospinning were not previously described in literature.

Understanding the molecular mechanisms that dominate the solvation of cellulose is essential for a correct choice of ILs solvents. Therefore, the capacity of ILs to dissolve carbohydrates and cellulose samples was also studied, aiming at providing novel insights into the mechanisms of biomass solvation. Besides the fact that carbohydrates are the simplest units of polysaccharides, allowing thus a deeper characterization, at the molecular level, of the interactions taking place in polysaccharides, they also play important roles in many biological processes, such as biological recognition and metabolic pathways. Monosaccharides and disaccharides are also vital components in the pharmaceutical and food industries. Most carbohydrates are soluble in protic solvents, such as water. However, their high number of hydroxyl groups hinders their dissolution in most common organic aprotic solvents, limiting thus some applications that require the use of aprotic solvents. The few organic and aprotic solvents that can effectively dissolve glucose, a simple and neutral monosaccharide, are pyridine, dimethylsulfoxide, and dimethylformamide [11]. Nevertheless, most of the enzymes used in carbohydrate chemistry can be inactivated in those

molecular solvents. Therefore, the study of ILs as key solvents for saccharides also play a significant task towards the improvement of carbohydrates dissolution in aprotic solvents [12].

1.2 Ionic Liquids

An ionic liquid (IL) is, by definition, a salt with a melting point below the boiling point of water [13]. Contrarily to common inorganic salts, ILs are liquid at low temperatures (even at room temperature depending on the IL chemical structure) due to the large size and conformational flexibility of their ions, which lead to small lattice enthalpies and large entropy changes upon melting [12]. The liquid state in ILs is thus thermodynamically favorable.

The ionic nature of ILs results in a unique combination of chemical/physical properties, such as high thermal stability, large liquid temperature range, high ionic conductivity, negligible vapor pressure, non-flammability and a high solvating capacity for the most diverse class of compounds [14]. Some of these characteristics contribute for their classification as "green" solvents. The substitution of organic solvents by ILs can provide significant environmental benefits, due to their low volatility at atmospheric conditions and their recycling possibility, reducing thus solvent losses to atmosphere. Therefore, it is expected that ILs may actually find multiple technological applications in the near future. Many academic and industrial studies have been carried out in the last decade to develop and increase the available information and knowledge about these new solvents [15-17]. Currently, ILs are being applied in organic synthesis, catalysis, and separation processes, including chromatography [18]. Several approaches in the past few years showed that ILs are highly effective in the recovery of acetone, antibiotics, ethanol and butanol from fermentation broths, and also in the removal of organic contaminants from aqueous waste streams [19]. More recently, there has been an increasing research on the use of ILs for the solubilization of (bio)macromolecules. These molecules range from polysaccharides (such as cellulose, chitin, amylose and pectin), to proteins (bovine serum albumine, collagen, and elastin, among others), to enzymes and nucleic acids [12, 20-22].

There is a massive number of cations and anions that can be used to synthesize ILs [23]. Based on their anion, ILs could be divided in four main groups [24]: (*i*) ILs based on $AlCl_3$ and organic salts combined with halogens, like 1-butyl-3-methylimidazolium chloride; (*ii*) ILs based on fluorinated anions like $[PF_6]^-$, $[BF_4]^-$, and $[SbF_6]^-$; (*iii*) more complex organic and fluorinated anions like $[CF_3SO_3]^-$ and $[NTf_2]^-$; and (*iv*) ILs based on alkylsulfates and alkylsulfonates anions [24]. The first group represents ILs with Lewis acid properties. This group of ILs is extremely hygroscopic, so its handling requires a dry atmosphere. The second group of ILs has the main disadvantage of being unstable, exothermically reacting with strong Lewis acids, as with $AlCl_3$, and suffering hydrolysis in the presence of water [24-25]. The third group of ILs is far more stable and can safely participate in a broad range of reactions. Moreover, these ILs are generally characterized by low melting points, low viscosity and high conductivity [24]. The fourth and last group does not contain

fluorine atoms, so the respective ILs can be easily prepared by reactions with organic bases of alkylsulfates and alkylsulfonates [24].

On the other hand, regarding the IL cation, there are several known families, such as imidazolium-, pyridinium-, pyrrolidinium-, piperidinium-, ammonium- and phosphonium–based ILs. Besides the phosphonium-based ILs all the remaining families are nitrogen-based ILs. Typical examples of ILs cations and anions are presented in Table 1 and Table 2, respectively.

Table 1 Common IL cations

Name	Abbreviation	Chemical Structure
1,3-dimethylimidazolium; R=CH_3	$[C_1mim]^+$	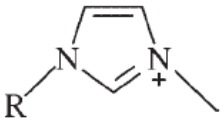
1-ethyl-3-methylimidazolium; R=C_2H_5	$[C_2mim]^+$	
1-butyl-3-methylimidazolium; R=C_4H_9	$[C_4mim]^+$	
1-pentyl-3-methylimidazolium; R=C_5H_{11}	$[C_5mim]^+$	
1-hexyl-3-methylimidazolium; R=C_6H_{13}	$[C_6mim]^+$	
1-decyl-3-methylimidazolium; R=$C_{10}H_{21}$	$[C_{10}mim]^+$	
1-butyl-3-methylpyridinium; R=C_4H_9	$[C_4mpy]^+$	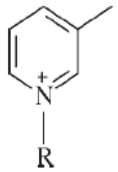
1-hexyl-3-methylpyridinium; R=C_5H_{11}	$[C_6mpy]^+$	
1-butyl-1-methylpyrrolidinium	$[C_4mpyr]^+$	
trihexyltetradecylphosphonium	$[P_{66614}]^+$	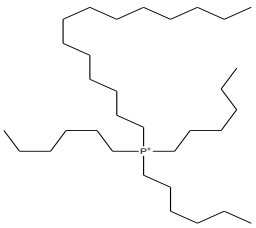

Table 2 Common IL anions

Name	Abbreviation	Chemical Structure
tetrafluoroborate	$[BF_4]^-$	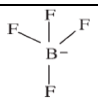
hexafluorophosphate	$[PF_6]^-$	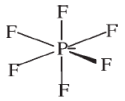
bis(trifluoromethylsulfonyl)imide	$[NTf_2]^-$	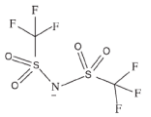
methylsulphate	$[CH_3SO_4]^-$	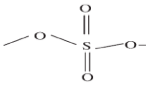
acetate	$[CH_3CO_2]^-$	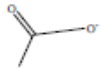
dicyanamide	$[N(CN)_2]^-$	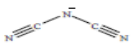
dimethylphosphate	$[DMP]^-$	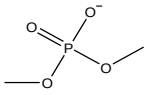
chloride	Cl^-	Cl^-
trifluoromethanesulfonate	$[CF_3SO_3]^-$	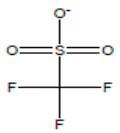

Among the possible ILs that can be synthesized, the *N*,*N*-dialkylimidazolium salts are probably the most investigated ILs [24]. Besides the nature of the IL cation and anion, ILs can additionally present specific functional groups. It was shown that ethers and hydroxyl groups in the imidazolium cation improve the solubility of inorganic salts [24]. Moroever, ILs with ester groups at the side chain of the imidazolium cation are more biodegradable and less toxic than their non-substituted counterparts [16, 26-27].

The chemical and physical properties of ILs are extremely important as they allocate the selection of these fluids for their most diverse applications. These properties depend on the nature and size of their anions and cations [28].

Salts with low-symmetry cations, like $[C_4mim]^+$, possess lower melting temperatures than analogous salts with higher symmetry. The cation side alkyl chain length also affects the melting point of ILs, albeit not following a monotonically pattern [29]. An increasing number of carbon atoms ($n < 7$) in the cation alkyl side chain decrease the melting temperature due to the lower

symmetry of the cation. For $n > 7$, the melting point increases because van der Waals interactions between the longer alkyl side chains become dominant outweighing the symmetry effect [29].

The presence or absence of strong hydrogen bonds also influences the melting temperature of ILs. Conventionally, the C-H$\cdots X$ (X = Cl^-, Br^-) interactions are characterized as being relatively weak interactions, but they become very strong in imidazolium-based halide ILs and may even possess some covalent character. These strong hydrogen bonds involving the imidazolium ring protons results in a three-dimensional ion-network with aromatic π-stacking interactions between the imidazolium cores [29].

The stability of ILs is crucial for their performance [23]. Most ILs have relatively high thermal stability. Their decomposition temperatures are usually above 573 K, and appear to be more dependent on the cation than on the anion, and decrease as the hydrophilicity of the anion increases [24]. The low melting temperature together with the high thermal stability of ILs define the large range of temperatures where it is possible to use ILs as main solvents in the diverse areas [24].

Density is also an important physical property with practical implications [30]. Most imidazolium-based ILs are denser than water. For instance, for 1-alkyl-3-methylimidazolium-based ILs density decreases with the increase of the side alkyl chain length [13].

Most ILs present viscosities comparable to common oils. This characteristic is a major disadvantage for the use of ILs as solvents, due to their negative effect through mass transfer processes and power requirements [13, 24]. Nevertheless, this property can be easily manipulated by changing the IL cation and anion nature composing the IL. Viscosity values at 293.15 K range from 430 mPa·s for $[C_4mim][PF_6]$ [13] to 154 mPa·s for $[C_4mim][BF_4]$ [31]. However, there are ILs with even lower viscosities such as $[C_2mim][CH_3CO_2]$ (10 mPa.s at 253.15 K) [32], $[C_2mim][N(CN)_2]$ (21 mPa.s at 298 K) [33], or $[C_4mim][N(CN)_2]$ (31 mPa.s at 298 K) [34]. Moreover, it was previously shown that the viscosity of ILs is very dependent on impurities [31]. The presence of water decreases the viscosity while the presence of chloride as main contaminant has the opposite effect [29]. The presence of co-solvents in ILs may decrease the viscosity because the aggregation of the ions in the liquid decreases. Experimental results indicate that the nature of the co-solvent plays a more important role than its effective amount [29]. In neat ILs, the branching of the alkyl chain in 1-alkyl-3-methylimidazolium salts reduces the viscosity, as it reduces intermolecular dipole-dipole interactions. The same reason accounts for the relatively low viscosity of most fluorinated anions [24]. The viscosity of fluorinated-based ILs with a fixed cation decreases in the following anion order: $[PF_6]^- > [BF_4]^- > [CF_3SO_3]^- > [CF_3CO_2]^- > [NTf_2]^-$ [29].

Fewer data has been published on the surface tension of ILs, although this property is quite important in multiphase processes. In general, the liquid/air surface tension values are higher than those observed with organic solvents, and usually range between (33 and 57) $mN \cdot m^{-1}$ [24]. Surface tensions of ILs usually decrease with the increasing size of both the IL cation and anion [14, 35-36].

There are some studies related with the toxicity of ILs towards some microorganisms. In general a longer alkyl side chain is responsible for higher toxicity levels [37-38]. Some authors also used the ILs lipophilicity to explain those results and concluded that the higher the lipophilicity of the cation the higher the ILs toxicity [39]. Fluorinated and more complex anions, such as $[NTf_2]^-$, also have a strong influence trough the toxicity of ILs [37-38]. However, it should be remarked that the toxicity of ILs can be adjusted by a proper selection of cation/anion combinations. In fact, many ILs display lower toxicity levels than common organic solvents [38]. Adequate ILs can be considered less dangerous to the environment due to their low toxicities and lack of vapor pressure at process conditions.

Polarity can be described as the capacity of a solvent to form intramolecular and intermolecular interactions that do not result in chemical reactions. This information provides an useful indication of general solvent properties suitable for indicating gross similarities and differences between conventional solvents and room temperature ILs [40]. Some authors reported the polarity of several ILs [41-44]; the main trends are that alkylammonium nitrate and thiocyanate ILs have a solvent strength similar to water, while the 1,3-dialkylimmidazolium salts are less polar than water with values near to polar organic solvents (*e.g.*, DMSO at the lower end of the range and short-chain aliphatic alcohols at the higher end) [40]. Moreover, the presence of an additional methyl group at the C-2 position on the imidazole ring in 1,3-dialkylidazolium ILs reduces the polarity of the IL, as would be expected, since the C-2 hydrogen is the most acidic hydrogen at the imidazolium core [40]. As a result, ILs are relatively good solvents for a wide range of organic, inorganic, organometallic components, biomolecules and metal ions, while their solvation ability can be easily manipulated by a proper selection of the cation and anion.

1.2 Cellulose Fibers

Cellulose is the most abundant renewable resource available throughout the world. Its production approaches 1.5×10^{12} tons *per* year [22]. Cellulose is the major component of cell walls of plant fibers representing, in the case of wood, 40-50 % of its dry weight [45].

Industrially, cellulose is isolated mainly from plant sources, such as wood, where it is embedded in a matrix of lignin and other polysaccharides (hemicelluloses) by accomplishing numerous chemical processes of separation and purification. The most pure cellulose is isolated from cotton, since it is composed by approximately 99.8 % of the polysaccharide. Cellulose can also be produced extra cellularly by non pathogenic bacteria, such as *Acetobacter xylinum* [46].

Cellulose is a homopolymer, strictly linear, with high molecular weight, and composed by repetitive units of β-D-glucopyranose which are linked by glycosidic β $(1 \rightarrow 4)$ bonds [45, 47-48]. The molecular formula of cellulose is $(C_6H_{10}O_5)_n$, where n is the number of carbohydrate units that are repeated or the degree of polymerization (DP) [49]. The degree of polymerization in native cellulose ranges between 10 000 and 15 000 units [50]. The basic structural unit which repeats itself is called cellobiose and consists of two molecules of glucose [51]. In Figure 2 it is shown the schematic representation of the partial structure of cellulose and its conformational configuration. Generally, in the cellulose chain, the basic units take the $^4C_1$ chair conformation. In this type of structure, the -OH and $-CH_2OH$ groups, and the glycosidic bonds, assume equatorial positions while the hydrogen atoms occupy the axial positions.

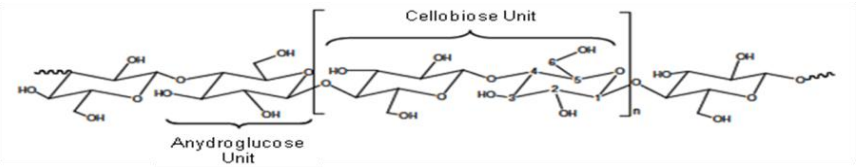

Figure 2 Partial structure of cellulose with the chair conformational configuration [52]

When the hydroxyl groups (-OH) are at the equatorial position, a type of conformation adopted by the glucopyranoside ring, there is the formation of a hydrophilic local position parallel to the plane of ring, conferring thus hydrophilic properties to cellulose. Moreover, the -OH groups that are connected in axial position to another glucopyranoside ring create a hydrophobic local position perpendicular to the plane of the ring [46].

Along the chains of cellulose there are three free hydroxyl groups *per* anhydroglucose unit in the positions C_2, C_3 and C_6 (Figure 2). These groups act as active sites that can interact with each other through the formation of links by hydrogen bonds. These links can be

intramolecular, occurring between the hydroxyl groups of the same molecule, or intermolecular, between hydroxyl groups of different chains of cellulose [46]. By conducting spectroscopic analysis it was demonstrated that the intramolecular hydrogen bonds occur between the hydroxyl group of C_3 of a AGU (anhydrous glucose unit) and the oxygen of the glucopyranoside ring adjacent chain, and between the hydroxyl group of C_6 and the hydroxyl group of C_2 of a neighbor unit of glucose [53].

The organization of the elementary fibrils results from the hydrogen bonding interactions between the cellulose chains, forming crystalline areas which alternate with amorphous zones. The elementary fibrils aggregate to form microfibrils and macrofibrils that in turn bind and form cellulose fibers [46, 54]. Figure 3 presents the organization of cellulose in plants cell walls.

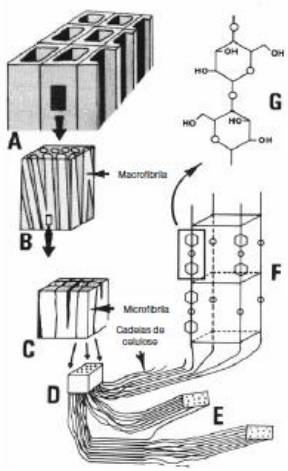

Figure 3 Scheme of cellulose chains organization in plants. A - Fibers; B - Fraction of the fiber wall, consisting of macrofibrils (clear zones) and non-cellulosic components (dark areas); C - Microfibrils; D - Elemental Fibrils; E - Chains of cellulose, crystalline regions alternating with amorphous zones; F - Unit cells of crystalline cellulose; G - Cellobiose unit [45]

Due to its fibrous structure, resulting from strong inter- and intramolecular hydrogen links, cellulose has a high mechanical strength and it is insoluble in water and most common solvents. Since the ordering of the macromolecules in cellulose fibers is not uniform throughout its structure, its reactivity depends on the accessibility factor. Cellulose fibers display crystalline areas which are responsible for the stiffness, density and resistance to traction, and amorphous areas with greater disorder and where the hydroxyl groups are more accessible, and thus reactions are easier to accomplish. Moreover, cellulose can undergo processes of inter and intrafibrilar swelling which lead to an increase in weight and volume of the material [46, 55].

The cellulose crystalline structure can be identified by X-ray diffraction analysis or through the absorption of polarized infrared radiation. The crystalline structure of native cellulose (Cellulose I) is shown in Figure 4. This structure can be described as a unit cell containing four residues of

glucose [46, 54]. It should be remarked that the degree of cellulose crystallinity varies with its origin and pretreatment issues.

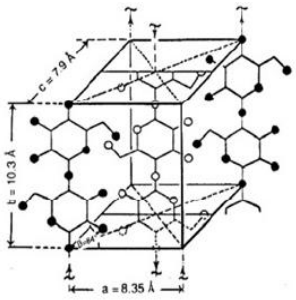

Figure 4 Representation of a unit cell of native cellulose (Cellulose I) [46]

The orientation of cellulose chains in the unit cell is still a subject of discussion. Meyer-Misch suggested an antiparallel orientation, as shown in Figure 4 [45]. However, most authors propose a parallel orientations [45, 50-51].

Due to its macromolecular structure, the cellulose solid state contains both crystalline and amorphous areas. The unit cell of Cellulose I contains two chains of cellulose with parallel orientation, as can be seen in the projection along the *a-c* plane represented in Figure 5. The cellulose chains form crystalline layers in the a-c plane which are linked by hydrogen bonds. However, between these crystal layers in the direction of b, cellulose does not form hydrogen bonds and is only connected by van der Waals dispersive forces [54].

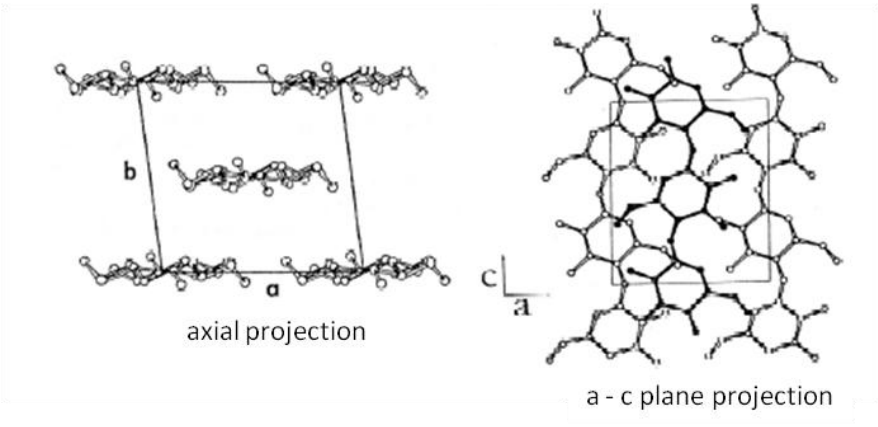

Figure 5 Structure of the unit cell of Cellulose I: axial projection along the a-b plane and projection along the a-c plane [54]

When dissolved in several fluids, regenerated cellulose chains can re-orientate and form other crystalline structure, Cellulose II, which is actually the most stable and presents the highest technical relevance. Depending on temperature, mechanical load, alkalinity and water content, it

is possible to convert Cellulose I into many crystalline forms - "hydrates of cellulose". During the washing and after a drying process Cellulose II is usually attained. Nevertheless, the way by which the chains of cellulose transit from the parallel arrangement to antiparallel orientation, without a dispersion intermediate of cellulose molecules, is yet not fully known [52].

The unit cell of Cellulose II contains two chains of cellulose orientated on an antiparallel way, as shown in the projection along the a-c plane represented in Figure 6 [52].

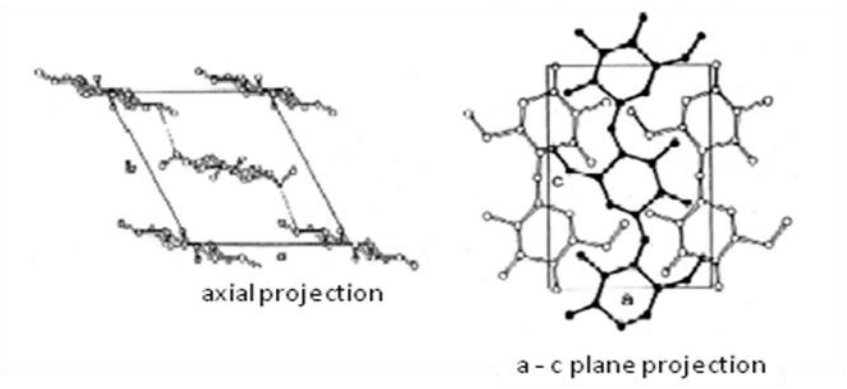

Figure 6 Structure of the unit cell of Cellulose II: axial projection along the a-b plane and projection along the a-c plane [54]

Regenerated cellulose origins an increased amount of links by intermolecular hydrogen bonds compared with the crystalline system of native cellulose. There are additional hydrogen bonds between cellulose chains in the a-c plane forming crystalline layers, and between crystal layers in the direction of b as displayed in Figure 6 [54].

The increased density of hydrogen bonding interaction, makes of regenerated cellulose thermodynamically more stable and that cannot be converted back into Cellulose I [46].

In addition to this two structures (Cellulose I and II), cellulose can also adopt other crystalline forms as Cellulose III and IV, which undergo changes trough the a-c axis [46, 54].

1.3 Carbohydrates

Carbohydrates are common and important organic compounds present in living systems. The lower molecular weight compounds are commonly designated by sugars. Carbohydrates are present in most biomass sources and are a main resource of energy in living systems. Carbohydrates are relatively inexpensive and a renewable feedstock, with many industrial applications in diverse areas, such as in chemistry and biotechnological applications, and in the food, paper, and pharmaceutical industries [56].

They were classified initially as "hydrates of carbon", because, in many cases, their molecular formula corresponds to $C_n(H_2O)_m$ [57]. The basic units of carbohydrates are the monosaccharides such as arabinose, glucose, galactose, xylose, mannose, and fructose, among others. More complex units are disaccharides, such as sucrose, lactose, maltose, lactulose and cellobiose. Monosaccharides when submitted to hydrolysis do not cleave into smaller units, while disaccharides origin two monosaccharides units under hydrolysis. Finally, polysaccharides are the most complex structures and are constituted by several monosaccharides units [57].

Monosaccharides are classified according to their most oxidized functional group, either an aldehyde or ketone group. Aldoses contain a single aldehyde group, while ketoses contain a ketone group. These compounds are thus designated with the prefix aldo- or keto-, while the prefix tri-, tetra-, pent-, and hex- indicate the number of carbon atoms in the monosaccharide [3].

Stereochemistry is a fundamental key for the understanding of the carbohydrates structure. This aspect was originally studied by Emil Fisher that introduced the projection formulas to represent the stereochemistry in chiral molecules [58]. Carbohydrates have chiral centers and Figure 7 presents a main example on this subject with the projections of aldoses containing from three to six carbon atoms [57-58].

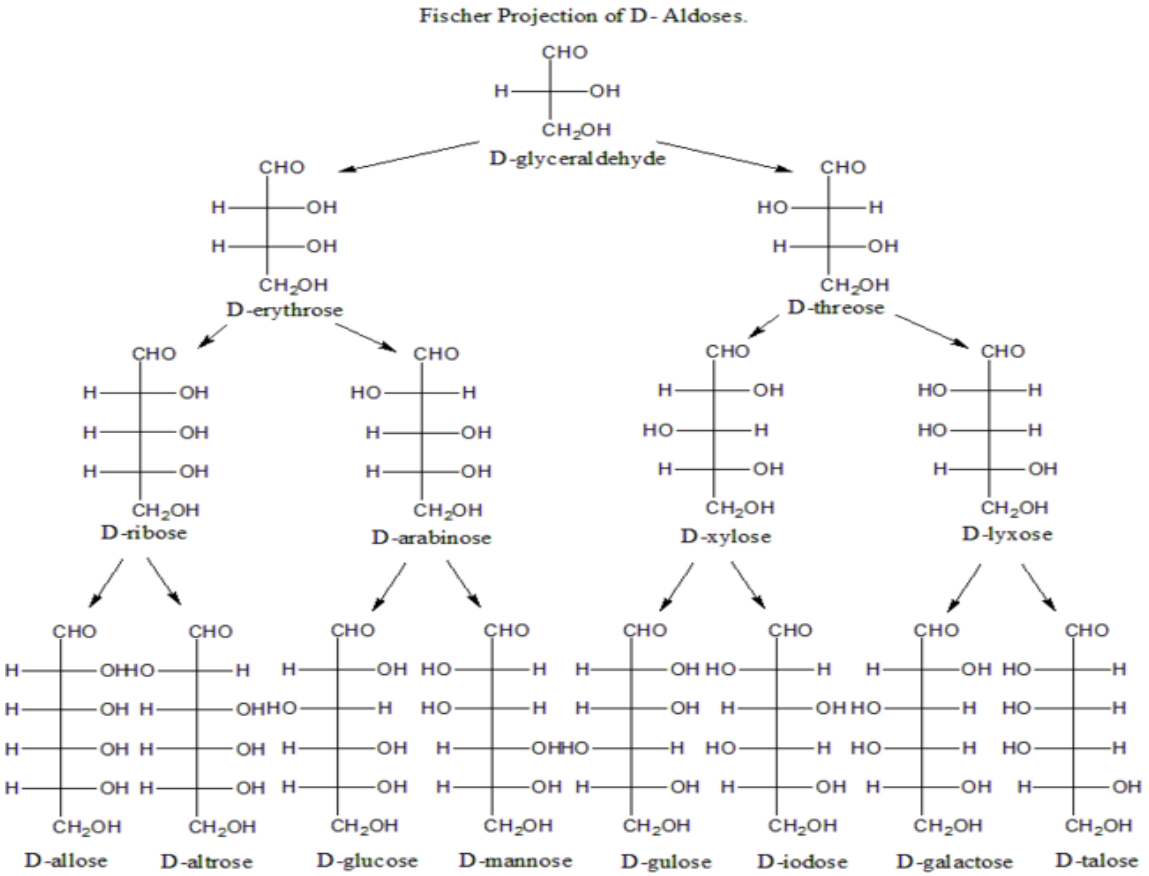

Figure 7 Configuration of aldoses containing from three to six carbon atoms [45]

Considering the projection of a three-dimensional structure of a glyceraldehyde there are two possibilities of rearrangement: (*i*) the hydroxyl group attached to the carbon neighbor of the primary alcohol function is on the right side of the plane (conformation D); (*ii*) the hydroxyl group is on the left of the plane (conformation L). These two forms correspond to the image of each other in a plane mirror, and are a pair of optical isomers (or enantiomers) with identical physical and chemical properties. As the number of carbon atoms increases, the number of asymmetric carbons also increases, and thus, the number of stereoisomers becomes larger.

For a long time the structure of carbohydrates was described by a linear chain, although this is not totally satisfactory, because this kind of structure did not allow the explanation of some of their properties. These inconveniences forced to the re-design of the carbohydrates structures, such as glucose. In 1895, Tollens, Fisher and Tanret, proposed a cyclic structure for this sugar [59]. Over the years, this structure has been adjusted and refined as shown in Figure 8 [59].

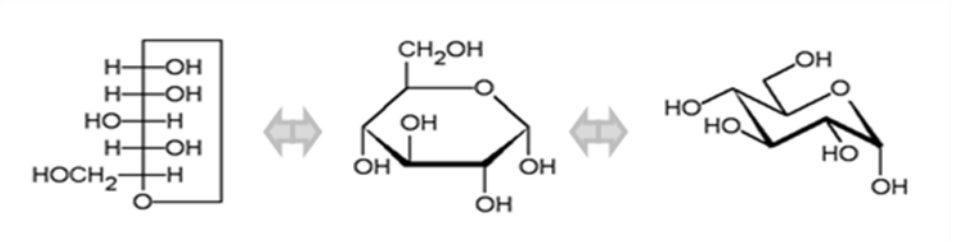

Figure 8 α-D-Glucose structures [57]

Polysaccharides are macromolecules formed by the union of many monosaccharides units by glycosidic bonds. These compounds may possess high molecular weights that further depend on the number of monosaccharides units. Polysaccharides can be hydrolyzed into smaller polysaccharides, as well as in monosaccharides or disaccharides, through the action of certain enzymes or by chemical hydrolysis (usually under acidic conditions). Frequently, these structures are linear, but they may contain various degrees of branching. Polysaccharides are often quite heterogeneous containing slight modifications of the repeating unit [58].

2. Electrospinning of Cellulose with Ionic Liquids

2.1 Introduction

2.1.1 Electrospinning

Electrospinning is one of the simplest and most effective methods for producing polymers micro and nanofibers. Hitherto many synthetic and natural biopolymers have been electrospun into ultra-thin fibers. The process is attractive since it is a cost-effective method of producing nanofibers from a large range of raw materials [60].

The most important applications of electrospun fibers are in fiber-reinforced composites, membranes, biosensors, electronic and optical devices, and enzyme and catalytic supports [21]. The electrospinning technique is even useful in large-scale manufacturing environments, such as in the textile, medical and pharmaceutical industries [9-10]. A variety of novel tissue engineering scaffolds have been prepared by electrospinning synthetic and natural biodegradable polymers [10]. However, the range of polymers that can be electrospun is still limited by the availability of volatile solvents and their limited capability of dissolving polymers [10].

Electrospinning involves the manipulation of the fluid, either in the form of molten polymer or polymer solution. Nevertheless, unlike conventional drawing methods, where there is an external mechanical force that pushes the molten polymer through a mold, electrospinning makes use of an electric potential that is applied to the fluid to provide a stretching force. Figure 9 shows a typical apparatus used in the electrospinning process.

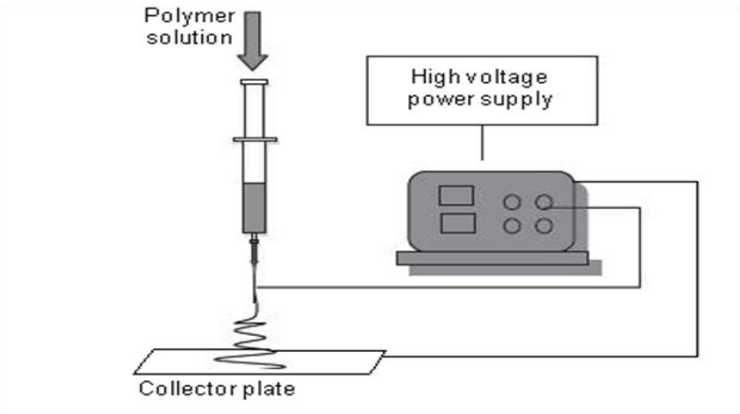

Figure 9 Scheme of electrospinning apparatus [6]

In electrospinning a high voltage is applied to a polymer solution and charges are induced within the fluid. A grounded conductive collector allows the voltage difference between the two electrically charged ends. When charges within the fluid reach a critical value (electrostatic repulsion within the droplet exceeds the liquid surface tension), a fluid jet erupts from the droplet

at the tip of the needle resulting in the formation of a Taylor cone (to minimize the droplets' surface area). After a certain threshold voltage is reached, the electrospinning jet travels towards the region of lower potential - the grounded collector. There are many parameters that influence the morphology of the resultant electrospun fibers, that may range from beaded or smooth fibers to fibers with pores on its surface [61].

The parameters that affect electrospinning are the polymer solution parameters, processing conditions and ambient conditions. By controlling these parameters, it is possible to come out with setups to yield fibrous structures of various forms and arrangements [61].

2.1.1.1 Polymer Solution Parameters

The polymer solution physical properties have the most significant influence in the electrospinning process and in the resultant fibers morphology. The polymer-solvent system plays an important role on the electrospinnability and final characteristics of the electrospun fibers. For a given polymer solvents system, surface tension has an important role in the formation of beads along the fiber length, while the viscosity of the solution, and its electrical properties, determine the extent of elongation of the solution in order to form fibers, thus affecting the diameter of the resultant electrospun fibers [61].

Polymer Molecular Weight and Solution Viscosity

The polymer molecular weight is a major factor that affects the viscosity of the solution to be electrospun. A polymer with high molecular weight dissolved in a specific solvent presents higher viscosity than a lower molecular weight polymer. For electrospinning to occurs the solution must present an adequate viscosity value, and for that purpose, both the molecular weight of the polymer and of the solvent must be in an adequate range [61].

One way of improving or decreasing viscosity is by changing the concentration of polymer in the overall solution. Increasing the polymer concentration results in greater polymer chain entanglements within the solution originating a continuous jet during electrospinning [61].

However, when the polymer solution has a high viscosity it is difficult to pump the solution through the syringe needle [62]. Furthermore, with high viscosity solutions, the solution may dry at the tip of the needle before the charge is applied and therefore making the electrospinning process highly difficult to be accomplished [63]. Moreover, an increase in viscosity usually leads to an increase in the fibers diameter [61].

Surface Tension

The electrospinning process only occurs if the charged solution overcomes the surface tension barrier. Surface tension has the effect of decreasing the surface area *per* unit mass of a fluid. For high concentrations of free solvent molecules there is a greater tendency for these molecules to aggregate and to take a spherical shape due to the surface tension differences. A higher surface tension/viscosity means that the interaction between the solvent and polymer molecules are more significant, and thus, when the solution is stretched under the influence of an applied charge, the solvent molecules will tend to spread over the entangled polymer molecules [61]. This phenomenon could be controlled by choosing a proper solvent with low surface tension. Another way to reduce the surface tension is by adding surfactants or amphiphilic molecules (cationic, anionic or nonionic) to the polymer/solvent mixture, improving thus the fiber morphology and size [64].

Solution Conductivity

During the electrospinning process there is the stretching of the solution caused by the repulsion of the charges at its surface. Therefore, if the conductivity of the solution is increased, more charges can be carried out by the electrospinning jet. The conductivity of the solution can be increased by the addition of ions. With the addition of polyelectrolytes the charges are increased and the solution stretch will increase. Thus, smooth fibers with small diameter are formed while preventing beaded fibers [63].
In some cases, the addition of salts may cause an increase in the viscosity of the solution. Thus, although the conductivity of the solution is improved, the viscoelastic force is stronger than the columbic forces resulting in increased fiber diameters [65].

Dielectric Constant

The dielectric constant of a solvent has great importance in the electrospinning process. Generally, a solution with a high dielectric constant reduces the beads formation and the diameter of the resultant electrospun fibers [61]. The bending instability of the electrospinning jet also increases with higher dielectric constants.

2.1.1.2 Processing Conditions

The conditions under which electrospinning occurs are very important as they affect the morphology and size of the obtained fibers. Parameters such as applied voltage, feed rate, solution

temperature, type of collector, needle diameter and distance between the tip of the needle and the collector are very important to control the characteristics of the obtained fibrous materials and to understand all the electrospinning results.

Voltage

The electrospinning only takes place if a high voltage is applied to the solution. Commonly, both high negative or positive voltages of more than 6 kV are able to cause the solution drop at the tip of the needle to turns into the shape of a Taylor cone during jet initiation. Depending on the feed rate of the solution, a higher voltage may be required so that the Taylor cone is stable. The columbic repulsive forces in the jet will then stretch the solution [61]. When the voltage is high, the large quantity of charges will accelerate the jet and more volume of solution will be drawn from the tip of the needle. This may results in a smaller and less stable Taylor Cone [63].

The flight time of the electrospinning jet is another feature that may influence the diameter of the fibers. A longer flight time allows more time for the fibers to stretch and elongate before being deposited on the collector. Consequently, at a lower voltage, the reduced acceleration of the jet and the weaker electric field may increase the flight time of the jet which generates smaller fibers [66].

High voltages result not only in different physical appearance of the fibers but also affect their crystallinity. The electrostatic field forces the polymer molecules to be more ordered during electrospinning, resulting in fibers with higher degree of crystallinity. Nevertheless, above a certain crucial voltage, the crystallinity of the fibers tends to be reduced [66].

Feed Rate

The feed rate will determine the amount of solution available for electrospinning *per* time. For a given voltage, there is an optimum feed rate if a stable Taylor cone is to be maintained. Usually an increase in the feed rate leads to higher fiber diameters or beads size [63].

Temperature

The increase on temperature increases the evaporation rate of the solvent, for a volatile solvent, and minimizes the viscosity of the polymer solution. With a lower viscosity, the columbic forces are able to exert a greater stretching force on the solution forming fibers of smaller diameter. Higher temperatures may increase polymer molecules mobility allowing the columbic forces to stretch the solution [61], decreasing the surface tension and viscosity and increase the conductivity

of the solution. Lower concentrations of polymer promote the decrease of the solution viscosity, but concentrations below 3 wt % of polymer could not allow the fiber formation due to the lower chain entanglement density [21].

Effect of Collector

There must be an electric field between the source and the collector, thus, the collector is made out of conductive material, such as aluminum foil that originates a stable potential difference between the source and the collector.

When a nonconducting material is used as the collector, charges on the electrospinning jet will quickly accumulate further resulting in fewer deposited fibers [67-68]. Fibers collected on a non-conducting material have a lower packing density compared to those collected on a conducting surface. This is caused by the repulsive forces of the accumulated charges on the collector as more fibers are deposited. With a conducting collector, charges on the fibers are dissipated, allowing more fibers to be attracted to the collector [67-68].

According to the desired fiber morphology and diameter, there are many types of collectors such as aluminum foil, rotating wire drum [6] or baths with molecular liquids (water or ethanol) [10]. When the electrospinning is made with solutions of a polymer in a non volatile system, such as, cellulose in ionic liquid, the collection of fibers could be made in a water or ethanol coagulation bath [9]. Ethanol is more efficient than water removing the ILs from cellulose fibers, but it has the disadvantage that it is highly flammable and can ignite easily. Water/ethanol mixtures can reduce the fire risk significantly, while improving the kinetics of RTIL removal from the fibers [21]

Diameter of the Needle

The internal diameter of the needle has a certain effect on the electrospinning process. A smaller diameter was found to reduce the clogging, as well as the amount of beads on the electrospun fibers [61]. The smaller diameter of needles could also reduce the diameter of the electrospun fibers.

When the size of the droplet at the tip of the needle is decreased, the surface tension of the droplet increases. For the same voltage supplied, a greater columbic force is required to cause jet initiation. As a result, the acceleration of the jet decreases and this allows more time for the solution to be stretched and elongated before being collected. However, if the diameter of the orifice is too small, it may not be possible to extrude a droplet of solution to be electrospun [66].

Distance between the Tip of the Needle and the Collector

The flight time, as well as the electric field strength, affects the electrospinning process and the resultant fibers. Changing the distance between the tip of the needle and the collector has a direct influence in both the flight time and in the electric field strength. When the distance between the tip and the collector is reduced, the jet travels a smaller distance before reaching the collector. Nevertheless, when the distance is too small, an excess of solvent may cause the fibers to merge resulting in inter and intra layer bonding as shown in Figure 10. These interconnected fibers mesh may provide additional strength to the resultant structure [69], but they would greatly reduce the porosity of the electrospun mat.

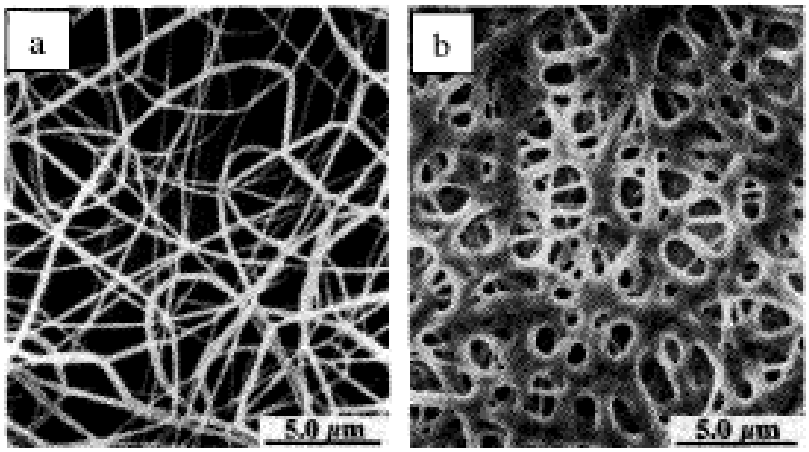

Figure 10 Nylon 6.6 fibers at (a) 2.00 cm deposition distance and (b) 0.50 cm deposition distance [69]

2.1.1.3 Ambient Parameters

The surrounding conditions where the electrospinning occurs are also important regarding the resulting fibers morphology. Parameters, such as humidity, could form pores on the surface of the fibers, and other factors, like atmosphere composition and pressure, may cause secondary effects on the fibers morphology [61]. The environmental conditions are a poorly studied field but it is well accepted that changes in the environment will affect the electrospun resultant fibers.

Humidity

At high humidity levels, water condensates on the surface of the fibers. As a result, this may have a strong influence on the fibers morphology, especially for polymers dissolved in volatile solvents

and when the solution has an hygroscopic polymer [61, 66]. On the other hand, it has been suggested that a high humidity level can help in the discharge of the electrospun fibers [61]. However, more research has to be done in this area to determine the effect of humidity on the electrical discharge during electrospinning and on the accumulation of residual charges on the collected fibers [61].

Type of Atmosphere

In the presence of some gases such as helium, the electrospinning is not possible to occurs, due to the helium behavior under high electrostatic field. On the other hand, when a gas with higher breakdown voltage is used, the fibers obtained have twice the diameter of those electrospun in air [61].

Pressure

Usually a reduction in the pressure surrounding the electrospinning jet does not improves the electrospinning process. With a pressure below atmospheric pressure, the polymer solution in the syringe tends to flow out of the needle causing unstable jet initiation. At sufficiently low pressures, electrospinning is indeed not possible due to the direct discharge of the electrical charges [61].

2.1.2.4 Cellulose dissolution in ionic liquids

In recent years there has been a growing interest in ILs applications thorough various fields [20]. ILs have already shown to effectively dissolve complex macromolecules and polymeric materials [9-10, 20-22, 29, 56, 70-81].

Cellulose, which is one of the most abundant renewable resources, and the main component of lignocellulosic materials, can be effectively dissolved in some ILs. The first case of dissolution of cellulose was reported in 1934, when Graenacher found that *N*-ethylpyridinium chloride was capable of its dissolution [22, 79]. Nowadays there is a wide range of ILs proficient for dissolving cellulose. Recently, it was found that cellulose could be dissolved in some hydrophilic ILs, such as 1-butyl-3-methylimidazolium chloride, $[C_4mim]Cl$[79], and 1-allyl-3-methylimidazolium chloride, [amim]Cl[82]. Solutions containing up to about 25 wt % of cellulose were prepared with $[C_4mim]Cl$ at 373.15 K using microwave heating while subsequent addition of water, ethanol or acetone allowed the easy precipitation of the polymer [79]. Moreover, it was shown that ILs based on dicyanamide, formate and acetate anions can dissolve up to 10-20 wt % of cellulose at lower temperatures [71]. These ILs anions form strong hydrogen bonds with the polymer to achieve the dissolution [71]. Solutions containing 12-39 wt % of cellulose at 278.15 K and 4-12 wt % at 353.15 K can be prepared with other types of ILs, such as 3-methyl-*N*-butylpyridinium chloride and 1-allyl-2,3-dimethylimidazolium bromide [72, 77], respectivelly.

In a recent study concerning a large range of IL anions, $[CH_3CO_2]$-based ILs have been reported as main solvent for cellulose [32, 79, 83]. For instance, microcrystalline cellulose can be dissolved up to 11.5 wt at 303.15 K [84]. Another evidence of the improved performance of $[C_2mim][CH_3CO_2]$ to dissolve lignocellulosic materials was presented be Sun et al. [32], showing that this IL is a better solvent for wood than $[C_4mim]Cl$. At the same conditions, $[C_2mim][CH_3CO_2]$ dissolved 93.5 % of wood powder while $[C_4mim]Cl$ dissolved only 26.0 % [32]. Moreover, $[C_2mim][CH_3CO_2]$ could be considered an interesting IL for cellulose dissolutions purposes since it is liquid at room temperature, presents a low viscosity, and it is a non-corrosive and biodegradable IL [71].

Aiming at obtaining nanometer- and micrometer-sized cellulose fibers for industrial and practical applications, electrospinning is a simple and versatile method. Nevertheless, typical organic and volatile solvents for cellulose dissolution are far from the green status, and new efforts already appeared in literature making use of ILs [6, 79]. Dissolving cellulose in IL results in a polymer solution which can be in fact electrospun. Xu et al. [6], showed that it was possible to perform cellulose electrospinning using 1-allyl-3-methylimidazolium chloride as solvent. Nevertheless, this IL is solid at room temperature, and thus it was introduced a co-solvent, dimethylsulfoxide (DMSO), which significantly decreased the surface tension and viscosity of the overall solution. Cellulose/[amim]Cl solutions with concentrations of cellulose in the order of 1 wt %, 3 wt % and

5 wt % were prepared in mass ratios of cellulose / [amim]Cl mixture solutions of 1:0, 1:1, 1:2, 1:4 and 1:8 to DMSO [6]. The authors additionally shown that the regenerated electrospun cellulose fibers had rather low crystalline degree compared with the initial dissolved cellulose [6, 85]. The fibers morphology was mainly determined by the method used to collect and solidify the cellulose [21]. This trend was also observed by other groups using common solvents for cellulose electrospinning [86-87]..

In an additional study regarding the electrospinning of cellulose from pure ILs both cellulose and cellulose-heparin composite fibers were obtained using 10 wt % of cellulose in [C_4mim]Cl and an applied voltage of 15-20 kV [10]. These authors found that heparin stays intact and bioactive after the electrospinning high voltage submission [10]. In addition, cellulose fibers showed a smooth surface, while the cellulose-heparin composite fibers showed a rough surface [10]. Nonetheless, this work made use of an extremely viscous and solid IL at room temperature [10]. Those properties are highly unfavorable to the electrospinning process requiring high energy consumptions because the dissolutipn was done at 343 K [10].

Electrospinning from ionic liquids polymeric solutions represents an interesting approach minimizing volatile emissions compared to typical solvents employed. Those non-volatile solvents remain in the fibers after electrospinning and can be removed by appropriate wash steps with solvents capable of dissolving the ILs employed allowing thus their further recovery.

In this study, the main goal is to produce micro- and nanoscale fibers from cellulose/IL solutions by an electrospinning process using the IL 1-ethyl-3-methylimidazolium acetate, [C_2mim][CH_3CO_2]. Attempts were carried out aiming at selecting a low viscous ionic liquid at room temperature with a high ability to dissolve cellulose. Such properties allow the use of the pure IL without requiring organic co-solvents addition or high temperature operating conditions. Parameters such as the cellulose type, cellulose concentration, dissolution time, and the addition of others ILs that could perform as surfactants, were evaluated along the morphology, diameter and crystallinity of the cellulose fibers obtained.

2.2 Experimental Section

2.2.1 Materials

Cellulose fibers, long fibers (CAS 9004-34-6), and microcrystalline cellulose, powder (CAS 9004-34-6), were acquired from Sigma Aldrich. The ILs used were $[C_2mim][CH_3CO_2]$ (> 95 wt % pure), $[C_{10}mim]Cl$ (> 98 wt % pure), $[C_4mim][BF_4]$ (> 99 wt % pure), $[C_4mim][NTf_2]$ (> 99 wt % pure), $[C_8mim][BF_4]$ (> 99 wt % pure), $[C_8mim][PF_6]$ (> 99 wt % pure) and $[C_8mim][NTf_2]$ (> 99 wt % pure). All ILs were purchased from IoLiTec. The solvent used on the coulometric Karl Fischer titration was Hydranal-Coulomat AG from Riedel de Haën.

Cellulose fibers were dried in an air oven at 378 K for at least 12 h before use. ILs samples were dried under vacuum, at constant stirring, and at 333 K for a minimum of 48 h, in order to reduce the water content and volatile compounds to negligible values. After that procedure, the ILs purity was further checked by ^{1}H and ^{13}C NMR spectroscopy.

2.2.2 Methods

Water contents of both individual cellulose samples and ILs were determined using a Metrohm 831 Karl-Fischer (KF) coulometer.

Cellulose/IL solutions for electrospinning purposes were prepared gravimetrically ($\pm 10^{-4}$ g). Cellulose/IL mixtures were homogenized under constant stirring in sealed glass vials at room temperature. In order to evaluate the progress of cellulose dissolution in ILs, periodical samples of the mixture were taken, and analyzed through optical polarized microscopy making use of an Olympus BX51 microscope.

Surface tensions and viscosities of pure ILs and ILs mixtures were determined at room temperature using a Dataphysics contact angle system OCA-20 (Figure 11) and a controlled stress rheometer AR 1000 (TA instruments) cone and plate geometry (4 cm diameter, 2º), respectively. Ionic liquids mixtures were prepared gravimetrically within $\pm 10^{-4}$ g. Surface tensions for mixtures of two ILs, $[C_2mim][CH_3CO_2]/[C_{10}mim]Cl$, were determined at (298 ± 1) K. The mole fraction composition of $[C_2mim][CH_3CO_2]$ ranged between 1.00 and 0.30**.**

Figure 11 Dataphysics contact angle system OCA-20

In order to validate the equipment and methodology used, the surface tensions of $[C_4mim][BF_4]$, $[C_4mim][NTf_2]$, $[C_8mim][BF_4]$, $[C_8mim][PF_6]$ and $[C_8mim][NTf_2]$ were also determined at (298 ± 1) K showing a good agreement with literature values [14, 35] (see Appendix A). It should be remarked that the surface tension of molecular solvents such as ultra-pure water was also determined, showing a relative deviation to literature within - 0.6 % [14].

Measurements of ILs density to correct surface tension values were performed using an automated SVM 3000 Anton Paar rotational Stabinger viscometer-densimeter at 298.15 K. Further details regarding the operation system can be found elsewhere [34]. The uncertainty in temperature is within 0.02 K and the absolute uncertainty in density is $\pm 5 \times 10^{-4}$ g·cm^{-3}.

The electrospinning equipment used in the study is an lab-made apparatus and it is composed by the following components (Figure 12): Syringe bomb Harvard Apparatus PHD 2000, with support for two syringes and infuse rate control between 10^{-7} cm^3/min and 220.82 cm^3/min; and an high voltage source Spellman CZE1000R, with a potential difference between 0 and 30 kV and continues electric current between 0 and 300 μA. Each cellulose/IL mixture aiming the electrospinning process was placed into a 10 cm^3 syringe with a capillary tip with an inner diameter of 1 mm. The syringe bomb at the equipment allowed the solution fed through the needle. The applied voltage was fixed at 20 kV, the feed rate of the syringe bomb was set to 0.002 cm^3/min and the tip-to-collector distance was fixed at 12 cm after minor optimizations tests where the Taylor cone was macroscopically evaluated. A water bath with a copper electrode was used as the grounded conductive collector. The water allowed the removal of $[C_2mim][CH_3CO_2]$ from the fibers since this IL is completely miscible with water at room temperature. The temperature of the electrospinning process was kept at ≈ 298 K.

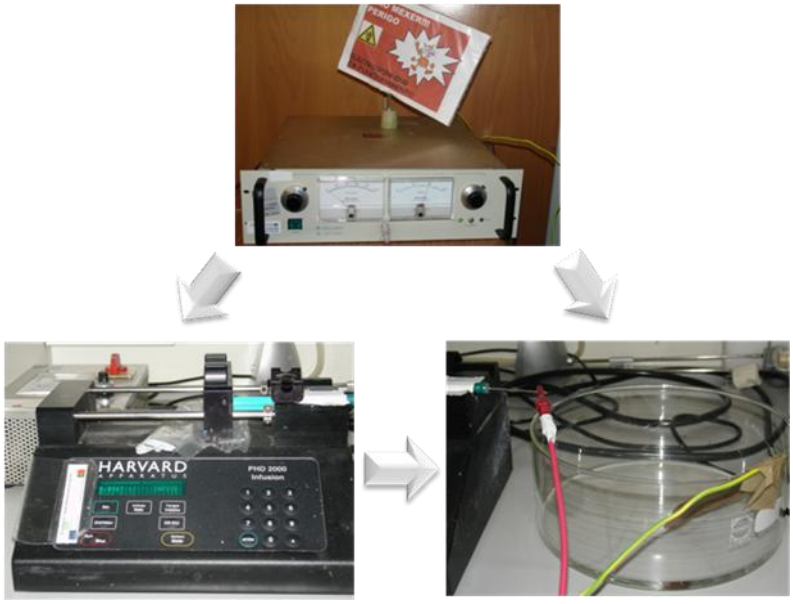

Figure 12 Electrospinning equipment

After the electrospinning process, cellulose fibers were collected and further immersed in ethanol for at least 24 h, and then repetitively washed with ethanol (at least 4 times with 20 cm^3 each). After the washing procedure to remove IL traces, electrospun cellulose fibers were placed into a vacuum oven at 298 K for at least 24 h. The resultant fibers were analyzed by Scan Electron Microscope (SEM) with a Hitachi SU – 70 microscope and by X-ray Diffraction (XRD) were performed on a Philips X'Pert diffractometer equipment. The diffracted intensity of Cu Kα radiation (λ = 0.1541 nm, 40 kv and 50 mA) was measured in a 2θ range between 10º and 45º.

2.3 Results

In order to optimize the electrospun fibers diameter size and homogeneity, and the fibers morphology, several parameters were tested: nature and molecular weight of cellulose, cellulose concentration, dissolution time of cellulose in the IL and physicochemical properties related to the IL solvent, like surface tension.

2.3.1 Cellulose Sample

Aiming at evaluating the initial cellulose samples that could be used in electrospinning (before the dissolution in ILs), SEM images were initially acquired (Figure 13).

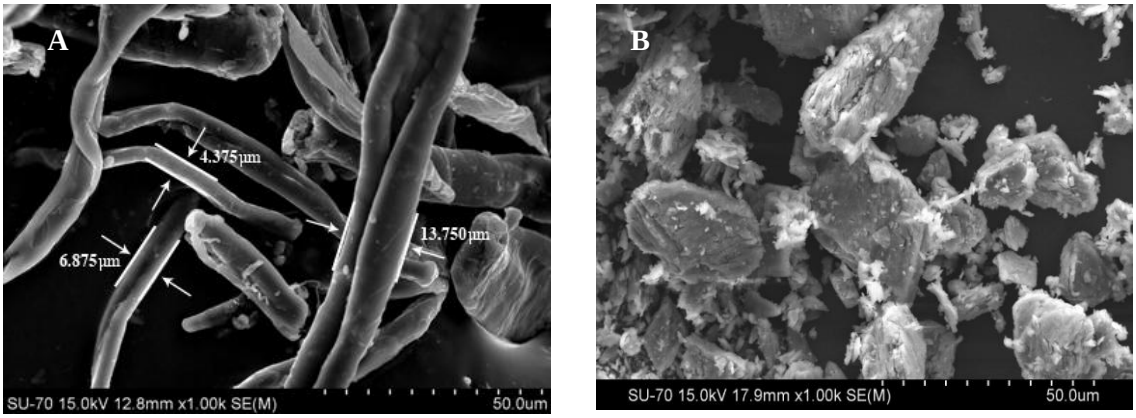

Figure 13 SEM images for Cellulose A: long fibrous cellulose **(A)**; and Cellulose B: microcrystalline cellulose particles **(B)**

As expected, the long fibrous cellulose sample (**cellulose A**) present long fibers morphology while the microcrystalline cellulose sample (**cellulose B**) presents particulate forms and few fibers morphology.

Both cellulose samples were dissolved, at 298 K, in $[C_2mim][CH_3CO_2]$ for a period of 72 h. It should be pointed out that the long fibers cellulose solution was at 8 wt % while microcrystalline cellulose was at 4 wt % due to its lower solubility in the selected IL. Figure 14 presents the SEM images for the resulting electrospun cellulose fibers of both cellulose samples.

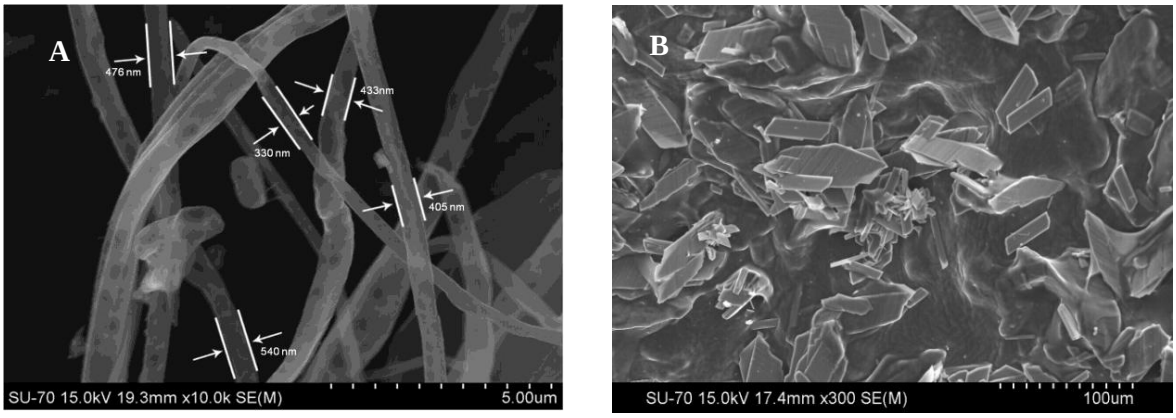

Figure 14 SEM images for electrospun cellulose fibers. Cellulose A: long fibrous cellulose **(A)**; and Cellulose B: microcrystalline cellulose **(B)**

2.3.2 Time for Cellulose Dissolution

In order to optimize the time for cellulose dissolution, and to guarantee that all the cellulose samples are completely dissolved in the IL, it was used polarized optical microscopy (POM) to periodically evaluate the dissolution status. The presence of crystalline parts of cellulose indicates that the solubility was not completely achieved; Figure 15 shows the macroscopic and microscopic trend on the cellulose dissolution at different times of dissolution at 298 K. In this section the cellulose sample used was the long fibers cellulose (cellulose A).

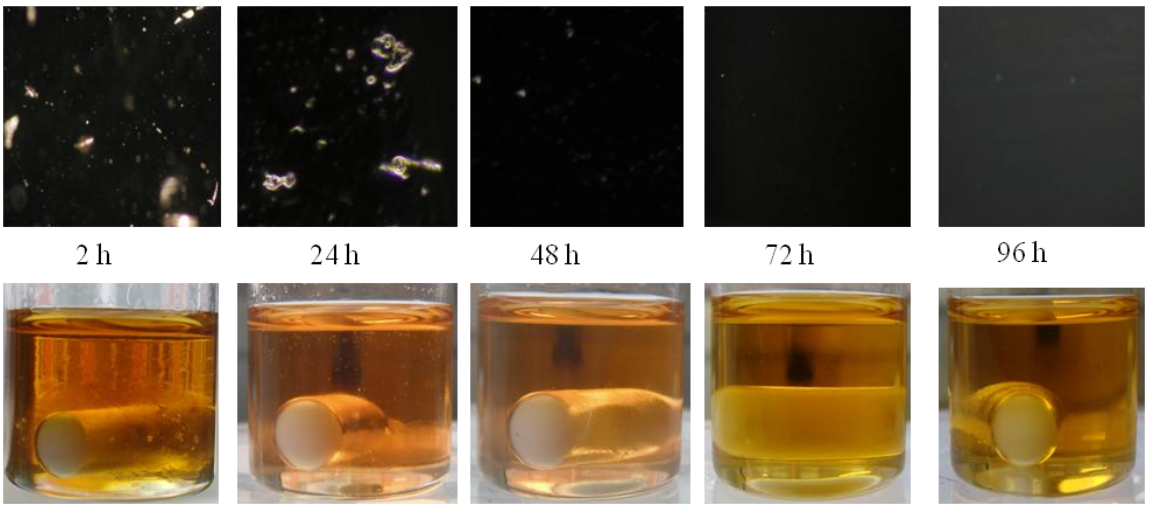

Figure 15 POM images and macroscopic aspect of the Cellulose A at 8 wt % in $[C_2mim][CH_3CO_2]$ after 2, 4, 6, 72 and 96 h of dissolution

Electrospinning was further performed with the cellulose A/[C_2mim][CH_3CO_2] mixtures with 24 h, 48 h, 72 h and 96 h of constant stirring at 298 K. It should be pointed out that in all samples it was macroscopically found two types of fibers: isolated fibers in suspension and matrix-based fibers as can be seen in Figure 16.

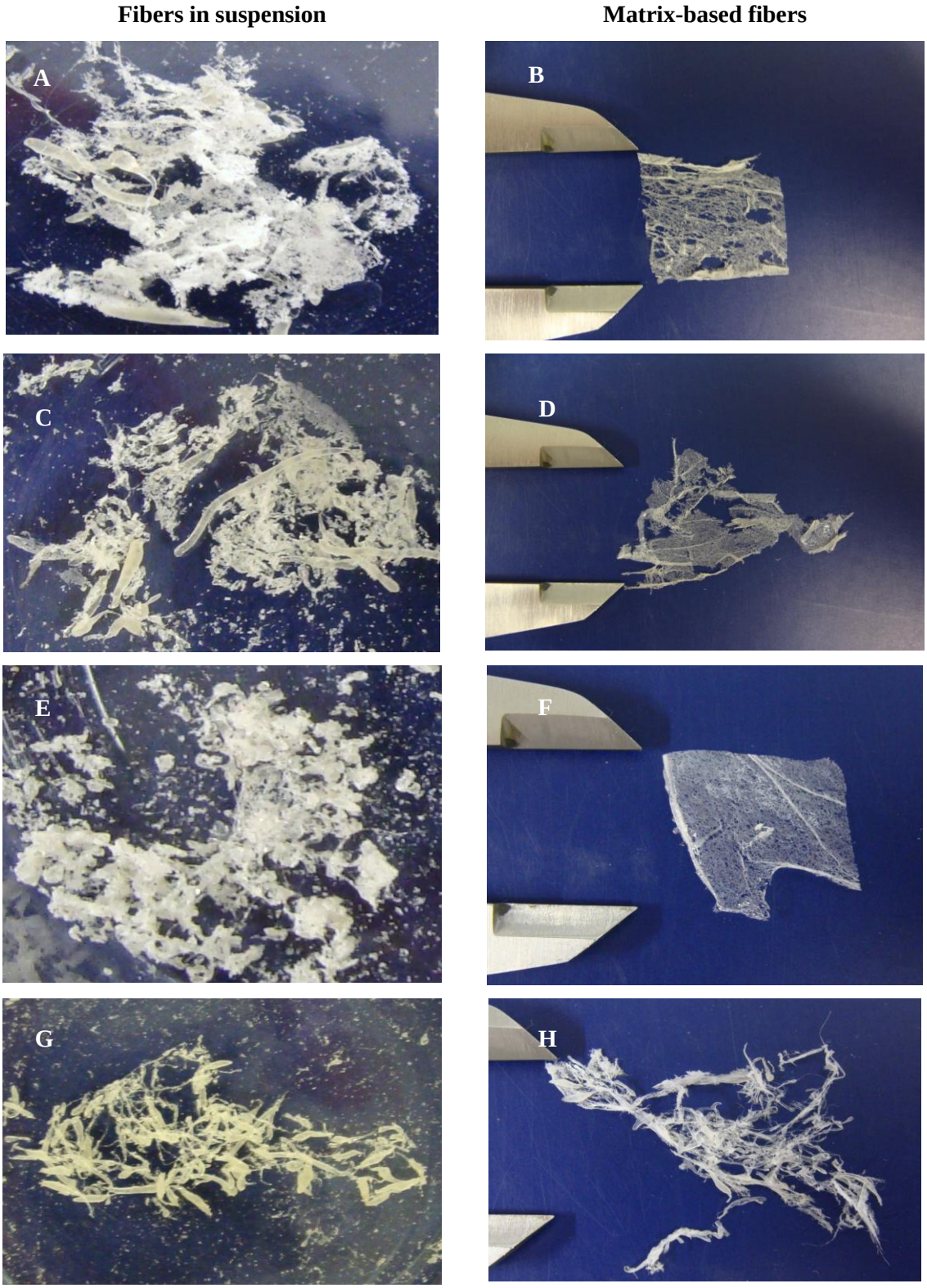

Figure 16 Macroscopic aspect of isolated fibers in suspension (**A**, **C**, **E** and **G**) and matrix-based fibers (**B**, **D**, **F** and **H**) for 24 h (**A** and **B**), 48 h (**C** and **D**), 72 h (**E** and **F**) and 96 h (**G** and **H**) after the electrospinning of 8 wt % Cellulose A in $[C_2mim][CH_3CO_2]$ solutions

Macroscopically, the matrixes obtained at 72 h of dissolution were more homogeneous. On the other hand, at 96 h of dissolution the matrixes obtained are partially destroyed. The results presented in Figure 15 show that after 72 h, Cellulose A is completely dissolved. This dissolution enables the greater homogeneity obtained in the fibers morphology.

Electrospun fibers obtained at the various times of dissolution were further analyzed with SEM. Results are shown in Figures 17 and 18. The matrix-based electrospun fibers are displayed in Figure 17 while the dispersed fibers are shown in Figure 18. The comparison between the two figures shows the differences between the two types of samples.

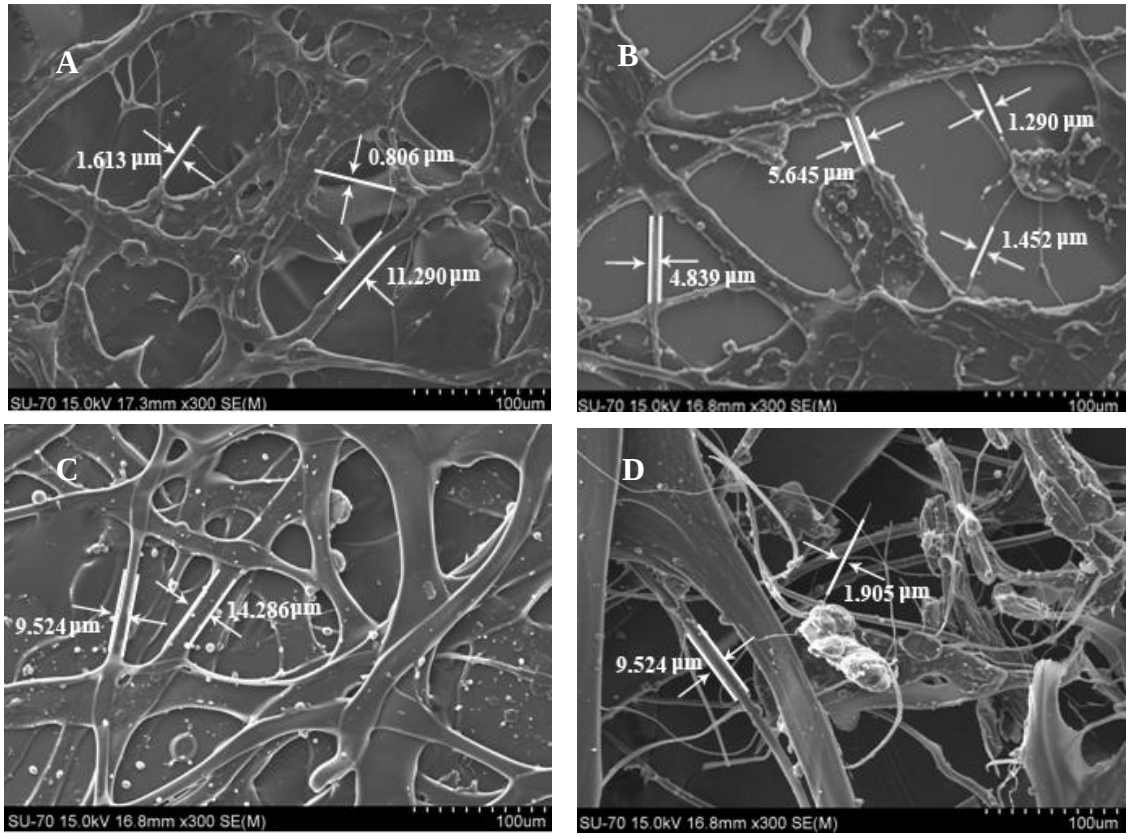

Figure 17 SEM images of matrix-based electrospun fibers with dissolution times of 24 h (**A**), 48 h (**B**), 72 h (**C**) and 96 h (**D**) for 8 wt % of Cellulose A in $[C_2mim][CH_3CO_2]$

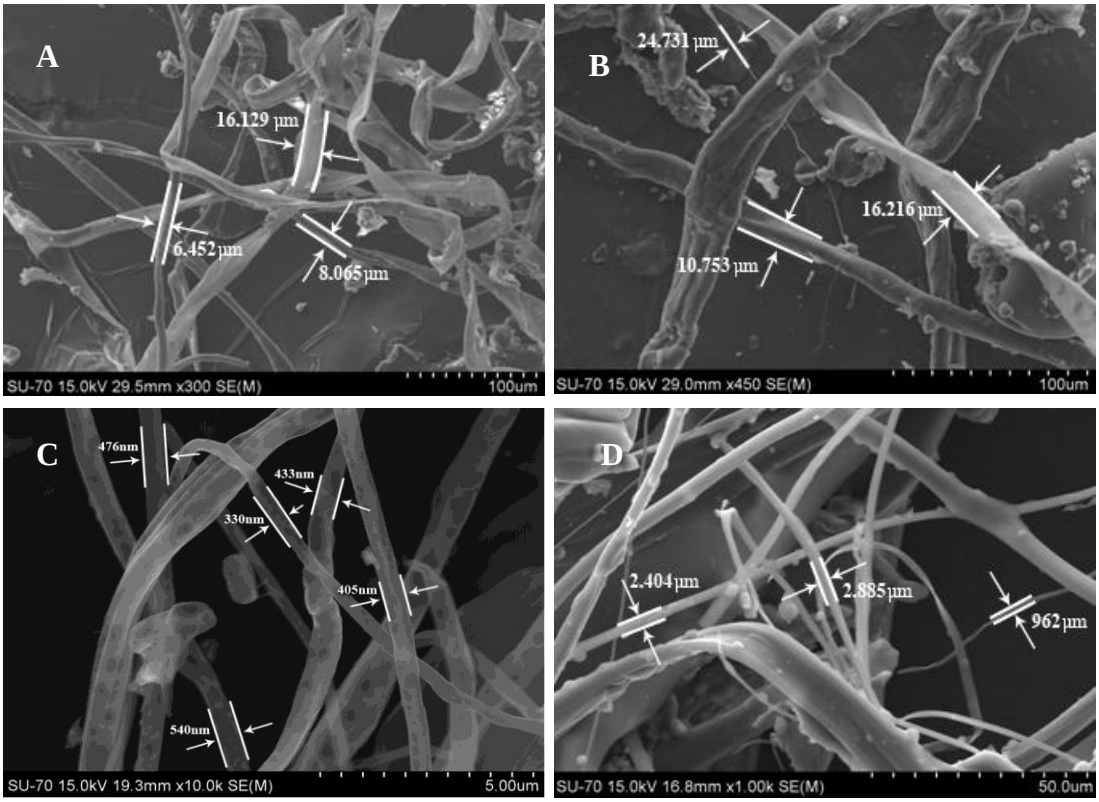

Figure 18 SEM images of electrospun fibers suspended in the water bath with dissolution times of 24 h (**A**), 48 h (**B**), 72 h (**C**) and 96 h (**D**) for 8 wt % of Cellulose A in $[C_2mim][CH_3CO_2]$

The images at Figure 17 show that the dissolution of cellulose at 72 h provides a higher homogeneity of the fibers, as well as smaller diameters. Despite the flat fiber morphologies and the extensive fiber branching observed, probably related to the low stretching of the polymer jet under the applied electric potencial and/or incomplete remotion of the IL, better results seem to be obtained for shorter times of dissolution (72 h) if compared with the 96 h results. Although it seems that smaller fibers diameters are obtained after 96 h of dissolution, a higher heterogeneity in the fibers size/morphology is observed.

Comparing the results gathered in Figure 18 with the SEM images for the initial cellulose sample displayed in Figure 13 it is patent a reduction in the fibers diameter from approximately 10 µm to 400-500 nm with a 8 wt % of Cellulose A in $[C_2mim][CH_3CO_2]$ solution with 72 h of dissolution. The electrospinning of cellulose in $[C_2mim][CH_3CO_2]$ showed a reduction in the fibers diameters size by 2 orders of magnitude.

2.3.3 Concentration of Cellulose

Two different concentrations for cellulose (Cellulose A) in the IL were evaluated preparing solutions with 5 wt % and 8 wt % in $[C_2mim][CH_3CO_2]$ with 72 h of dissolution. Figure 19 depicts the SEM images for both samples.

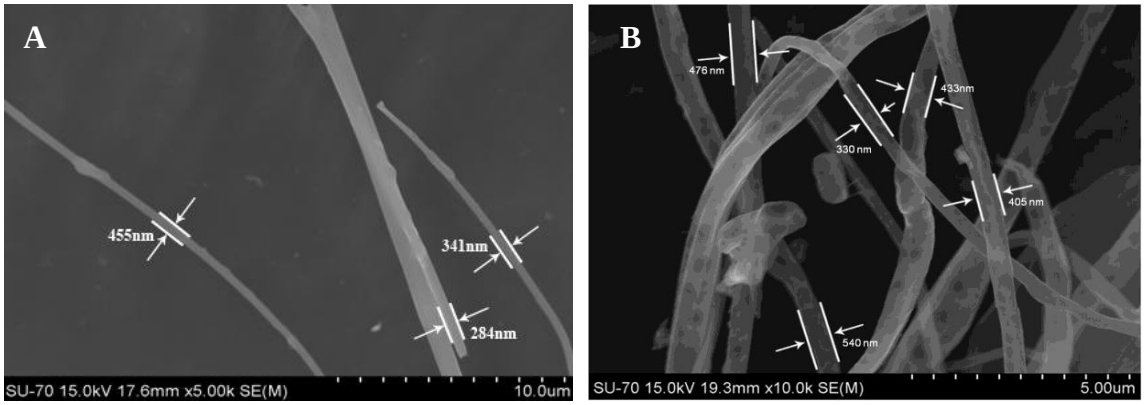

Figure 19 Electrospun cellulose A fibers with 5 wt % and 8 wt % of cellulose in $[C_2mim][CH_3CO_2]$ (72 h of dissolution)

Albeit the cellulose fibers present almost the same diameter for both concentrations of cellulose studied, the 8 wt % solutions provide improved homogeneity with a decreasing distribution of diameters within the obtained fibers.

2.3.4 Physical Properties of the Solvent

Since lower surface tension solutions are expected to improve the fibers diameter and morphology, additional tests were carried out using mixtures of $[C_2mim][CH_3CO_2]$ and $[C_{10}mim]Cl$. The longer alkyl chain length IL can factually act as a surfactant and decrease the surface tension of the mixture. Indeed it was already shown that $[C_{10}mim]Cl$ is an effective surfactant in aqueous solution [88]. $[C_{10}mim]^+$ cation possess a long alkyl chain coupled to an highly charged imidazolium core allowing the formation of micellar aggregates. Although, in this work the main solvent is another IL besides water, and thus, it is expected that the critical micelle concentration moves towards higher concentrations. Even so, it was already shown that surface active ILs can also perform as surfactants in ILs solutions [89]. On the other hand, $[C_{10}mim]Cl$ presents an higher viscosity compared to $[C_2mim][CH_3CO_2]$ [32] and a careful selection of the binary mixture composition should be considered. Surface tensions for the mixture composed by $[C_2mim][CH_3CO_2]$ and $[C_{10}mim]Cl$ were determined at 298 K, with a mole fraction composition of $[C_{10}mim]Cl$ ranging between 0 and 0.70. Since density data is required to correct surface tension values, the densities of the mixtures at 298.15 K were also determined and are presented in Appendix A. The methodology and equipment used were properly validated measuring surface tensions for pure ILs well established in literature [14, 35]. Surface tensions for pure $[C_4mim][BF_4]$, $[C_4mim][NTf_2]$, $[C_8mim][BF_4]$, $[C_8mim][PF_6]$ and $[C_8mim][NTf_2]$ were determined and the comparison between the results gathered in this work and those previously reported [14, 35] are shown in Appendix A.

Several solutions of $[C_2mim][CH_3CO_2]$ and $[C_{10}mim]Cl$ were prepared in different molar ratios to evaluate the decrease in the surface tension values and further use a mixture of ILs with improved low surface tension aiming the cellulose electrospinning. Surface tension dependence of the $[C_{10}mim]Cl$ content, at 298 K, is displayed in Figure 20.

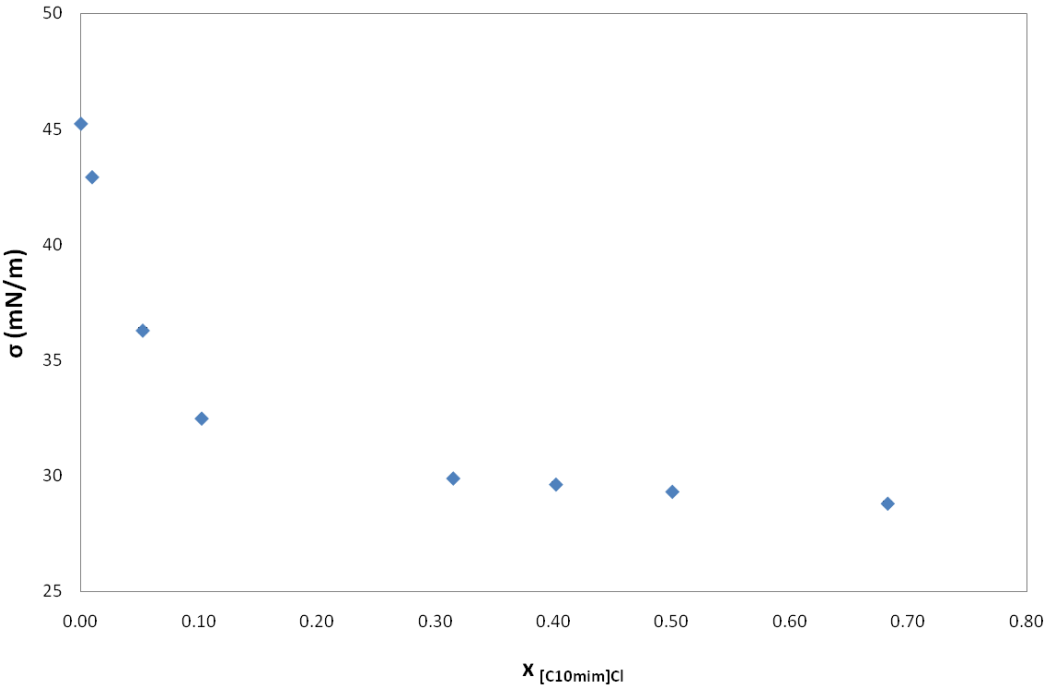

Figure 20 Surface tension of $[C_2mim][CH_3CO_2]$ / $[C_{10}mim]Cl$ mixtures as function of $[C_{10}mim]Cl$ mole fraction at 298 K

In Figure 21 it is shown the viscosity values for the ILs mixtures used to evaluate the surface tension decrease. It is possible to see that a increment in the $[C_{10}mim]Cl$ molar ratio is proportional to the viscosity of the solution. Because of the extremely high viscosity of pure $[C_{10}mim]Cl$, it was not possible to measure its surface tension by the method described.

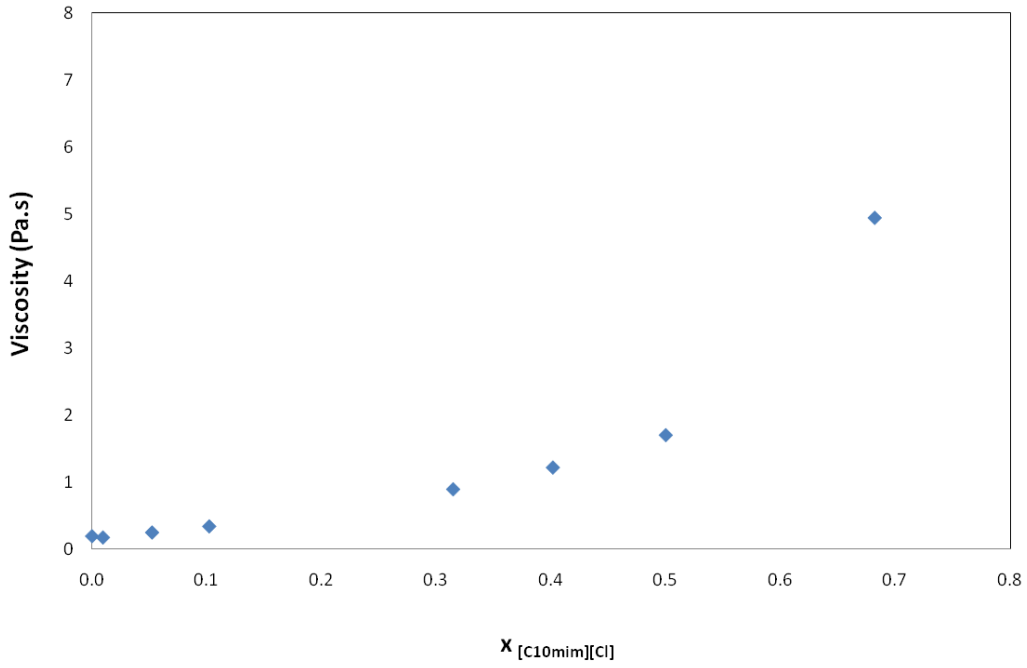

Figure 21 Viscosity of $[C_2mim][CH_3CO_2]$ / $[C_{10}mim]Cl$ mixtures as function of $[C_{10}mim]Cl$ mole fraction at 298 K

Due to the high viscosity of the longer alkyl chain IL and the pattern in the surface tension decrease, the mole fraction ratio selected of ILs for further cellulose dissolution and electrospinning was 0.90 of $[C_2mim][CH_3CO_2]$ and 0.10 of $[C_{10}mim]Cl$.

Both types of cellulose (Cellulose A and Cellulose B) in the 0.90:0.10 mole fraction mixture $[C_2mim][CH_3CO_2]$:$[C_{10}mim]Cl$ were subjected to electrospinning and SEM results for the electrospun fibers are shown in Figures 22 and 23. It should be pointed out that the time of dissolution was kept at 72 h for both samples and mixtures were prepared at 298 K. The main problem associated to the addition of $[C_{10}mim]Cl$ to $[C_2mim][CH_3CO_2]$ is the decrease in the cellulose solubility. Preliminary tests of saturation were performed and Cellulose A dissolves up to 8 wt % while cellulose B content in this ILs mixture was within 4 wt %. Also the SEM images for the electrospun fibers of the same cellulose sample dissolved in pure $[C_2mim][CH_3CO_2]$ are displayed in Figures 23 and 24 for comparison purposes.

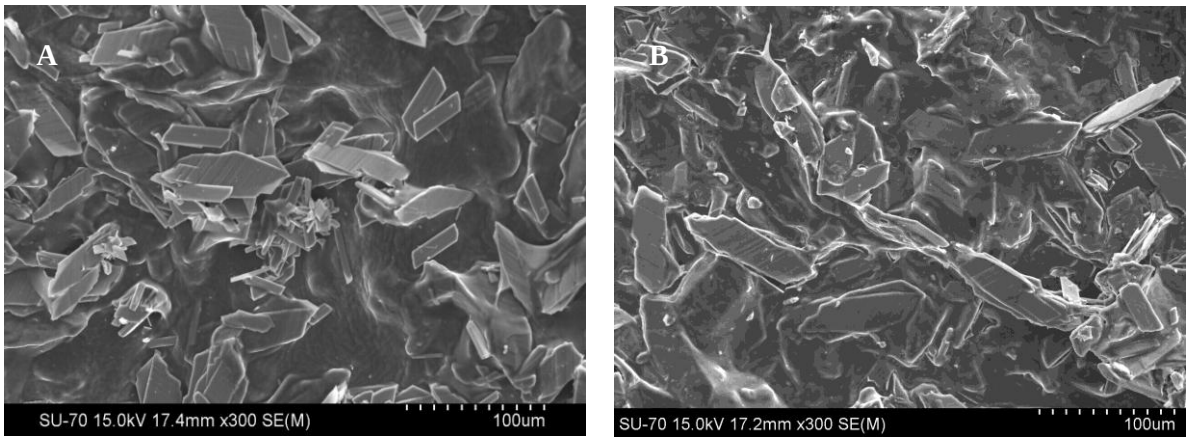

Figure 22 Microcrystalline cellulose (Cellulose B) after electrospinning in pure $[C_2mim][CH_3CO_2]$ (**A**) and in $[C_2mim][CH_3CO_2]$: $[C_{10}mim]Cl$ mixture (mole fraction ratio 0.90:0.10) (**B**)

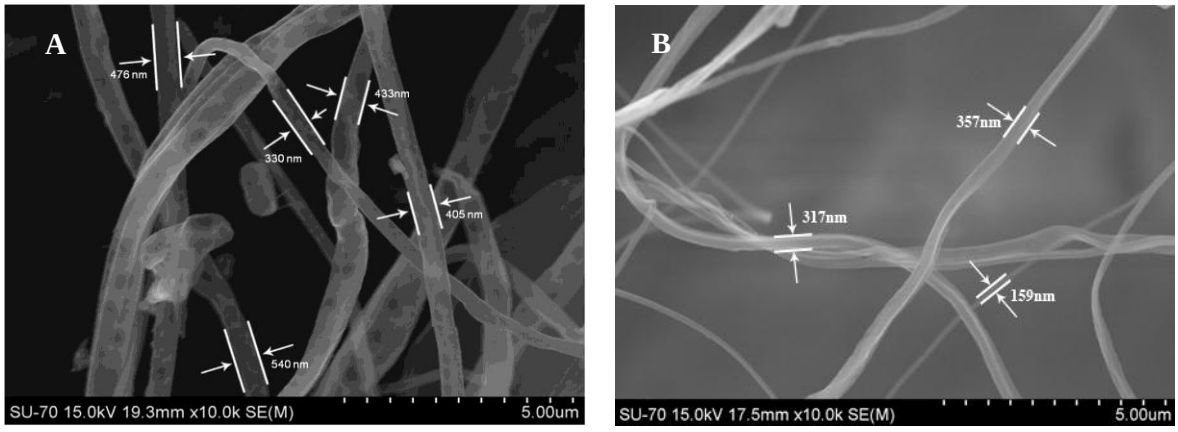

Figure 23 Cellulose A fibers after electrospinning in pure $[C_2mim][CH_3CO_2]$ (**A**) and in $[C_2mim][CH_3CO_2]$: $[C_{10}mim]Cl$ mixture (mole fraction ratio 0.90:0.10) (**B**)

Figure 24 presents several SEM images obtained for the Cellulose A fibers after electrospinning in the $[C_2mim][CH_3CO_2]$: $[C_{10}mim]Cl$ mixture.

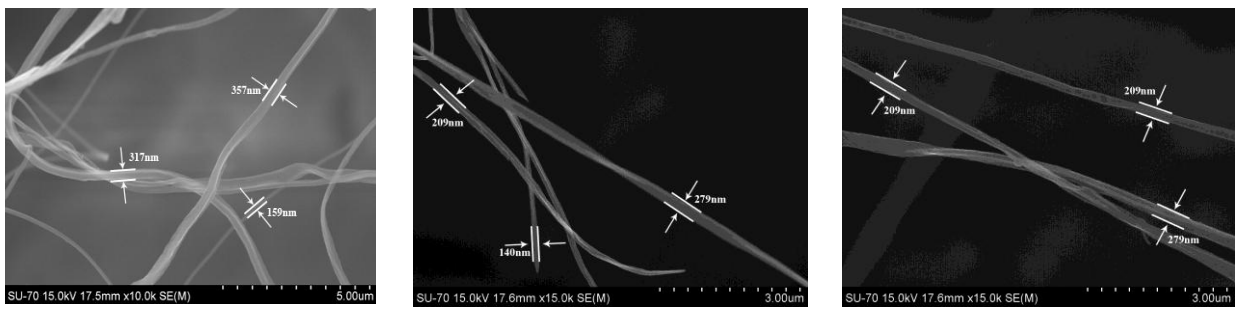

Figure 24 Cellulose A fibers after electrospinning in the $[C_2mim][CH_3CO_2]$: $[C_{10}mim]Cl$ mixture (mole fraction ratio 0.90:0.10)

Cellulose B (microcrystalline cellulose) does not show any improvements after the electrospinning in the mixture of ILs. In fact it seems that the size of the microscopic fibers increased when compared with the results obtained with pure $[C_2mim][CH_3CO_2]$. On the contrary, the electrospun fibers of Cellulose A in the presence of the surfactant $[C_{10}mim]Cl$ are of smaller size than those obtained from pure $[C_2mim][CH_3CO_2]$. The fibers diameter seems to decrease from 500 nm to ≈ 300 nm. The reduction of the fibers size is a result of the surface tension decrease in the overall polymeric solution that facilitates the formation of fibers.

In Figure 25, X-ray diffraction results for electrospun fibers are shown in an attempt to understand if the electrospinning process affects the crystallinity of the fibers. The comparison is made by the direct analysis of the original cellulose A and regenerated cellulose obtained from a solution of $[C_2mim][CH_3CO_2]$ and subsequent precipitation of the dissolved cellulose with water. It is possible to see a loss of crystallinity from the original cellulose A to the electrospun fibers obtained from a $[C_2mim][CH_3CO_2]$: $[C_{10}mim]Cl$ mixture**.**

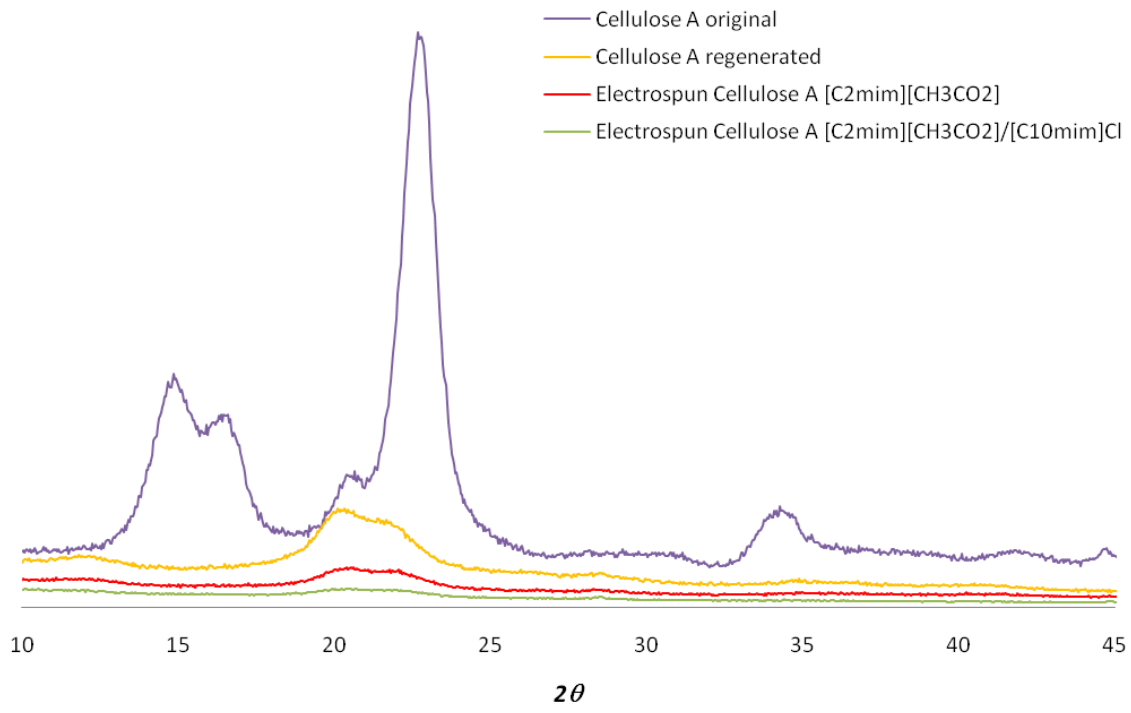

Figure 25 XRD results for original cellulose A, cellulose A regenerated, electrospun cellulose A with pure $[C_2mim][CH_3CO_2]$ and electrospun cellulose A in $[C_2mim][CH_3CO_2]$: $[C_{10}mim]Cl$ mixture (mole fraction ratio 0.90:0.10)

Original Cellulose A used for electrospinning revealed to be of Type-I polymorph with characteristic peaks at 2θ = 14.9º, 16.3º, 22.5º and 34.6º. Nevertheless, after dissolution of cellulose in the ionic liquid and subsequent regeneration, both electrospun cellulose fibers and regenerated casting film are mainly amorphous (polymorphs of Type-II with a characteristic peak at 2θ = 20.8º) [90]. Thus, most of the intra- and intermolecular hydrogen bonding network present in the original cellulose A was destroyed when dissolving it in $[C_2mim][CH_3CO_2]$ (with or without undergoing trough electrospinning).

These results could be explained by what happens in the recrystallization of cellulose with or without electrospinning. For regenerated cellulose, the process of dissolution is responsible for the loss of crystallinity because the IL destroys the majority of the crystalline zones of cellulose.

Comparing the crystallinity of electrospun fibers obtained from a pure IL solution and the fibers obtained from a mixture of ILs, the explanation to this fact resides in the interactions of the solvents with cellulose in each case. Despite any cinetic study made, it is possible that the acetate and the chloride anions have different ways to be removed from the fibers during the collection of in the electrospinning process affecting thus the recrystallization of the cellulose over the original polymer. On the other hand, the rapid re-crystallization of the fibers affects the crystallinity of cellulose.

2.4 Conclusions

In this work a study for the optimization of the conditions aiming at obtaining micro and nanosized cellulose fibers by electrospinning using ionic liquid as solvents was carried out. A room temperature IL, 1-ethyl-3-methylimidazolium acetate, $[C_2mim][CH_3CO_2]$, with low viscosity and high solvation ability for cellulose, was selected as main solvent. This selection allowed the use of the pure IL without requiring the addition of organic volatile co-solvents or high temperature operating conditions, contrarily to that previously reported in literature [6, 10, 21].

With the goal of obtaining nanometer- and micrometer-sized cellulose fibers several parameters were evaluated, such as, the cellulose nature, cellulose concentration, dissolution time, and the use of an additional IL as additive ($[C_{10}mim]Cl$) that could perform as an active surface specie. The results were analyzed according to the electrospun fibers morphology, diameter and crystallinity obtained.

Two types of cellulose were evaluated: long fibrous cellulose (Cellulose A) and microcrystalline cellulose (Cellulose B). Cellulose A has shown to better dissolve in $[C_2mim][CH_3CO_2]$ with a concentration value of 8 wt % at 298 K. This is related with the high crystallinity of Cellulose B compared to Cellulose A. ILs anions are hydrogen bond acceptors and dissolve polysaccharides by disrupting the extensive network of hydrogen bonds in the crystalline polymer. While Cellulose A has more amorphous zones, Cellulose B is mainly composed by crystalline particles which decrease the solubility in the IL. Moreover, comparing electrospun fibers from the two samples, improved results were obtained with Cellulose A probably due to its higher ability to be completely dissolved before electrospinning operations.

In order to optimize the time for cellulose dissolution, electrospinning was also performed with the 8 wt % cellulose A/$[C_2mim][CH_3CO_2]$ mixtures with 24 h, 48 h, 72 h and 96 h of constant stirring. The results gathered indicated that the dissolution of cellulose during 72 h provides higher homogeneity of the fibers morphology, as well as smaller diameters. With longer times of dissolution, for instance 96 h, a higher heterogeneity in the fibers size/morphology was observed.

Two different concentrations for Cellulose A in $[C_2mim][CH_3CO_2]$ were evaluated to optimize the cellulose concentration. Solutions with 5 wt % and 8 wt % of cellulose in $[C_2mim][CH_3CO_2]$ were electrospun and the SEM results indicated that the 8 wt % solutions provide improved homogeneity through the fibers diameter.

The optimized conditions of 72 h of dissolution at 298 K of a 8 wt % Cellulose A mixture in $[C_2mim][CH_3CO_2]$ leaded to a reduction in the fibers diameter from approximately 10 μm to 400-500 nm.

Trying to optimize the physical properties of the IL solvent, an additional active surface IL ($[C_{10}mim]Cl$) was used aiming at decreasing the mixture surface tension. Taking into account the

surface tensions decrease as a function of [C_{10}mim]Cl content, the mole fraction ratio selected for further cellulose dissolution and electrospinning was 0.90 of [C_2mim][CH_3CO_2] and 0.10 of [C_{10}mim]Cl. Both Cellulose A and Cellulose B were dissolved in the mixture of ILs and both cellulose samples were maintained at the same concentration as in pure [C_2mim][CH_3CO_2]. Although no major improvements were observed with Cellulose B, on the other hand, electrospun fibers of Cellulose A decreased in size from 500 nm to ≈ 300 nm. XRD results have shown that electrospinning affects the crystallinity of the polysaccharide due to the rapid solidification of the fibers and the solvent removal from the fibers.

In this work a room temperature IL was used, for the first time, to produce cellulose fibers by electrospinning. The results obtained are promissory and should be further explored aiming at producing nanosized cellulose fibers with practical applications. The relative simplicity and versatility of the electrospinning process, coupled with the high ability of ILs to dissolve polymers and their benign characteristics, show a great promise for future productions of other biopolymer-based fibrous materials with enhanced functionalities and advanced applications.

3. Solubility of Carbohydrates in Ionic Liquids

3.1 Carbohydrates Dissolution in Ionic Liquids

ILs have been known as "greener" solvents when compared with volatile organic compounds (VOCs), essentially due to their negligible vapor pressure and high thermal and chemical stability [91]. They have been shown capable of dissolving numerous polar and non-polar compounds. In the past few years several research studies have demonstrated their potential to dissolve carbohydrates, including glucose, cellulose, sucrose, lactose, mannose, xylose, amylose, amylopectin, chitin, chitosan, inulin, pectin, starch, xylan, agarose, dextrin, and cyclodextrin [11, 56, 76, 79, 91-92]. Moreover, experimental methods such as Nuclear Magnetic Resonance (NMR) [93], UV-Vis spectroscopy and Fourier Transform Infrared spectroscopy (FTIR) [94] were used to gather a broader picture of the underlying molecular mechanisms responsible for such high solvation capability. In addition, room temperature ILs are factual solvents in which carbohydrates can be chemically and enzymatically converted into useful new chemicals and materials with many potential applications [74].

Park et al. [95] and Kimizuka et al. [92] reported the solubility of glucose in ILs based on the imidazolium cation. The authors mentioned such ILs as "sugar-philic" due to their capacity to hydrogen bonding with the carbohydrates hydroxyl groups [92, 95]. On the other hand, MacFarlane et al. [33] shown dicyanamide-based ILs to present enhanced ability to dissolve glucose due to the donor solvent properties caused by the Lewis basicity provided by the IL anion [33]. In addition, a further study regarding carbohydrates solubility in ILs aiming enzyme-catalysed transformations showed that $[C_4mim][N(CN)_2]$ dissolved glucose in concentrations between 211 and 405 $g.dm^{-3}$ (in the temperature range from 313.15 to 348.15 K) [76]. Sheldon et al. [76] observed that glucose solubility was more dependent on the IL anion (with the dicyanamide anion being the improved anion among all ILs evaluated) than on the IL cation. However, among the several IL cations evaluated, 1-butyl-3-methylimidazolium cation, was the one that showed higher solubility values [76]. Although, it was further shown that the IL cation has also an important role in the solubility process of carbohydrates, particularly when functionalized groups, such as an ether substituent group, are added to the alkyl chain of the imidazolium ring [78]. Glucose dissolved up to 450 $mg \cdot cm^{-3}$ and α-cyclodextrin to 350 $mg \cdot cm^{-3}$ in ether-containing imidazolium-bromide-based ILs [78]. The enhanced solvating capacity of these ILs was attributed to the additional functionalized ether groups [78].

Attempts at understanding the mechanisms responsible for the carbohydrates dissolution process in ILs are available in literature [96]. Molecular dynamics simulation results indicated

that the solvation of glucose in 1,3-dimethylimidazolium chloride involves interactions between the chloride anion and glucose, whereas the cation only interacts weakly with the sugar. Chloride ions form a primary solvation shell around the perimeter of the glucose ring [96]. Only a small presence of the cation was found in the first solvation shell, while the main association occurs between the most acidic hydrogen at the C2-position of the imidazolium ring and the oxygen atoms of the secondary sugar hydroxyls [96].

The vast majority of studies that exist on the carbohydrates solubility in ILs are mainly based in ILs with the imidazolium cation and few cases included benzotriazonium-, pyridinium-, pyrrolidinium- and ammonium-based ILs [56]. Therefore it would be interesting to extend solubility studies to others classes of ILs, including phosphonium-based ILs. When compared to imidazolium- and pyridinium-based ILs, phosphonium-based ILs are thermally more stable and have no acidic protons which make them more stable towards nucleophilic and basic conditions [97]. Accordingly, some of these inherent characteristics of phosphonium-based ILs can be valuable for specific applications. Another interesting characteristic regarding phosphonium-based ILs is their low density values, even lower than water, that could provide potential benefits for particular applications [97]. Despite the studies concerning the solubility of carbohydrates in ILs available in literature, no comprehensive and detailed studies with the dependency on temperature were found.

The study of the solubility of six monosaccharides in different ILs was here conducted in a large temperature range. Monosaccharides evaluated were D-(+)-Glucose, D-(+)-Mannose, D-(-)-Fructose, D-(+)-Galactose, D-(+)-Xylose and L-(+)-Arabinose. Solubilities of all monosaccharides in two hydrophilic ILs, 1-butyl-3-methylimidazolium dicyanamide and 1-butyl-3-methylimidazolium dimethylphosphate, were determined in the temperature range between 288.15 K and 348.15 K. Aiming at evaluating the IL anion influence on the solubility of carbohydrates two additional hydrophobic ILs were considered: trihexyltetradecylphosphonium dicyanamide and trihexyltetradecylphosphonium chloride. In the phosphonium-based ILs the solubility of D-(+)-Glucose was determined in the temperature interval from 298.15 K to 338.15 K. Table 3 presents the molecular structures of the six monosaccharides considered in this study.

Table 3 Molecular structures of the monosaccharides used in this study

Monosaccharide	Molecular Structure
D-(+)-Glucose	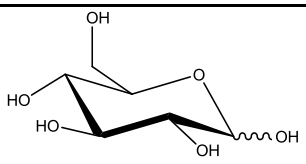
D-(+)-Mannose	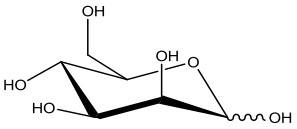
D-(+)-Galactose	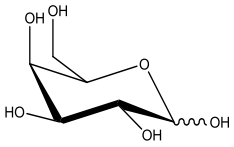
L-(+)-Arabinose	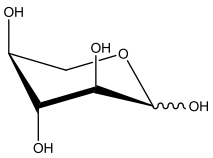
D-(-)-Fructose	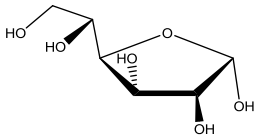
D-(+)-Xylose	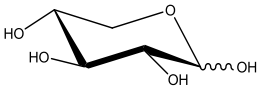

3.2 Experimental Section

3.2.1 Hydrophilic Ionic Liquids

3.2.1.1 Chemicals

The monosaccharides studied were D-(+)-glucose > 99.5 wt % pure from Scharlau, D-(+)-mannose > 99 wt % pure from Aldrich, D-(+)-galactose > 98.0 wt % pure from GPR Rectapur, D-(+)-xylose 99.0 wt % pure from Carlo Erba, L-(+)-arabinose ≥ 99.0 wt % pure from BHD Biochemicals, and D-(-)-fructose > 98.0 wt % pure from Panreac. The ILs used were 1-butyl-3-methylimidazolium dicyanamide, $[C_4mim][N(CN)_2]$, and 1-butyl-3-methylimidazolium dimethylphosphate, $[C_4mim][DMP]$. Both ILs were acquired at Iolitec with mass fraction purities > 99 %. The solvent used on the coulometric Karl Fischer titration was Hydranal-Coulomat AG from Riedel de Haën.

To reduce the water content and volatile compounds to negligible values, ILs were dried at vacuum and at 333 K, using continuous stirring, for a minimum of 48 h. ILs and carbohydrates purities were further checked by ^{1}H and ^{13}C NMR spectroscopy.

It was previously shown that the water content influences the sugars solubility in ILs [11]. Therefore, after the drying procedure the water content of both ILs and carbohydrates was determined by Karl Fischer titration and is presented in Table 4.

Table 4 Water content in the carbohydrates and ILs used

Carbohydrate	Water Content (wt %)
D-(+)-Glucose	0.598
D-(+)-Mannose	0.654
D-(-)-Fructose	0.080
D-(+)-Galactose	0.373
D-(+)-Xylose	0.142
L-(+)-Arabinose	0.510
$[C_4mim][N(CN)_2]$	0.010
$[C_4mim][DMP]$	0.078

3.2.1.2 Methods

Water contents of both carbohydrates samples and ILs were determined using a Metrohm 831 Karl-Fischer (KF) coulometer.

Approximately 2 g of each carbohydrate/IL solution was prepared by adding both ionic liquid and carbohydrate in excess amounts to achieve saturation conditions. The solid-liquid mixture was left under constant stirring for at least 72 h at constant temperature. Sample glass tubes were thermostatized making use of a water bath as shown in Figure 26. The temperature was maintained within +/-0.5 K.

Figure 26 Temperature control bath and equilibrium cell

After the equilibration the samples were centrifuged during 20 min at 4500 rpm to completely separate both phases in an Eppendorf centrifuge 5804. Approximately 1 g (gravimetrically determined) of each ionic liquid-saturated solution was taken and diluted in pure water in a volumetric ratio previously established and dependent on the concentration of sugar. The monosaccharides quantification was performed by a coulorimetric method making use of the dinitrosalicylic acid reagent. 1 cm^3 of a standard 3,5-dinitrosalycilic acid (DNS) solution was added to 1 cm^3 of each diluted IL-carbohydrate sample, vigorously stirred, and finally placed in a water bath at 373 K for 5 min to accomplish the reaction. After the reaction, the samples were placed in ice for a few minutes and further diluted in 10 cm^3 of ultra-pure water. The amount of the reduced product 3-amino-5-nitrisalicylate was determined by UV-Vis spectroscopy using a SHIMADZU UV-1700, Pharma-Spec Spectrometer, at a wavelength of 540 nm. Calibration curves for each monosaccharide were properly determined. Three samples of each saturated solution were quantified. Figure 27 presents the overall scheme reaction occurring in the coulorimetric method using DNS and reducing carbohydrates. Moreover, Figure 28 presents the

macroscopic aspect of an aqueous solution containing carbohydrates before and after the reaction with DNS.

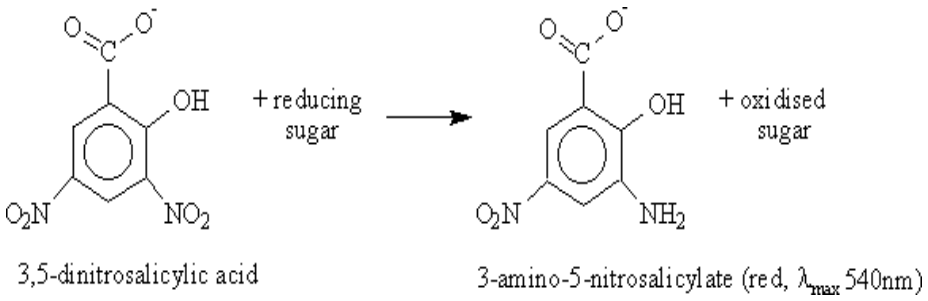

Figure 27 Reaction scheme of the coulorimetric method involving DNS and reducing carbohydrates

Figure 28 Macroscopic aspect of the DNS-involving reaction with a reducing sugar

The calibration curves obtained for each carbohydrate in water are presented in Appendix B.

3.2.2 Results and Discussion

The coulorimetric method here adopted was validated with the quantification of D-(+)-Glucose in $[C_4mim][N(CN)_2]$ according to literature values determined by high-performance liquid-chromatography (HPLC) [11]. Table 5 shows the values for the solubility of D-(+)-Glucose in $[C_4mim][N(CN)_2]$ obtained in this work and those presented in literature [11].

Table 5 Solubility of D-(+)-Glucose in $[C_4mim][N(CN)_2]$ obtained in this work and presented in literature **[11]**

T/ K	**IL water content wt %**	**[D-(+)-Glucose] Literature / (g.cm^{-3})**	**T/ K**	**IL water content wt %**	**[D-(+)-Glucose] this work / (g.cm^{-3})**
298.15	< 0.05	0.145	**298.15**	0.010	0.142
313.15	< 0.05	0.211	**318.15**	0.010	0.229
348.15	<0.05	0.405	**348.15**	0.010	0.319

The results obtained in this work show good agreement with literature values. Both positive and negative deviations in the solubility of glucose were observed and they result probably from the IL water content, equilibration conditions, analytical method used for quantification, among others.

The solubility of the six carbohydrates in $[C_4mim][N(CN)_2]$ between 288.2 K and 348.2 K is presented in Table 6. Note that the mass fraction of water in $[C_4mim][N(CN)_2]$ at all measurements performed was kept at approximately, or below, 0.01 wt %.

Table 6 Experimental mole fraction solubility data of carbohydrates (x_{CH}) in $[C_4mim][N(CN)_2]$ as a function of temperature

Carbohydrate	T / K	$(1/T)$ / (K^{-1})	x_{CH}	$\ln x_{CH}$	$\sigma(x_{CH})$	$\sigma(\ln x_{CH})$
	288.2	0.00347	0.142	-1.952	0.005	0.035
	298.2	0.00335	0.170	-1.772	0.006	0.035
	308.2	0.00325	0.191	-1.655	0.006	0.031
D-(+)-Glucose	318.2	0.00314	0.229	-1.476	0.006	0.026
	328.2	0.00305	0.250	-1.387	0.006	0.024
	338.2	0.00296	0.280	-1.273	0.006	0.021
	348.2	0.00287	0.319	-1.142	0.006	0.018
	288.2	0.00347	0.172	-1.76	0.004	0.024
	298.2	0.00335	0.197	-1.62	0.0040	0.020
	308.2	0.00325	0.226	-1.49	0.004	0.016
D-(+)-Mannose	318.2	0.00314	0.261	-1.34	0.004	0.014
	328.2	0.00305	0.301	-1.20	0.004	0.012
	338.2	0.00296	0.331	-1.11	0.004	0.011
	348.2	0.00287	0.390	-0.94	0.010	0.026
	288.2	0.00347	0.132	-2.02	0.005	0.038
	298.2	0.00335	0.153	-1.88	0.005	0.033
	308.2	0.00325	0.178	-1.72	0.005	0.028
D-(-)-Fructose	318.2	0.00314	0.201	-1.60	0.005	0.025
	328.2	0.00305	0.220	-1.51	0.005	0.023
	338.2	0.00296	0.245	-1.41	0.005	0.020
	348.2	0.00287	0.275	-1.29	0.010	0.036
	288.2	0.00347	0.142	-1.95	0.008	0.056
	298.2	0.00335	0.165	-1.80	0.008	0.048
	308.2	0.00325	0.192	-1.65	0.008	0.042
D-(+)-Galactose	318.2	0.00314	0.221	-1.51	0.008	0.036
	328.2	0.00305	0.248	-1.39	0.008	0.032
	338.2	0.00296	0.268	-1.32	0.008	0.030
	348.2	0.00287	0.298	-1.21	0.008	0.027

Carbohydrate	***T* / K**	**(1/*T*) / (K^{-1})**	x_{CH}	$\ln x_{CH}$	$\sigma(x_{CH})$	$\sigma(\ln x_{CH})$
D-(+)-Xylose	288.2	0.00347	0.182	-1.71	0.009	0.050
	298.2	0.00335	0.208	-1.57	0.009	0.043
	308.2	0.00325	0.250	-1.39	0.009	0.036
	318.2	0.00314	0.280	-1.27	0.009	0.032
	328.2	0.00305	0.314	-1.16	0.009	0.029
	338.2	0.00296	0.355	-1.04	0.009	0.025
	348.2	0.00287	0.402	-0.91	0.009	0.022
L-(+)-Arabinose	288.2	0.00347	0.142	-1.95	0.009	0.063
	298.2	0.00335	0.165	-1.80	0.009	0.055
	308.2	0.00325	0.185	-1.69	0.009	0.049
	318.2	0.00314	0.221	-1.51	0.009	0.041
	328.2	0.00305	0.241	-1.42	0.009	0.037
	338.2	0.00296	0.270	-1.31	0.009	0.033
	348.2	0.00287	0.301	-1.20	0.009	0.030

Figure 29 presents the experimental values obtained for the solubility of D-(+)-Glucose, D-(+)-Mannose, D-(+)-Xylose, D-(+)-Galactose, D-(-)-Fructose and L-(+)-Arabinose in $[C_4mim][N(CN)_2]$ as a function of temperature.

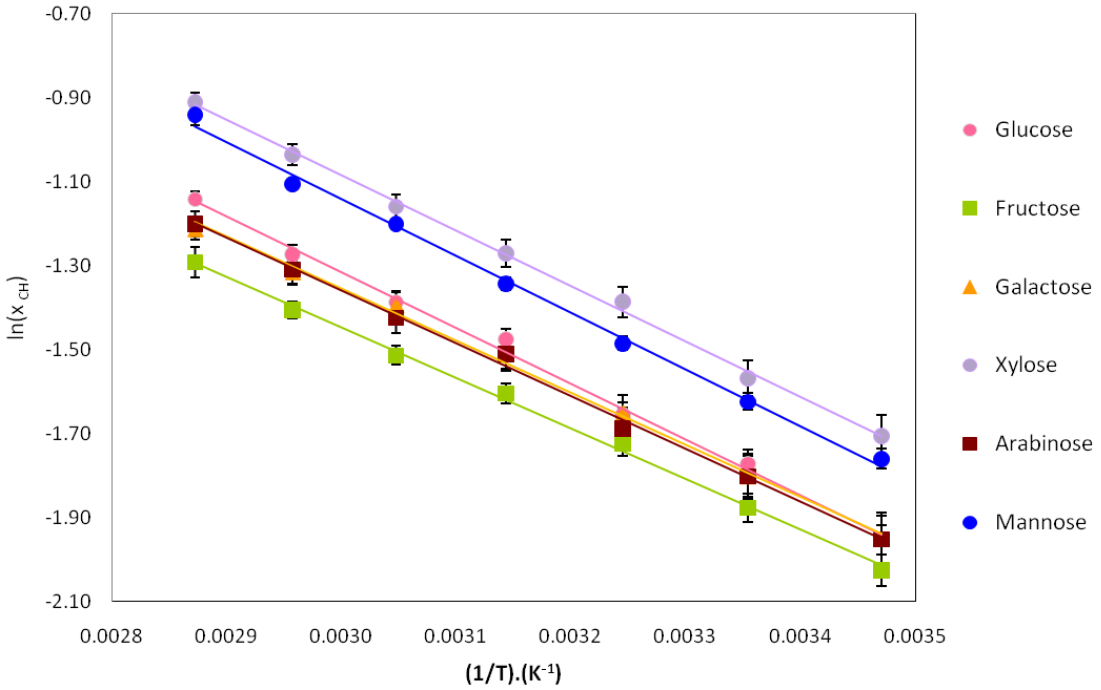

Figure 29 $\ln x_{CH}$ as a function of $1/T$ in $[C_4mim][N(CN)_2]$

It shows that all monosaccharides have the same solubility tendency as a function of temperature. The solubility increases monotonically with the temperature and presents a similar dependency for all the sugars studied. This fact is quite interesting since in common molecular solvents, such as water and short chain alcohols, the solubility dependence on temperature of different monosaccharides does not follows a similar pattern [98-100]. Xylose, a pentose, presents the higher solubility in $[C_4mim][N(CN)_2]$, while fructose, a hexose, presents the lower solubility in the same IL. The solubility of monosaccharides in $[C_4mim][N(CN)_2]$ decreases in the following order: xylose > mannose > glucose ≈ galactose ≈ arabinose > fructose.

The results obtained for the solubility of monosaccharides in 1-butyl-3-methylimidazolium dimethylphosphate, $[C_4mim][DMP]$, are presented in Table 7. The water content in $[C_4mim][DMP]$ in all measurements was maintained at or below 0.07 wt %.

Table 7 Experimental mole fraction solubility data of carbohydrates (x_{CH}) in [C_4mim][DMP] as a function of temperature

Carbohydrate	***T* / K**	**(1/*T*) / (K^{-1})**	x_{CH}	$\ln x_{CH}$	$\sigma(x_{CH})$	$\sigma(\ln x_{CH})$
D-(+)-Glucose	288.2	0.00347	0.035	-3.35	0.010	0.286
	298.2	0.00335	0.045	-3.10	0.010	0.222
	308.2	0.00325	0.074	-2.61	0.010	0.135
	318.2	0.00314	0.132	-2.02	0.010	0.076
	328.2	0.00305	0.158	-1.85	0.010	0.063
	338.2	0.00296	0.232	-1.46	0.010	0.043
D-(+)-Mannose	288.2	0.00347	0.029	-3.53	0.020	0.68
	298.2	0.00335	0.052	-2.96	0.020	0.38
	308.2	0.00325	0.070	-2.66	0.020	0.29
	318.2	0.00314	0.121	-2.11	0.020	0.17
	328.2	0.00305	0.175	-1.74	0.020	0.11
	338.2	0.00296	0.230	-1.47	0.020	0.09
D-(-)-Fructose	288.2	0.00347	0.015	-4.19	0.003	0.23
	298.2	0.00335	0.028	-3.58	0.003	0.12
	308.2	0.00325	0.042	-3.16	0.003	0.08
	318.2	0.00314	0.056	-2.89	0.015	0.27

Carbohydrate	***T* / K**	**(1/*T*) / (K^{-1})**	x_{CH}	$\ln x_{CH}$	$\sigma(x_{CH})$	$\sigma(\ln x_{CH})$
	328.2	0.00305	0.099	-2.31	0.015	0.15
	338.2	0.00296	0.125	-2.08	0.015	0.12
	288.2	0.00347	0.070	-2.66	0.010	0.14
	298.2	0.00335	0.112	-2.19	0.010	0.09
	308.2	0.00325	0.182	-1.70	0.010	0.05
D-(+)-Galactose	318.2	0.00314	0.220	-1.51	0.010	0.05
	328.2	0.00305	0.344	-1.07	0.010	0.03
	338.2	0.00296	0.412	-0.89	0.010	0.02
	288.2	0.00347	0.080	-2.53	0.030	0.37
	298.2	0.00335	0.126	-2.07	0.030	0.24
	308.2	0.00325	0.211	-1.56	0.030	0.14
D-(+)-Xylose	318.2	0.00314	0.302	-1.20	0.030	0.10
	328.2	0.00305	0.453	-0.79	0.030	0.07
	338.2	0.00296	0.503	-0.69	0.030	0.06
	288.2	0.00347	0.050	-3.00	0.020	0.40
L-(+)-Arabinose	298.2	0.00335	0.078	-2.55	0.020	0.26
	308.2	0.00325	0.115	-2.17	0.020	0.17

Carbohydrate	***T* / K**	**(1/*T*) / (K^{-1})**	x_{CH}	$\ln x_{CH}$	$\sigma(x_{CH})$	$\sigma(\ln x_{CH})$
	318.2	0.00314	0.182	-1.71	0.020	0.11
	328.2	0.00305	0.235	-1.45	0.020	0.09
	338.2	0.00296	0.332	-1.10	0.020	0.06

Figure 30 presents the experimental values for the solubility of D-(+)-Glucose, D-(+)-Mannose, D-(+)-Xylose, D-(+)-Galactose, D-(-)-Fructose and L-(+)-Arabinose in [C_4mim][DMP] and their respective dependence on temperature.

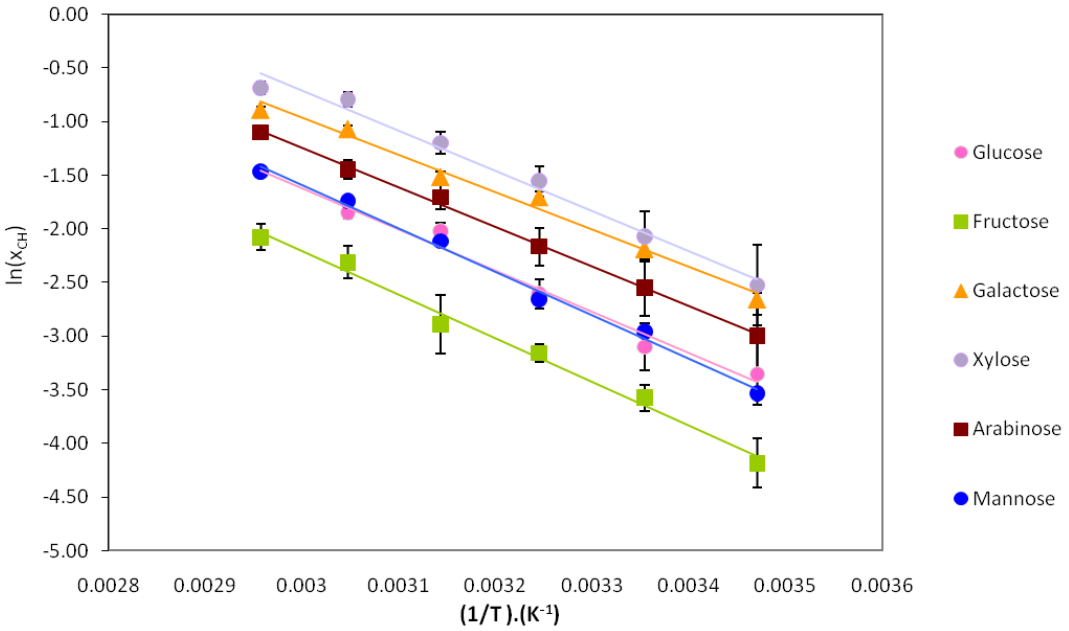

Figure 30 $\ln x_{CH}$ as a function of $1/T$ in [C_4mim][DMP]

As previously observed with [C_4mim][$N(CN)_2$], also for [C_4mim][DMP] the carbohydrates solubility increases with the temperature. The monosaccharide with higher solubility is xylose while the carbohydrate less soluble in [C_4mim][DMP] is fructose. These two extremes in solubilities follow the same pattern verified before with [C_4mim][$N(CN)_2$]. The solubility of the carbohydrates studied, at constant temperature, in [C_4mim][DMP] follows the increasing order: fructose < mannose ≈ glucose < arabinose < galactose < xylose. The solubility trend of

monosaccharides does not follow the same order in both hydrophilic ILs evaluated. These tendencies reflect a major role played by the IL anion towards the monosaccharides solvation. Figure 31 displays a general comparison on the solubility of the six carbohydrates in both ILs studied and water at different temperatures.

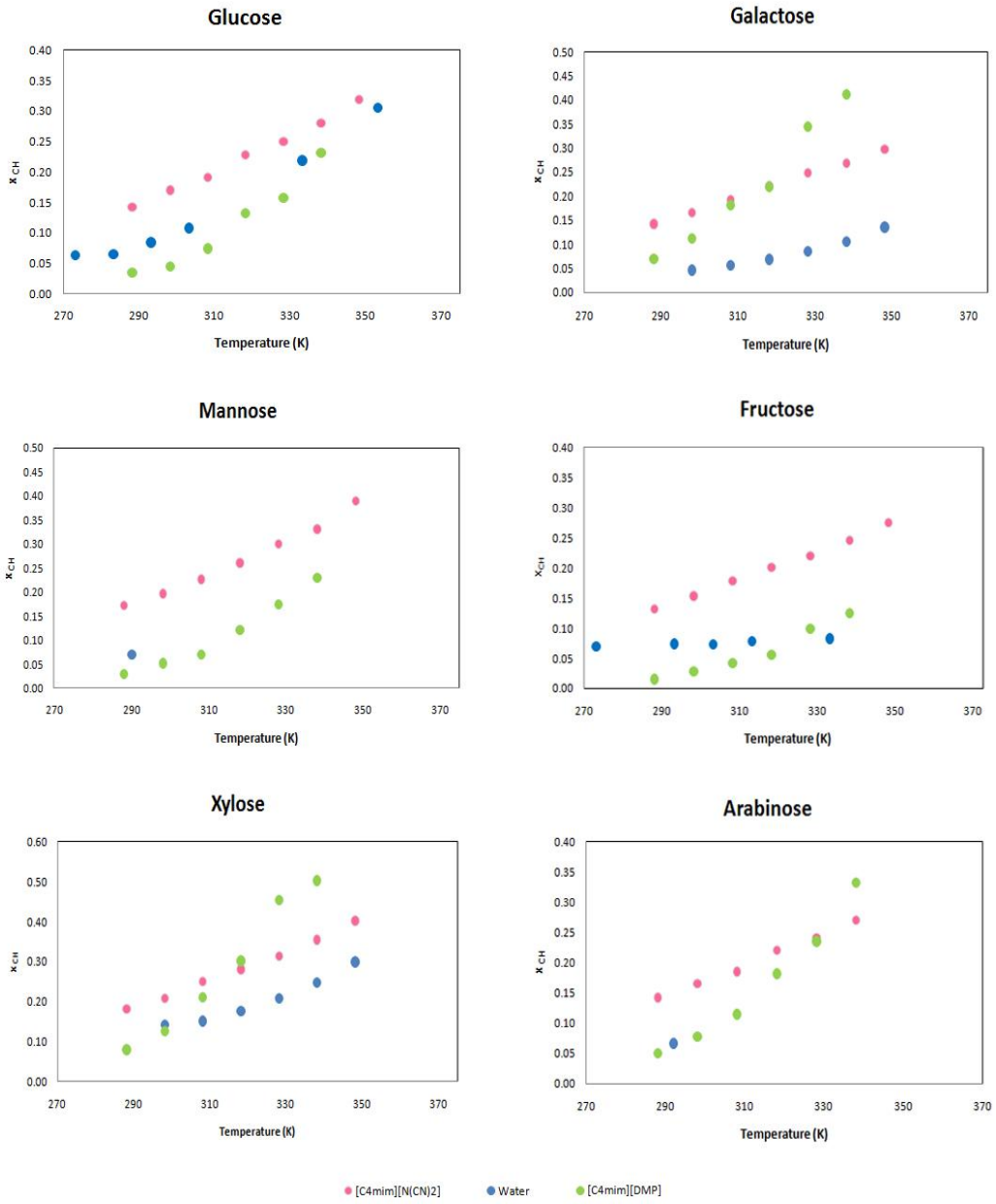

Figure 31 Mole fraction solubility of monosaccharides as a function of temperature in $[C_4mim][N(CN)_2]$, $[C_4mim][DMP]$ and water

From the results depicted it is patent that the selected ILs present enhanced capacity to dissolve carbohydrates. Moreover, in a molar fraction basis, the solubility of monosaccharides in ILs is of the same order of magnitude, or higher than, the solubility in water (a major solvent for sugars).

At most temperatures studied (lower temperatures) [C_4mim][$N(CN)_2$] is more efficient in dissolving the monosaccharides studied. However, with the temperature increase there is a temperature at which [C_4mim][DMP] becomes more able to dissolve carbohydrates. These tendencies could be explained by the basicity of the anion of each IL, *i.e.*, the capacity of the anion for hydrogen bonding with the monosaccharide. Solvatochromic parameter values of hydrogen-bond basicity, β, taken from literature (0.470 for water [101], 0.596 for [C_4mim][$N(CN)_2$] and 1.118 for [C_4mim][DMP] [102]) could be useful in interpreting the solubility trends obtained. From the β values, water is the solvent less capable of hydrogen-bonding while the dimethylphosphate-based IL is the solvent with higher ability to hydrogen bond with the carbohydrates hydroxyl groups. These values explain the solubility trends observed at higher temperatures. Nevertheless, the enthalpy of solution of each carbohydrate in both ILs seems to be highly different accordingly to the solubility trends observed along temperature. The enthalpy of solution of carbohydrates in [C_4mim][DMP] is substantially higher than that observed in [C_4mim][$N(CN)_2$].

Aiming at better understanding the enhanced solubility of carbohydrates in hydrophilic ILs, the activity coefficients for each monosaccharide were further determined. Solvents with low capacity to dissolve carbohydrates, namely methanol and ethanol, were also considered for comparison purposes. The activity coefficients of each carbohydrate were determined accordingly to the following equation,

$$\gamma = \left(\frac{1}{x_{CH}}\right) e^{\left(\left(-\frac{\Delta H_f}{R}\right)\left(\frac{1}{T}-\frac{1}{T_m}\right)+\frac{\Delta C_p}{R}\left(\left(\frac{T_m}{T}\right)-\ln\left(\left(\frac{T_m}{T}\right)-1\right)\right)\right)} \qquad \text{Eq.1}$$

Where $\Delta_f H$ represents the enthalpy of fusion ($J \cdot mol^{-1}$ at 298 K) of each carbohydrate, R is the universal gas constant (8.314 $J \cdot mol \cdot K^{-1}$), T is temperature (K), T_m is the melting temperature of each carbohydrate (K), x_{CH} is the mole fraction solubility of the solute in each solvent and ΔC_p is the heat capacity of the monosaccharide. The physical properties of each carbohydrate are indicated in Table 8 and were taken from literature [42-43].

Table 8 Carbohydrate physical properties [42-43]

Carbohydrate	$\Delta_f H$ / (J·mol^{-1} at 298 K)	T_m / (K)	ΔCp / (J / (mol · K))
D-(+)-Glucose	32 248	423.15	120.0
D-(+)-Mannose	24 687	407.15	120.0
D-(-)-Fructose	26 030	378.15	120.0
D-(+)-Galactose	43 778	436.15	120.0
D-(+)-Xylose	31 650	423.15	120.0
L-(+)-Arabinose	35 626	428.65	120.0

Results for the activity coefficients of each carbohydrate in both ILs evaluated are displayed in Table 9.

Table 9 Experimental activity coefficients of each carbohydrate (γ_{CH}) in [C_4mim][$N(CN)_2$] and [C_4mim][DMP] at different temperatures

Carbohydrate	x_{CH}	γ_{CH} [C_4mim][$N(CN)_2$]	x_{CH}	γ_{CH} [C_4mim][DMP]
	0.142	0.324	0.035	1.316
	0.170	0.342	0.045	1.292
	0.191	0.384	0.074	0.994
D-(+)-Glucose	0.229	0.406	0.132	0.703
	0.250	0.469	0.158	0.742
	0.280	0.528	0.232	0.637
	0.319	0.583		
	x_{CH}	γ_{CH} [C_4mim][$N(CN)_2$]	x_{CH}	γ_{CH} [C_4mim][DMP]
	0.172	0.755	0.029	4.443
	0.197	0.769	0.052	2.915
	0.226	0.785	0.070	2.540
D-(+)-Mannose	0.261	0.803	0.121	1.736
	0.301	0.824	0.175	1.417
	0.331	0.889	0.230	1.280
	0.390	0.898		

	x_{CH}	γ_{CH} [C_4mim][$N(CN)_2$]	x_{CH}	γ_{CH} [C_4mim][DMP]
	0.132	1.024	0.015	8.889
	0.153	1.102	0.028	6.027
	0.178	1.183	0.042	4.967
D-(-)-Fructose	0.201	1.312	0.056	4.747
	0.220	1.499	0.099	3.332
	0.245	1.683	0.125	3.300
	0.275	1.876		

	x_{CH}	γ_{CH} [C_4mim][$N(CN)_2$]	x_{CH}	γ_{CH} [C_4mim][DMP]
	0.142	0.060	0.070	0.121
	0.165	0.075	0.112	0.110
	0.192	0.092	0.182	0.097
D-(+)-Galactose	0.221	0.114	0.220	0.115
	0.248	0.144	0.344	0.104
	0.268	0.188	0.412	0.122
	0.298	0.236		

	x_{CH}	γ_{CH} [C_4mim][$N(CN)_2$]	x_{CH}	γ_{CH} [C_4mim][DMP]
	0.182	0.275	0.080	0.623
	0.208	0.300	0.126	0.495
D-(+)-Xylose	0.250	0.313	0.211	0.371
	0.280	0.350	0.302	0.325
	0.314	0.392	0.453	0.272
	0.355	0.434	0.503	0.306
	0.402	0.480		

	x_{CH}	γ_{CH} [C_4mim][$N(CN)_2$]	x_{CH}	γ_{CH} [C_4mim][DMP]
	0.142	0.197	0.050	0.560
	0.165	0.222	0.078	0.470
L-(+)-Arabinose	0.185	0.259	0.115	0.418
	0.221	0.283	0.182	0.344
	0.241	0.338	0.235	0.346

	0.270	0.390	0.332	0.318
	0.301	0.453		

The activity coefficient is typically used in thermodynamics to account for deviations from the ideal behaviour in a particular solution. In an ideal mixture, the interactions between each pair of chemical species are similar. For an ideal solution, the value of the activity coefficient should be 1. So, the higher the activity coefficients, the lower the interactions occurring between the solvent and solute [103].

Representing thus the activity coefficients as a function of the mole fraction of each sugar can provide us the information regarding the interactions strength (favorable or not favorable) between the carbohydrate and the ionic liquid. Figure 32 and Figure 33 present the activity coefficients of the distinct carbohydrates in $[C_4mim][N(CN)_2]$ and $[C_4mim][DMP]$.

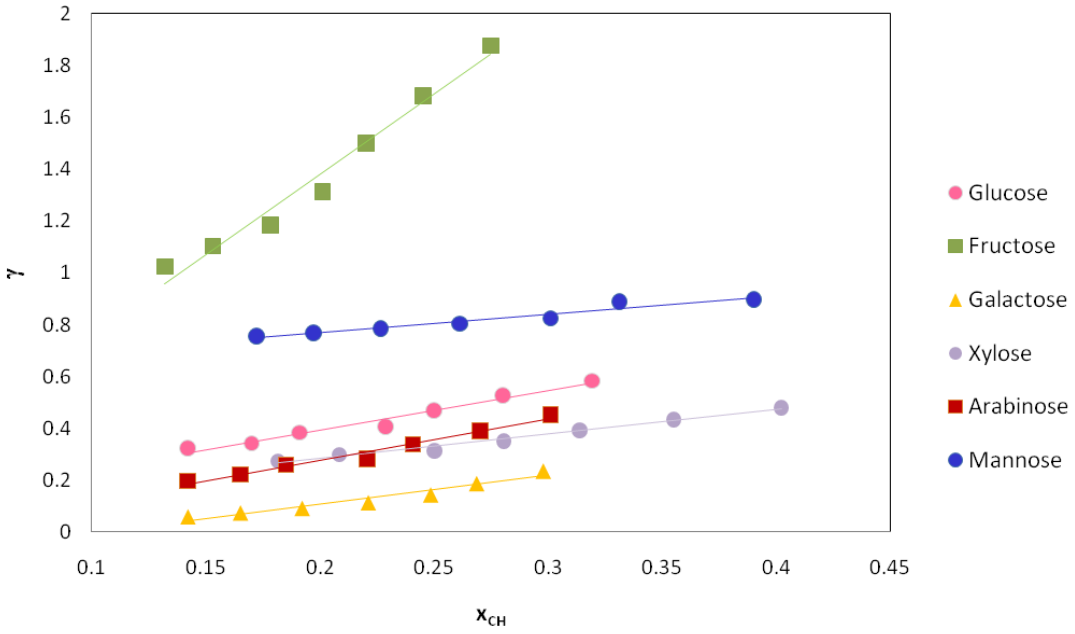

Figure 32 Activity coefficients for carbohydrates in $[C_4mim][N(CN)_2]$. The lines are just guides to the eye

Considering Figure 32, it can be observed that fructose is the only carbohydrate presenting positive deviations reflecting the non favorable interactions between the sugar and the IL. The remaining carbohydrates present activity coefficients below 1 at all the temperatures studied indicating favourable interactions between the monosaccharides and $[C_4mim][N(CN)_2]$.

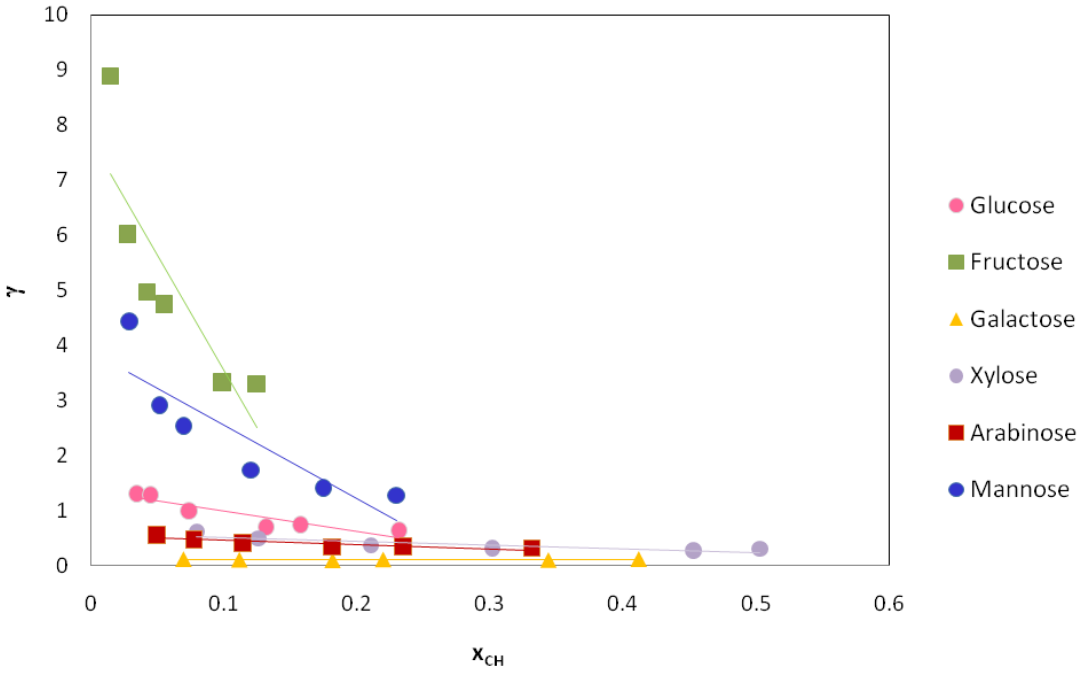

Figure 33 Activity coefficients for carbohydrates in $[C_4mim][DMP]$. The lines are just guides to the eye

For $[C_4mim][DMP]$, fructose and mannose are the carbohydrates that present positive deviations. Both carbohydrates display non favorable interactions with $[C_4mim][DMP]$ and are reflected by the low solubility values observed with these two sugars. The remaining carbohydrates present favorable interactions with the IL at all composition regimes evaluated. Moreover, arabinose and xylose, both pentoses, present similar activity coefficient values.

3.2.3 Hydrophobic Ionic Liquids

3.2.3.1 Chemicals

D-(+)-glucose, > 99.5 wt % pure, was from Scharlau. The hydrophobic ILs selected were based on the trihexyltetradecylphosphonium cation combined with different anions. Trihexyltetradecylphosphonium dicyanamide, $[P_{66614}][N(CN)_2]$, (mass fraction purity ≈ 97 %) and trihexyltetradecylphosphonium chloride, $[P_{66614}]Cl$, (mass fraction purity ≈ 93-95 %) were kindly provided by Cytec Industries. To reduce the water content and volatile compounds to negligible values, IL samples were dried at vacuum and at 333 K, using continuous stirring, for a minimum of 48 h. After that procedure, the IL and carbohydrates purities were checked by ^{1}H, ^{13}C, ^{19}F and ^{31}P NMR spectroscopy. The solvent used on the coulometric Karl Fischer titration was Hydranal-Coulomat AG from Riedel de Haën.

3.2.3.2 Methods

The water content in both ILs and glucose samples were determined using a Metrohm 831 Karl-Fischer (KF) coulometer.

Glucose and ILs were added in excess amounts and equilibrated by means of an air oven under constant agitation using an Eppendorf Thermomixer Comfort equipment. Previous optimizing equilibration conditions conducted to a stirring velocity of 750 rpm, at least for 24 h, and at each temperature of interest. After the saturation conditions achievement all samples were centrifuged in a Hettich Mikro 120 centrifuge to properly separate both macroscopic phases during 20 minutes at 4500 rpm. Approximately 1 g (gravimetrically determined within 10^{-5} g) of the saturated IL solution with glucose was taken and the sugar was precipitated using an antisolvent - dichloromethane. The precipitated sugar was filtrated and further washed with dichloromethane to completely remove IL traces. The glucose content was determined by weight with an uncertainty of $\pm 10^{-5}$g.

Aiming at calibrating the temperature maintained in the air oven it was used a Pt100 calibrated probe. The Pt 100 probe was immersed in the IL-carbohydrate solution and temperatures were registered. The results are presented in Appendix C and no major deviations in temperature were found.

3.2.4 Results and Discussion

Table 10 shows the experimental values for the solubility of D-(+)-glucose in $[P_{66614}][N(CN)_2]$ obtained in this work and those shown in literature [11] obtained by a different quantitative method - HPLC. The results gathered in this work show a good agreement with literature values [11]. The results obtained are slightly inferior to literature values [11] but it should be remarked the lower water contents in the IL used in this work that tend to reduce the solubility of carbohydrates.

Table 10 Mole fraction solubility of D-(+)-glucose in $[P_{66614}][N(CN)_2]$ obtained in this work and literature values [11]

Carbohydrate	T/ K	Water content wt %	x_{CH} literature	Water content wt %	x_{CH} this work
D-(+)-Glucose	308.15	0.03 [11]	0.015	0.02	0.010

Experimental results for the solubility of D-(+)-glucose in $[P_{66614}][N(CN)_2]$ at different temperatures are presented in Table 11. The maximum water content in $[P_{66614}][N(CN)_2]$ in all measurements at different temperatures was 0.08 wt %.

Table 11 Mole fraction solubility of D-(+)-glucose in $[P_{66614}][N(CN)_2]$ obtained in this work at different temperatures

Carbohydrate	T / K	$(1/T)$ / (K^{-1})	x_{CH}	$\ln x_{CH}$	$\sigma(x_{CH})$	$\sigma(\ln x_{CH})$
D-(+)-Glucose	288.15	0.00347	0.007	-4.957	0.003	0.332
	308.15	0.00325	0.010	-4.635	0.002	0.228
	318.15	0.00314	0.011	-4.519	0.002	0.214

The experimental solubility values of D-(+)-Glucose in $[P_{66614}]Cl$ at different temperatures are displayed in Table 12. The mass fraction values of water in $[P_{66614}]Cl$ were maintained below 0.118 wt %.

Table 12 Experimental data for the solubility of D-(+)-Glucose in $[P_{66614}]Cl$

Carbohydrate	T / K	$(1/T)$ / (K^{-1})	x_{CH}	$\ln x_{CH}$	$\sigma(x_{CH})$	$\sigma(\ln x_{CH})$
D-(+)-Glucose	298.2	0.00336	0.008	-4.828	0.001	0.125
	308.2	0.00325	0.012	-4.423	0.002	0.167
	318.2	0.00314	0.021	-3.863	0.004	0.190
	328.2	0.00305	0.047	-3.058	0.006	0.128
	338.2	0.00296	0.052	-2.957	0.004	0.077

Figure 34 presents the experimental solubility values of D-(+)-glucose in $[P_{66614}][N(CN)_2]$ and $[P_{66614}][Cl]$ from 288.15 K to 348.15 K.

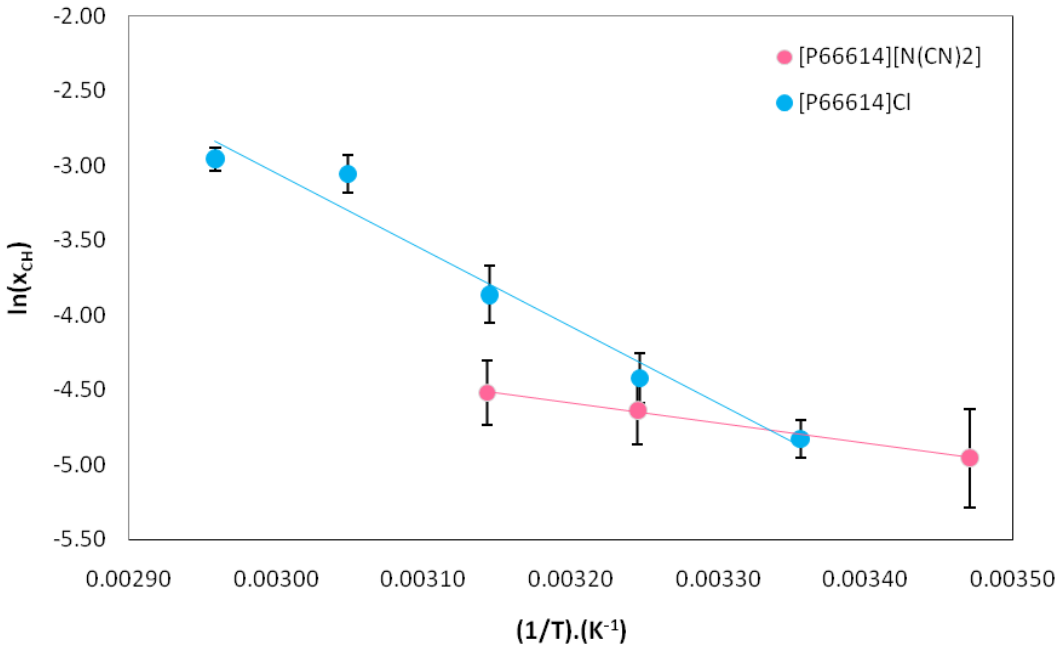

Figure 34 $\ln x_{CH}$ (D-(+)-glucose) as a function of $1/T$ in $[P_{66614}][N(CN)_2]$ and $[P_{66614}]Cl$

The solubility of D-(+)-glucose is higher in $[P_{66614}]Cl$ than in $[P_{66614}][N(CN)_2]$. Curiously, and as observed with hydrophilic ILs, there is a temperature were the dicyanimide-based IL dissolves more glucose than the chloride-based IL. Nevertheless, it should be remarked the higher water content in $[P_{66614}]Cl$ that could increase the solubility values of the carbohydrate.

Figure 35 shows a comparison of the solubility of glucose in both hydrophilic and hydrophobic ILs studied in the temperature range between 288.15 K and 348.15 K.

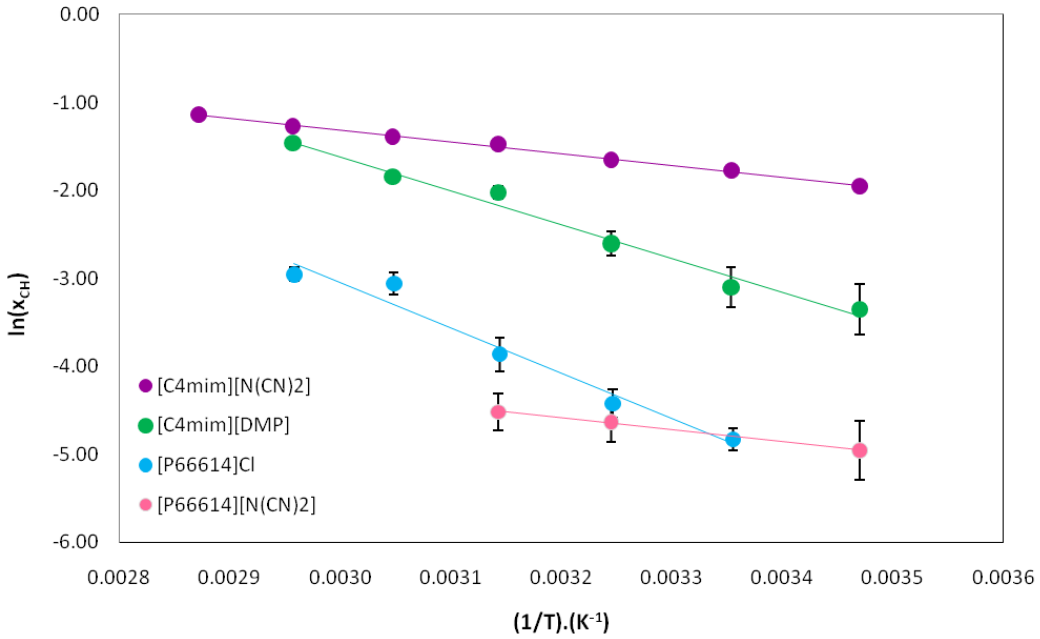

Figure 35 $\ln x_{CH}$ (D-(+)-glucose) as a function of $1/T$ in hydrophobic and hydrophilic ILs

As expected the phosphonium-based ILs, $[P_{66614}][N(CN)_2]$ and $[P_{66614}]Cl$, present a lower capability to dissolve glucose, since their cationic ability to hydrogen bond with the carbohydrates hydroxyl groups is largely reduced (compared to imidazolium cores). Nevertheless, from the results gathered it seems that the IL cation also plays an important role in the carbohydrates solubility. The solvation of carbohydrates is manly defined by the IL anion – trend that is visible from the enthalpy of solution derived from the solubilities temperature dependence.

3.3 Conclusions

The solubility of six monosaccharides in selected ILs were studied in a broad range of temperatures aiming at better understanding the solubility dependence on temperature of carbohydrates in these novel systems. Indeed, no systematic studies concerning the temperature influence on the carbohydrates dissolution in ILs were found in literature.

The ionic liquids nature was also investigated using two hydrophilic ILs, $[C_4mim][N(CN)_2]$ and $[C_4mim][DMP]$, and two hydrophobic ILs, $[P_{66614}][N(CN)_2]$ and $[P_{66614}]Cl$. With such a combination it was possible to analyze the IL anion and cation effects through the solubilization of carbohydrates. Hydrophilic ILs present solubility values 10 orders of magnitude higher than hydrophobic ILs. In fact, the results obtained among the hydrophilic ILs are of the same order of magnitude than those observed in water if a molar fraction basis is considered. At lower temperatures dicyanamide-based ILs dissolve more sugars than chloride- or dimethylphosphate-based ILs. For both families it was observed a critical temperature turnover where $[C_4mim][DMP]$ and $[P_{66614}]Cl$ start to dissolve more carbohydrate contents than their dicyanamide-counterparts. From all the results it was observed that the IL anion plays the major goal in the solubility capacity of ILs for carbohydrates.

This study showed the high potential of ILs to dissolve carbohydrates and represents a new contribution towards the carbohydrates chemistry.

4. General Conclusions

Typical environmentally friendly resources (such as cellulose) are usually processed by environmentally damaging processes making use of volatile and non benign solvents. Environmentally friendly processes that use biomass must be coupled to other materials capable of minimizing the actual critical concerns related to the declining resources of fossil fuels and global heating. Therefore, in this work ionic liquids (ILs) are proposed as greener and potential solvents for cellulose and monosaccharides. The combination of biomass resources with greener solvents will contribute to the improvement of our living standards.

In the first section of this work it was shown that pure ILs, or ILs mixtures, can be used in electrospinning processes and appropriately replace typical volatile organic solvents commonly used. The results obtained indicated a decrease in the cellulose fibers diameter from 10 μm to 300 nm. These nanosized fibers could lead to the enhancement of certain properties, such as surface energy, glass transition, thermal and electrical conductivity, and surface reactivity enhancing the biopolymer practical applications.

In the second section of this thesis it was shown the high potential of adequate ILs for dissolving monosaccharides. Hydrophilic ILs present enhanced abilities to dissolve carbohydrates compared to hydrophobic ILs (10 orders of magnitude in a mole fraction basis). Moreover, the solubilities of carbohydrates in hydrophilic ILs are of the same order of magnitude of those observed in a molecular solvent – water. For the first time a systematic study on the solubility of carbohydrates in ILs and their dependence on temperature was demonstrated. From the patterns obtained it was shown that the enthalpies of solution of carbohydrates are more dependent on the IL anion than on the IL cation.

5. Future Work

As future work, it would be interesting to process other polysaccharides in ILs solutions by electrospinning or even dissolve cellulose in different ionic liquids to assess whether there are any differences in the morphology of the obtained fibers.

In order to understand the interactions at the molecular level between the ILs and monosaccharides, some NMR in situ studies should be conducted.

To complete the knowledge related to hydrophobic ILs, the study will be extended to other monosaccharides.

An extensive study of the anion effect in the solubility of the carbohydrates should be performed as well, in order to corroborate the anion effect for both families of ILs, both hydrophilic and hydrophobic.

6. Bibliographic References

1. Klass, D.L., *Biomass for renewable energy, fuels and chemicals*. Academic Press ed. 1998, San Diego, CA.

2. Demirbas, A., *Biofuels - Securing the planet's future energy needs*. 2009, London: Springer.

3. Brown, R.C., *Biorenewable resources - Engineering new products from agriculture*, ed. 1st. 2003, Ames - Iowa.

4. Fernando, S., Adhikari, S., Chandrapal, C.Murali, N., *Biorefineries: current status, challenges, and future Direction.* Energy & Fuels, 2006(20): p. 1727-1737.

5. Sjöström, E., *Wood Chemistry:Fundamentals and Applications*. 2 ed, ed. A. Press. 1992, San Diego - Calofornia.

6. Xu, S., Zhang, J., He, A., Li, J., Zhang, H.Han, C.C., *Electrospinning of native cellulose from nonvolatile solvent system.* Polymer, 2008. 49: p. 2911 - 2917.

7. Frey, M.W., *Electrospinning Cellulose and Cellulose Derivatives.* Polymer Reviews, 2008. 48: p. 378 - 391.

8. Lu, P.Ding, B., *Applications of Electrospun Fibers.* Recent Patents on Nanotechnology, 2008. 2: p. 169 - 182.

9. Quan, S.L., Kang, S.G.Chin, I.J., *Characterization of cellulose fibers electrospun using ionic liquids.* Cellulose, 2010. 17: p. 223-230.

10. Viswanathan, G., Murugesan, S., Pushparaj, V., Nalamasu, O., Ajayan, P.M.Linhardt, R.J., *Preparation of biopolymer fibers by electrospinning from room temperature ionic liquids.* Biomacromolecules, 2006. 7(2): p. 415 - 418.

11. Rosatella, A.A., Branco, L.C.Afonso, C.A.M., *Studies on dissolution of carbohydrates in ionic liquids and extraction from aqueous phase.* Green Chemistry, 2009. 11: p. 1406-1413.

12. Seoud, O.A., Koschella, A., Fidale, L.C., Dorn, S.Heinze, T., *Applications of ionic liquids in carbohydrates chemistry: A window of opportunities.* Biomacromolecules, 2007. 8(9): p. 2629-2647.

13. Marsh, K.N., Boxall, J.A.Lichtenthaler, R., *Room temperature ionic liquids and their mixtures-a review.* Fluid phase equilibria, 2004. 219: p. 93 - 98.

14. Freire, M.G., Carvalho, P.J., Fernandes, A.M., Marrucho, I.M., Queimada, A.J.Coutinho, J.A.P., *Surface tensions of imidazolium based ionic liquids: Anion, cation, temperature and water effect.* Journal of Colloid and Interface Science 2007. 314: p. 621 - 630.

15. Earle, M.J., Esperança, J.M.S.S., Gilea, M.A., Lopes, J.N.C., Rebelo, L.P.N., Magee, J.W., Seddon, K.R.Widegren, J.A., *The distillation and volatility of ionic liquids.* Nature, 2006. 439: p. 831 - 834.

16. Gathergood, N., Garcia, M.T.Scammells, P.J., *Biodegradable ionic liquids: Part I. Concept, preliminary targets and evaluation.* Green Chemistry, 2004. 6: p. 166 -175.

17. Plechkova, N.V.Seddon, K.R., *Applications of ionic liquids in the chemical industry.* Chemical Society Reviews, 2007. 37: p. 123 - 150.

18. Soto, A., Arce, A.Khoshkbarchi, M.K., *Partitioning of antibiotics in a two liquids phase system formed by water and room temperature ionic liquids.* Separation and Purification Technology, 2005. 44: p. 242 - 246.

19. Huddleston, J.G., Willauer, H.D., Swatloski, R.P., Visser, A.E.Rogers, R.D., *Room temperature ionic liquids as novel media for 'clean' liquid-liquid extraction* Chemical Communications, 1998. 16: p. 1765 - 1766.

20. Earle, M.J.Seddon, K.R., *Ionic Liquids. Green solvents for the future.* Pure Applied Chemistry, 2000. 72(7): p. 1391 - 1398.

21. Meli, L., Miao, J., Dordick, J.S.Linhardt, R.J., *Electrospinning from room temperature ionic liquids for biopolymer fiber formation.* Green Chemistry, 2010. 12: p. 1883 - 1892.

22. Zhu, S., Wu, Y., Che, Q., Yu, Z., Wang, C., Jin, S., Ding, Y.Wu, G., *Dissolution of cellulose with ionic liquids and its application: a mini-review.* Green Chemistry, 2006. 8: p. 325-327.

23. Keskin S., K.-T.D., Akman U., Hortaçsu O. , *A review of ionic liquids towards supercritical fluid applications.* J. of Supercritical Fluids 2007. 43: p. 150 - 180.

24. Chiappe, C.Pieraccini, D., *Ionic liquids: solvents properties and organic reactivity.* Journal of physical Organic Chemistry, 2005. 18: p. 275 - 297.

25. Freire, M.G., Neves, C.M.S.S., Marrucho, I.M., Coutinho, J.A.P.Fernandes, A.M., *Hydrolysis of tetrafluoroborate and hexafluorophosphate counter ions in imidazolium-based ionic liquids.* Journal of Physical Chemistry A, 2010. 114: p. 3744 - 3749.

26. Coleman, D.Gathergood, N., *Biodegradation studies of ionic liquids.* Chemical Society Reviews, 2010. 39: p. 600 - 637.

27. Garcia, M.T., Gathergood, N.Scammells, P.J., *Biodegradable ionic liquids. Part II. Effect of the anion and toxicology.* Green Chemistry, 2005. 7: p. 9 -14.

28. Dong, K., Zhang, S., Wang, D.Yao, X., *Hydrogen Bonds in Imidazolium Ionic Liquids.* Journal of Physical Chemistry A, 2006. 110(31): p. 9775 - 9782.

29. Pinkert, A., Marsh, K.N., Pang, S.Staiger, M.P., *Ionic liquids and their interactions with cellulose.* Chemical Reviews, 2009.

30. Wilkes, J.S., *Properties of ionic liquid solvents for catalysis.* Journal of Molecular Catalysis, 2004. 214: p. 11 - 17.

31. Seddon, K.R., Stark, A.Torres, M.J., *Influence of chloride, water, and organic solvents on the physical properties of ionic liquids.* Pure Applied Chemistry, 2000. 72(12): p. 2275 - 2287.

32. Sun, N., Rahman, M., Qin, Y., Maxim, M.L., Rodríguez, H.Rogers, R.D., *Complete dissolution and partial delignification of wood in the ionic liquid 1-ethyl-3-methylimidazolium acetate.* Green Chemistry, 2009. 11: p. 646 - 655.

33. MacFarlane, D.R., Golding, J., Forsyth, S., Forsyth, M.Deacon, G.B., *Low viscosity ionic liquids based on organic salts of the dicyanamide anion.* Chemical Communications, 2001: p. 1430 - 1431.

34. Carvalho, P.J., Regueira, T., Santos, L.M.N.B.F., Fernandez, J.Coutinho, J.A.P., *Effect of water on the viscosities and densities of 1-butyl-3-methylimidazolium dicyanamide and 1-butyl-3-methylimidazolium tricyanomethane at atmospheric pressure.* Journal of Chemical & Engeneering Data 2010. 55: p. 645 - 652.

35. Carvalho, P.J., Freire, M.G., Marrucho, I.M., Queimada, A.J.Coutinho, J.A.P., *Surface Tensions for the 1-Alkyl-3-methylimidazolium Bis(trifluoromethylsulfonyl)imide Ionic Liquids.* Journal of Chemical & Engeneering Data 2008. 53: p. 1346-1350.

36. Law, G.Watson, P.R., *Surface tension measurements of N-alkylimidazolium ionic liquids.* Langmuir, 2001. 17(20): p. 6138-6141.

37. Matzke, M., Stolte, S., Thiele, K., Juffernholz, T., Arning, J., Ranke, J., Welz-Biermannd, U.Jastorff, B., *The influence of anion species on the toxicity of 1-alkyl-3-methylimidazolium ionic liquids observed in an (eco)toxicological test battery.* Green Chemistry, 2007. 9: p. 1198 - 1207.

38. Ventura, S.P.M., Gonçalves, A.M.M., Gonçalves, F.Coutinho, J.A.P., *Assessing the toxicity on [C_3mim][NTf_2] to aquatic organisms of different trophic levels.* Aquatic Toxicology 2010. 96: p. 290 - 297.

39. Stolte, S., Matzke, M., Arning, J., Böschen, A., Pitner, W.-R., Welz-Biermann, U., Jastorffa, B.Ranke, J., *Effects of different head groups and functionalised side chains on the aquatic toxicity of ionic liquids.* Green Chemistry, 2007. 9: p. 1170 - 1179.

40. Poole, C.F.Poole, S.K., *Extraction of organic compounds with room temperature ionic liquids.* Journal of Chromatography A, 2009.

41. Carmichael, A.J.Seddon, K.R., *Polarity study of some 1-alkyl-3-methylimidazolium ambient-temperature ionic liquids with the solvatochromic dye, Nile Red.* Journal of Physical Organic Chemistry, 1998. 76: p. 32 - 37.

42. Dyekjær, J.D.Jónsdóttir, S.Ó., *QSPR models for various physical properties of carbohydrates based on molecular mechanics and quantum chemical calculations.* Carbohydrate Research, 2004. 339: p. 269 - 280.

43. Ferreira, O., Brignole, E.A.Macedo, E.A., *Phase equilibria in sugar solutions using the A-UNIFAC model.* Industrial & Engineering Chemistry Research, 2003. 42: p. 6212 - 6222.

44. Fredlake, C.P., Crosthwaite, J.M., Hert, D.G., Aki, S.N.V.K.Brennecke, J.F., *Thermophysical properties of imidazolium-based ionic liquids.* Journal of Chemical & Engeneering Data 2004. 49: p. 954 - 964.

45. Sjöström, E., *Wood Chemistry:Fundamentals and Applications*, ed. A. Press. 1993.

46. Klemm, D., Philipp, B., Heinze, T., Heinze, U.Wagenknecht, W., *Comprehensive Cellulose Chemistry - Fundamentals and Analytical Methods*. Vol. Volume I. 1998, Weinheim: Wiley-VCH.

47. Sixta, H., *Handbook of pulp*, ed. Wiley-VCH. 2006, Weinheim.

48. Fengel, D.Wegener, G., *Wood: Chemistry, Ultrastructure, Reactions*, ed. W.d. Gruyter. 1984, New York.

49. Smook, G.A., *Handbook for Pulp and Paper Technologists*, ed. 3. 2002, Vancouver: Angus Wilde Publications Inc.

50. Rowell, R.M., *Handbook of Wood Chemistry and Wood Composites*, ed. R. Rowell. 2005, Florida: CRS Press.

51. Dumitriu, S., *Polysaccharides: Structural Diversity and Functional Versatility*. 2 ed. 2004, New York: CRC Press.

52. Klemm, B.D., Heublein, H.P.Fink, A.B., *Cellulose: Fascinating biopolymer and sustainable raw material.* Angewandte Chemie, 2005. 44(22): p. 3358 - 3393.

53. Kondo, T., *Hydrogen Bonds in Cellulose and Cellulose Derivatives*, in *Polysaccharides: structural diversity and functional versatility*. 2005, Marcel Dekker: New York.

54. Sjöström, E., *Wood Chemistry: Fundamentals and Applications*. 1993, London: Academic Press.

55. Gilbert, R.D.Kadla, J.F., *Preparation and Properties of Cellulosic Biocomponent Fibers*, in *Polysaccharides: structural diversity and functional versatility*, S. Dumitriu, Editor. 2005, Marcel Dekker: New York.

56. Zakrzewska, M.E., Bogel-Lukasik, E.Bogel-Lukasic, R., *Solubility of carbohydrates in ionic liquids.* Energy & Fuels, 2010. 24: p. 737 - 745.

57. Carey, A.F., *Organic Chemistry 6st editon*. 2003, New York: McGraw-Hill.

58. Weil, J.H., *Bioquímica Geral*. Fundação calouste Gulbenkian, ed. edição. 2000, Lisboa.

59. Morrison, R., *Química orgânica*. Fundação Calouste Gulbenkian, ed. 13st. 1996, Lisboa.

60. Schiffman, J.D.Schauer, C.L., *A Review: Electrospinning of Biopolymer Nanofibers and their Applications.* Polymer Reviews, 2008. 48: p. 317 - 352.

61. Ramakrishna, S., Fujihara, K., Teo, W.-E., Lim, T.C.Ma, Z., *An introduction to electrospinning and nanofibres*. 2005, Singapore: World Scientific Publishing Co. Pte. Ltd.

62. Kameoka, J., Orth, R., Yang, Y.N., Czaplewski, D., Mathers, R., Coates, G.W.Craighead, H.G., *A scanning tip electrospinning source for deposition of oriented nanofibres.* Nanotechnology, 2003. 14(10): p. 1124 - 1129.

63. Zong, X.H., Kim, K., Fang, D.F., Ran, S.F., Hsiao, B.S.Chu, B., *Structure and process relationship of electrospun bioabsorbable nanofiber membranes.* Polymer, 2002. 43: p. 4403 - 4412.

64. Zeng, J., Xu, X., Chen, X., Liang, Q., Bian, X., Yang, L.Jing, X., *Biodegradable electrospun fibers for drug delivery.* Journal of Controlled Release, 2003. 92: p. 227 - 231.

65. Mit-uppatham, C., Nithitanakul, M.Supaphol, P., *Ultrafine electrospun polyamide-6 fibers: Effect of solution conditions on morphology and average fiber diameter.* Macromolecular Chemistry and Physics, 2004. 205: p. 2327 - 2338.

66. Zhao, S., Wu, X., Wang, L.Huang, Y., *Electrospinning of Ethyl-Cyanoethyl Cellulose/Tetrahydrofuran Solutions.* Journal of Applied Polymer Science 2004. 91: p. 242 - 246.

67. Kessick, R., Fenn, J.Tepper, G., *The use of AC potentials in electrospraying and electrospinning processes.* Polymer, 2004. 45: p. 2981 - 2984.

68. Liu, H.Q.Hiseh, Y.L., *Ultrafme fibrous cellulose membranes from electrospinning of cellulose acetate.* Joournal Polymer Science B Polymer Physics, 2002. 40: p. 2119- 2129.

69. Buchko, C.J., Chen, L.C., Shen, Y.Martin, D.C., *Processing and microstructural characterization of porous biocompatible protein polymer thin films.* Polymer, 1999. 40(26): p. 7397-7407.

70. Egorov, V.M., Smirnova, S.V., Formanovsky, A.A., Pletnev, I.V.Zolotov, Y.A., *Dissolution of cellulose in ionic liquids as a way to obtain test materials for metal-ion detection.* Analitycal and Bioanalitycal Chemistry, 2007. 387(2263-2269).

71. Liebert, T.Heinze, T., *Interaction of ionic liquids with polysaccharides 5. Solvents and reaction media for the modification of cellulose.* Bioresources, 2008. 3(2): p. 576-601.

72. Dadi, A.P., Varanasi, S.Schall, C.A., *Enhancement of cellulose saccharification kinetics using an ionic liquid pretreatment step.* Biotechnology and Bioengineering, 2006. 95(5).

73. Singh, S., Simmons, B.A.Vogel, H.P., *Visualization of biomass solubilization and cellulose regeneration during ionic liquid pretreatment of switchgrass.* Biotechnology and Bioengineering, 2009. 104(1): p. 68-75.

74. Murugesan, S.Linhardt, R.J., *Ionic liquids in carbohydrate chemistry - Current trends and future directions.* Current Organic synthesis, 2005. 2(437-451).

75. Fukaya, Y., Hayashi, K., Wada, M.Ohno, H., *Cellulose dissolution with polar ionic liquids under mild conditions required factors for anions.* Green Chemistry, 2008. 10: p. 44 - 46.

76. Liu, Q., Janssen, M.H.A., Rantwijk, F.v.Sheldon, R.A., *Room-temperature ionic liquids that dissolve carbohydrates in high concentrations.* Green Chemistry, 2004. 7: p. 39 - 42.

77. Zhao, H., Baker, G.A., Song, Z., Olubajo, O., Crittle, T.Peters, D., *Designing enzyme-compatible ionic liquids that can dissolve carbohydrates.* Green Chemistry, 2008. 10: p. 696 - 705.

78. Tan, S.S.Y.MacFarlane, D.R., *Ionic liquids in biomass processing*, in *Ionic liquids* B. Kirchner, Editor. 2010: Leipzig. p. 311 - 333.

79. Swatloski, R.P., Spear, S.K., Holbrey, J.D.Rogers, R.D., *Dissolution of cellulose with ionic liquids.* Journal of the American Chemical Society 2002. 124: p. 4974-4975.

80. Zhao, H., Jones, C.L., Xia, G.A., Baker, S., Olubajo, O.Person, V.N., *Regenerating cellulose fron ionic liquids for an accelerated enzymatic hydrolysis.* Journal of Biotechnology, 2009. 139: p. 47-54.

81. Zhao, H., Xia, S.Q.Ma, P.S., *Use of ionic liquids as 'green' solvents for extractions.* Journal of Chemical Technology and Biotechnology, 2005. 80(10): p. 1089 - 1096.

82. Zhang, H., Wu, J., Zhang, J.He, J., *1-allyl-3-methylimidazolium chloride room temperature ionic liquid: a new ans powerful nonderivatizing solvent for cellulose.* Macromolecules, 2005. 38: p. 8272-8277.

83. Zhang, J., Zhang, H., Wu, J., Zhang, J., Hea, J.Xiang, J., *NMR spectroscopic studies of cellobiose solvation in EmimAc aimed to understand the dissolution mechanism of cellulose in ionic liquids.* Physical Chemistry Chemical Physics, 2010. 12: p. 1941 - 1947.

84. Xu, A., Wang, J.Wang, H., *Effects of the anionic structure and lithium salts addition on the dissolution of cellulose in 1-butyl-3-methylimidazolium-based ionic liquids solvent systems.* Green Chemistry, 2010. 10: p. 268-275.

85. Kim, C.-W., Frey, M.W., Marquez, M.Joo, Y.L., *Preparation of submicron-scale, electrospun cellulose fibers via direct dissolution.* Journal of Polymer Science B: Polymer Physics, 2005. 43: p. 1673 - 1683.

86. Kim C., e.a., *Preparation of submicron-scale, electrospun cellulose fibers via direct dissolution.* Journal of Polymer Science Part B Polym Phys, 2005. 43: p. 1673 - 1683.

87. Kulpinski, P., *Cellulose Nanofibers Prepared by the N-methylmorpholine-N-oxide Method.* Journal of Applied Polymer Science, 2005. 98: p. 1855 - 1859.

88. Blesic, M., Marques, M.H., Plechkova, N.V., Seddon, K.R., Rebelo, L.P.N.Lopes, A., *Self-aggregation of ionic liquids: micelle formation in aqueous solution.* Green Chemistry, 2007. 9(5): p. 481 - 490.

89. Velasco, S.B., Turmine, M., Caprio, D.D.Letellier, P., *Micelle formation in ethyl-ammonium nitrate (an ionic liquid).* Colloids and Surfaces A 2006. 275(1-3): p. 50 - 54.

90. Zugenmaier, P., *Crystalline Cellulose and Cellulose Derivatives - Characterization and Structures*. Springer Series in Wood Science, ed. T.E.T.a.R. Wimmer. 2008, Berlin: Springer.

91. Forsyth, S.A., MacFarlane, D.R., Thomsonb, R.J.Itzsteinb, M.v., *Rapid, clean, and mild O-acetylation of alcohols and carbohydrates in an ionic liquid.* Chemical Communications, 2002: p. 714 - 715.

92. Kimizuka, N.Nakashima, T., *Spontaneous self-assembly of glycolipid bilayer membranes in sugar-philic ionic liquids and formation of ionogels.* Langmuir, 2001. 17(22): p. 6759 - 6761.

93. Remsing, R.C., Hernandez, G., Swatloski, R.P., Massefski, W.W., Rogers, R.D.Moyna, G., *Solvation of carbohydrates in N,N'-dialkylimidazolium ionic liquids: A multinuclear NMR spectroscopy study.* Journal of Physical Chemistry, 2008. 112: p. 11071-11078.

94. Kiefer, J., Obert, K., Bçsmann, A., Seeger, T., Wasserscheid, P.Leipertz, A., *Quantitative analysis of alpha-d-glucose in an ionic liquid by using infrared spectroscopy*. Journal of Chemical Physics and Physical Chemistry 2008. 8: p. 1317 - 1322.

95. Park, S.Kazlauskas, R.J., *Improved preparation and use of room-temperature ionic liquids in lipase-catalyzed enantio- and regioselective acylations.* Journal of Organic Chemistry, 2001. 66: p. 8395 - 8401.

96. Youngs, T.G.A., Hardacre, C.Holbrey, J.D., *Glucose Solvation by the Ionic Liquid 1,3-Dimethylimidazolium Chloride: A Simulation Study.* Journal of Physical Chemistry B 2007. 111(13765 - 13774).

97. Atefi, F., Garcia, M.T., Singer, R.D.Scammells, P.J., *Phosphonium ionic liquids: design, synthesis and evaluation of biodegradability.* Green Chemistry, 2009. 11: p. 1595 - 1604.

98. Spiliotis, N.Tassios, D., *A UNIFAC model for phase equilibrium calculations in aqueous and nonaqueous sugar solutions.* Fluid Phase Equilibria, 2000. 173: p. 39 - 55.

99. Jónsdóttir, S.Ó., Cooke, S.A.Macedo, E.A., *Modeling and measurements of solid–liquid and vapor–liquid equilibria of polyols and carbohydrates in aqueous solution.* Carbohydrate Research 2002. 337: p. 1563 - 1571.

100. Montañes, F., Olano, A.Ibáñez, E., *Modeling solubilities of sugars in alcohols based on original experimental data.* AIChE Journal, 2007. 53(9): p. 2411 - 2418.

101. Herodes, K., Leito, I., Koppel, I.Rosés, M., *Solute-solvent and solvent-solvent interactions in binary solvent mixtures. Part 8. The $E_T(30)$ polarity of binary mixtures of formamides with hydroxylic solvents.* Journal of Physical Organic Chemistry 1999. 12: p. 109 - 115.

102. Brandt, A., Hallett, J.P., Leak, D.J., Murphyb, R.J.Welton, T., *The effect of the ionic liquid anion in the pretreatment of pine wood chips.* Green Chemistry, 2010. 12: p. 672 - 679.

103. Prausnitz, J.M., Lichtenthaler, R.N.Azevedo, E.G.d., *Molecular thermodynamics of fluid phase equilibria*. 3th Edition ed, ed. N.R. Amundson. 1999, New Jersey: Prentice Hall, Inc.

List of Publications

Mariana B. Oliveira, Rita R. Teles, António J. Queimada, João A.P. Coutinho, *"Phase equilibria of glycerol containing systems and their description with the Cubic-Plus-Association (CPA) Equation of State"*, Fluid Phase Equilibria 280 (2009) 22-29.

Luciana I.N. Tomé, Vítor R. Catambas, Rita R. Teles, Mara G. Freire, Isabel M. Marrucho, João A.P. Coutinho, *"Tryptophan extraction using hydrophobic ionic liquids"*, Separation and Purification Technology, 72 (2010) 167-173.

Rita R. Teles, Mara G. Freire, José N. Canongia Lopes, Luís P. N. Rebelo, João A. P. Coutinho, and Isabel M. Marrucho, *"Extraction of caffeine and nicotine from aqueous solutions using tetradecyltrihexylphosphonium-based ionic liquids",* in preparation.

Ana Rita R. Teles, Mara G. Freire, José A. Lopes da Silva and João A. P. Coutinho, *"Electrospun nanosized cellulose fibers using a neat and room temperature ionic liquid"*, in preparation.

Appendix A

A1 Surface Tension Related Data

Table A1 shows the water contents of the ILs studied in the surface tension measurements. Moreover, the water contents in cellulose samples after the drying procedure are also displayed in Table A1.

Table A 1 Water content in the ILs used to validate the surface tension measurements

Ionic Liquid	Water Content (wt %)
$[C_2mim][CH_3CO_2]$	0.270
$[C_{10}mim]Cl$	1.264
$[C_4mim][BF_4]$	0.056
$[C_4mim][NTf_2]$	0.047
$[C_8mim][BF_4]$	0.045
$[C_8mim][PF_6]$	0.497
$[C_8mim][NTf_2]$	0.159
Cellulose A	6.545
Cellulose B	6.705

Table A2 presents the surface tension for the pure ILs considered as references to validate the surface tension measurements.

Table A 2 Surface tension values [14, 35]

Ionic liquid	σ (this work) / ($mN.m^{-1}$)	σ (literature)/ ($mN.m^{-1}$)	Δσ%
$[C_4mim][BF_4]$	44.49 ± 0.030	44.50[14]	-0.017
$[C_4mim][NTf_2]$	33.01 ± 0.008	33.33[14]	-0.969
$[C_8mim][BF_4]$	33.43 ± 0.051	33.44[14]	-0.037
$[C_8mim][PF_6]$	34.92 ± 0.030	34.95[14]	-0.080
$[C_8mim][NTf_2]$	31.53 ± 0.039	31.59[35]	-0.187
Water	71.54 ± 0.166	71.98[14]	-0.615

Table A3 presents the density and molar fraction for the mixtures of ILs considered to the surface tension measurements.

Table A 3 Density values for the mixtures of ILs

$x_{[C2mim][CH3CO2]}$	$x_{[C10mim]Cl}$	ρ / (g/cm^3) 298 K
1.000	0.000	1.104
0.991	0.009	1.103
0.948	0.052	1.097
0.898	0.102	1.091
0.685	0.315	1.064
0.598	0.402	1.053
0.500	0.500	1.041

Table A4 displays the viscosity values for the ILs mixtures

Table A 4 Viscosity values for the mixture of ILs

$x_{[C2mim][CH3CO2]}$	$x_{[C10mim]Cl}$	*Shear Rate / (1.s^{-1})*	*Viscosity / (Pa.s)*
1.000	0.000	1.822	0.1987
0.991	0.009	2.387	0.1796
0.948	0.052	2.223	0.2543
0.898	0.102	2.192	0.3453
0.685	0.315	2.396	0.8987
0.598	0.402	2.244	1.223
0.500	0.500	2.45	1.706
0.318	0.682	2.164	4.947
0.000	1.000	2.526	50.41

Figure A1 is the representation of the viscosity as a function of [C_{10}mim]Cl molar fraction, including the values for the pure Ils.

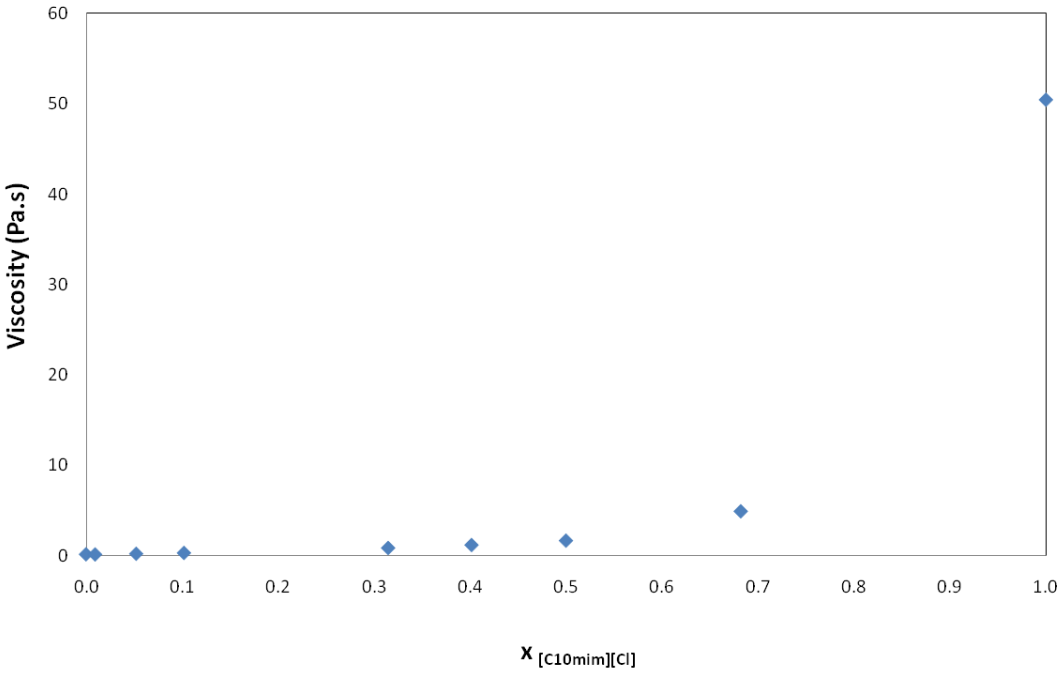

Figure A 1 Viscosity of ILs mixtures as a function of molar ration of [C_{10}mim]Cl

Appendix B

B.1 Calibration Curves for Carbohydrates

In order to quantify the carbohydrates saturation in hydrophilic ILs several calibration curves were determined. At least 7 standard solutions, of different known concentrations, were prepared for each carbohydrate from an initial stock solution and the respective absorbance was measured at wavelength of 540 nm by UV-Vis spectroscopy using a SHIMADZU UV-1700, Pharma-Spec Spectrometer.

B.1.1 D-(+)-Glucose

Results for the calibration curve of D-(+)-Glucose are presented in Table B 2 and Figure B 1. The concentration of the D-(+)-Glucose stock solution was 1.0084 g·dm^{-3}.

Table B 2 Concentration of D-(+)-Glucose and respective absorbance at λ = 540 nm

Standard	[D-(+)-Glucose] / (g.dm^{-3})	Abs
1	0.101	0.037
2	0.202	0.094
3	0.303	0.155
4	0.403	0.208
5	0.504	0.266
6	0.605	0.325
7	0.807	0.413

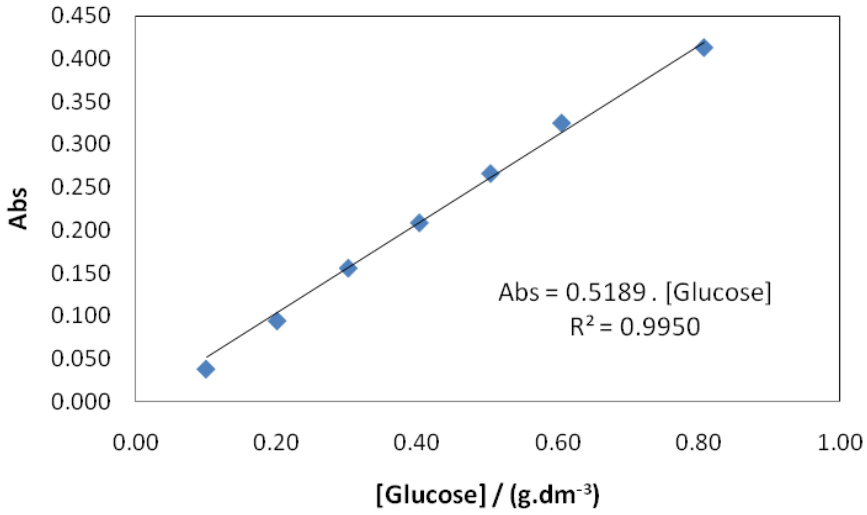

Figure B 1 Calibration curve for D-(+)-Glucose at λ = 540 nm

B.1.2 D-(+)-Mannose

For D-(+)-Mannose, 9 standards of different known concentrations (Table B 2) from the initial stock solution ([D-(+)-Mannose] = 1.0176 g.dm^{-3}) were prepared. Absorbance was measured at wavelength of 540 nm. Results are displayed in Figure B 2.

Table B 3 Concentration of D-(+)-Mannose and respective absorbance at λ = 540 nm

Standard	[D-(+)-Mannose] / (g.dm^{-3})	Abs
1	0.102	0.042
2	0.204	0.102
3	0.305	0.171
4	0.407	0.253
5	0.509	0.295
6	0.611	0.369
7	0.712	0.431
8	0.814	0.484
9	0.916	0.615

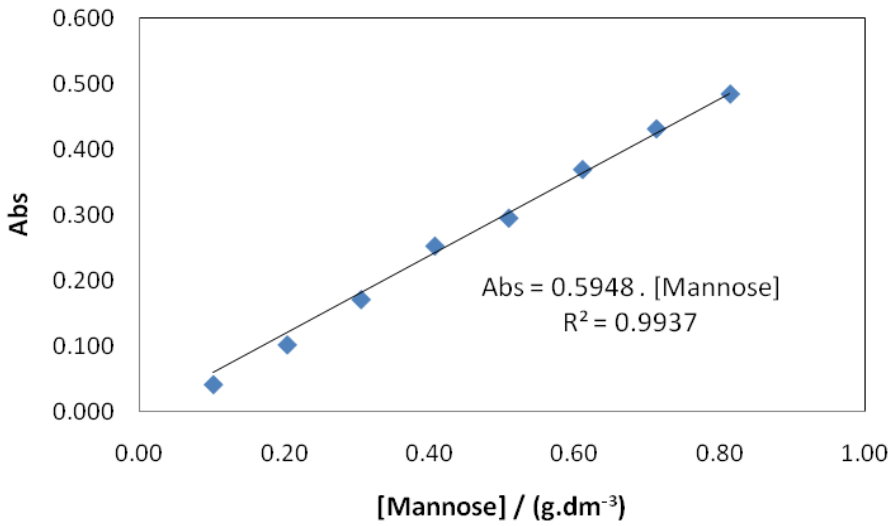

Figure B 2 Calibration curve for D-(+)-Mannose at λ = 540 nm

B.1.4 D-(-)-Fructose

For D-(-)-Fructose 7 standards of different known concentrations (Table B 3) from the initial stock solution ([D-(-)-Fructose] = 1.0176 $g.dm^{-3}$) were prepared. Absorbance was measured at wavelength of 540 nm and the calibration curve is displayed in Figure B 3.

Table B 4 Concentration of D-(-)-Fructose and respective absorbance at λ = 540 nm

Standard	[D-(-)-Fructose] / ($g.dm^{-3}$)	Abs
1	0.203	0.089
2	0.304	0.148
3	0.406	0.205
4	0.507	0.266
5	0.608	0.329
6	0.710	0.379
7	0.811	0.438

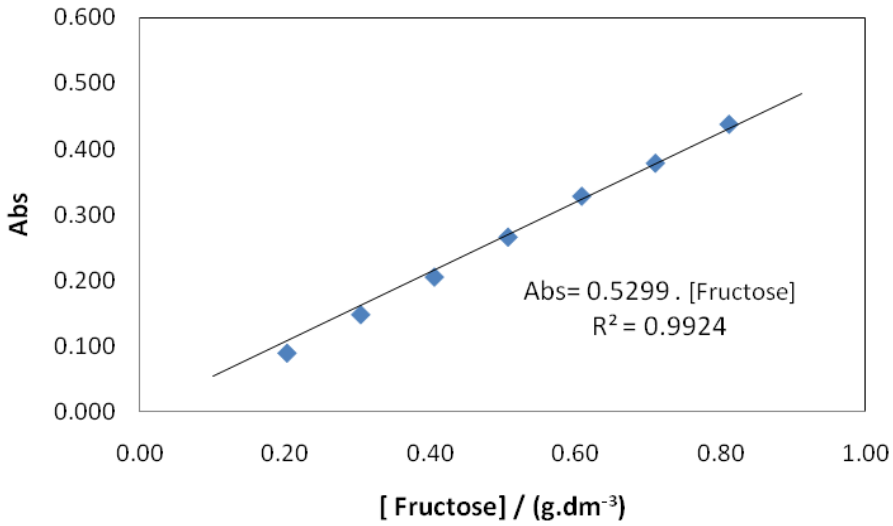

Figure B 3 Calibration curve for D-(-)-Fructose at λ = 540 nm

B.1.5 L-(+)-Arabinose

For L-(+)-Arabinose, 8 standards of different known concentrations (Table B 4) from the initial stock solution ([L-(+)-Arabinose] = 1.0012 g.dm^{-3}) were considered. Absorbance was measured at wavelength of 540 nm. Figure B 4 presents the graphical representation of the calibration curve obtained.

Table B 5 Concentration of L-(+)-Arabinose and respective absorbance at λ = 540 nm

Standard	[L-(+)-Arabinose] / (g.dm^{-3})	Abs
1	0.100	0.040
2	0.200	0.103
3	0.300	0.177
4	0.400	0.239
5	0.501	0.314
6	0.601	0.379
7	0.701	0.445
8	0.801	0.508

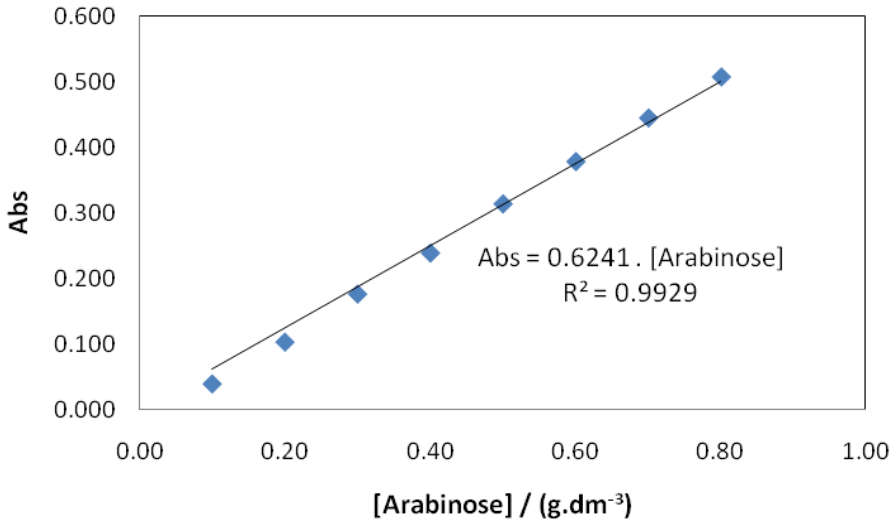

Figure B 4 Calibration curve for L-(+)-Arabinose at λ = 540 nm

B.1.6 D-(+)-Xylose

For D-(+)-Xylose, 8 standards of different known concentrations (Table B 5) prepared from the initial stock solution ([D-(+)-Xylose] = 1.0096 $g.dm^{-3}$) were used. Absorbance was measured at wavelength of 540 nm. Results for the calibration curve are shown in Figure B 5.

Table B 6 Concentration of D-(+)-Xylose and respective absorbance at λ = 540 nm

Standard	[D-(+)-Xylose] / ($g.dm^{-3}$)	Abs
1	0.101	0.043
2	0.202	0.103
3	0.303	0.184
4	0.404	0.250
5	0.505	0.311
6	0.606	0.375
7	0.707	0.443
8	0.808	0.510

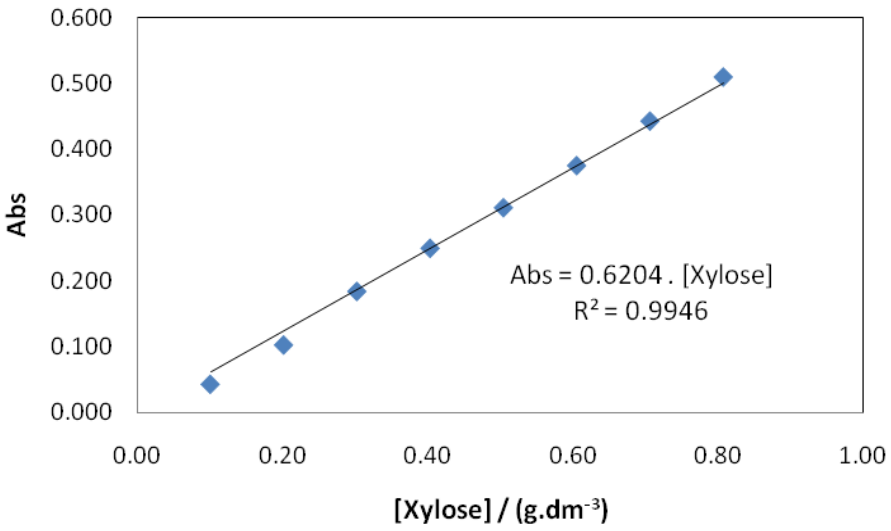

Figure B 5 Calibration curve for D-(+)-Xylose at λ = 540 nm

B.1.7 D-(+)-Galactose

For D-(+)-Galactose, 8 standards of different known concentrations (Table B 6) were prepared using the initial stock solution ([D-(+)-Galactose] = 1.0056 g.dm^{-3}). Absorbance was measured at wavelength of 540 nm. The calibration curve for D-(+)-galactose is presented in Figure B 6.

Table B 7 Concentration of D-(+)-Galactose and respective absorbance at λ = 540 nm

Standard	[D-(+)-Galactose] / (g.dm^{-3})	Abs
1	0.101	0.044
2	0.201	0.110
3	0.302	0.175
4	0.503	0.302
5	0.603	0.355
6	0.704	0.420
7	0.804	0.510
8	0.905	0.619

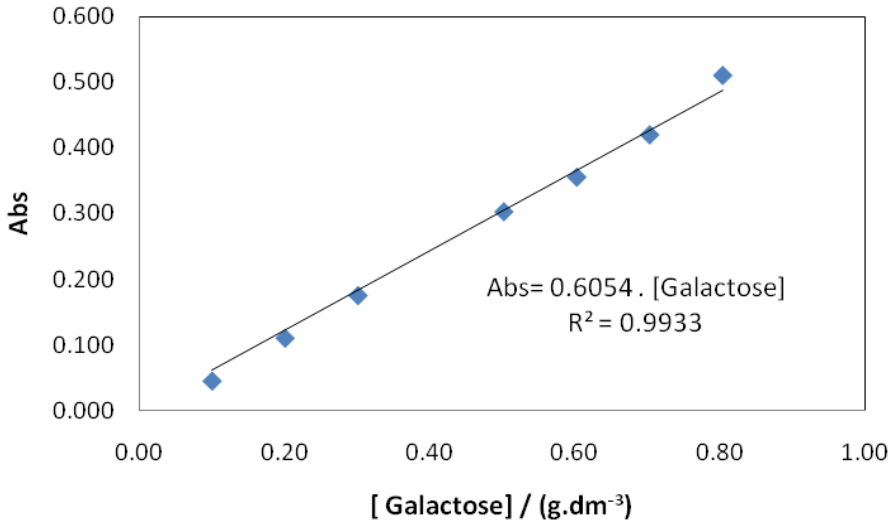

Figure B 6 Calibration curve for D-(+)-Galactose at λ = 540 nm

Appendix C

C.1 Temperature Calibration

To calibrate the temperature provided by the Eppendorf Thermomixer Comfort commercial air oven, a Pt 100 probe with an uncertainty within 0.01 K was used and directly immersed in the solutions. Experimental temperatures are presented in Table C 1 and the linear correlation between both temperatures is displayed in Figure C 1.

Table C Correlation between the temperature provided by the thermomixer equipment and a Pt 100 probe immersed in the solution

$T_{\text{thermomixer}}$ / (ºC)	$T_{\text{thermomixer}}$ / (K)	T_{Pt100} / (ºC)	T_{Pt100} / (K)
15	288.15	15.40	288.55
20	293.15	20.20	293.35
25	298.15	25.00	298.15
30	303.15	29.90	303.05
35	308.15	34.70	307.85
40	313.15	39.60	312.75
45	318.15	44.50	317.65
50	323.15	49.30	322.45
55	328.15	54.10	327.25
60	333.15	58.80	331.95
65	338.15	63.70	336.85
70	343.15	68.50	341.65
75	348.15	73.10	346.25

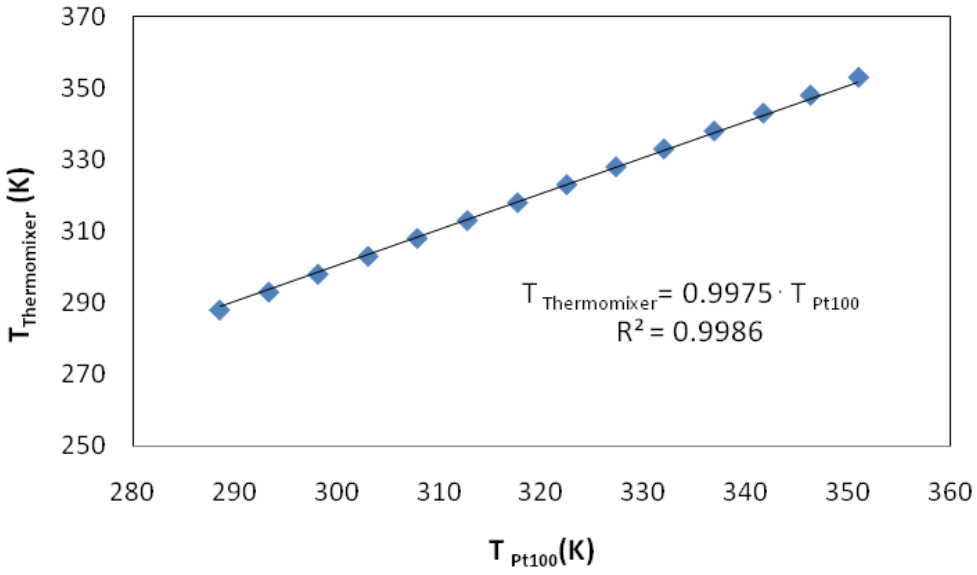

Figure C 1 Temperature calibration of the thermomixer equipment with a Pt 100 probe